Hydroformylation of post-metathesis product using rhodium-based catalysts

by

Nicholas Claus Carl Breckwoldt

Dissertation presented for the Degree

of

DOCTOR OF PHILOSOPHY
(CHEMICAL ENGINEERING)

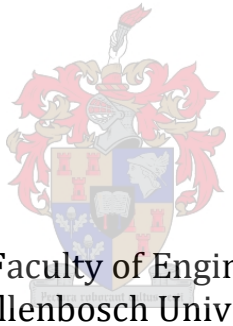

in the Faculty of Engineering
at Stellenbosch University

Supervisor
Dr. N. Goosen

Co-Supervisor/s
Prof. G. Smith
Prof. P. Van der Gryp

December 2019

DECLARATION

By submitting this dissertation electronically, I declare that the entirety of the work contained therein is my own, original work, that I am the sole author thereof (save to the extent explicitly otherwise stated), that reproduction and publication thereof by Stellenbosch University will not infringe any third party rights and that I have not previously in its entirety or in part submitted it for obtaining any qualification.

This dissertation includes three original papers published in peer-reviewed journals or books and one unpublished publication. The development and writing of the papers (published and unpublished) were the principal responsibility of myself and, for each of the cases where this is not the case, a declaration is included in the dissertation indicating the nature and extent of the contributions of co-authors.

Date: December 2019

ABSTRACT

This study forms part of the overall scope of the RSA Olefins Programme for the upgrading of low-value α-alkene feedstocks to higher value detergent-range products within the South African context. The programme is motivated by the unique α-alkene market position in South Africa, as a producer of both odd- and even-numbered α-alkenes via Fischer-Tropsch conversion of syngas. Based on currently available technologies, the beneficiation of these low-value short-chain α-alkenes (C_5-C_9) via consecutive transition-metal-catalysed alkene metathesis and hydroformylation reactions is under consideration in South Africa. This study focused on evaluating the hydroformylation reaction within the scope of the proposed catalytic beneficiation process.

The contributions of the study were thus two-fold in firstly describing the application of commercially available rhodium-based catalysts and secondly the application of non-commercial Schiff base derived rhodium-based precatalysts for the identified model hydroformylation reaction of the post-metathesis product 7-tetradecene. For both sets of catalyst systems, the study aimed to i) understand the catalytic performances of different rhodium-based catalysts for model reaction system, ii) to evaluate the effect of process conditions on the hydroformylation performance and iii) to evaluate and describe the reaction kinetics through phenomenological rate law model development that can be used in the reaction-engineering context.

In terms of commercial rhodium-based catalysts:

The performance of three commercially available catalyst systems, Rh-tris(2,4-ditertbutylphenyl)phosphite (**1**), Rh-triphenylphosphine (**2**) and Rh-triphenylphosphite (**3**) were evaluated for the model reaction by varying operating conditions such as temperature (60-90°C) and pressure (10-30 bar). Catalyst performance was characterised according to the activity (turnover numbers) and selectivity. It was found that all three commercial catalysts showed hydroformylation and isomerisation behaviour that was largely temperature- and pressure-dependent. Optimal conditions were established at 70°C (30 bar, $CO:H_2$, 1:1) within the investigated ranges, for which **1** was exclusively hydroformylation-selective, while **2** and **3** were both hydroformylation- and isomerisation-selective. Overall, it was found that **1** was the most effective commercial catalyst system in terms of both activity (TON of 980) and regioselectivity toward targeted branched aldehyde product 2-hexylnonanal (>99%).

It was further proposed and found that the reaction kinetics of the model reaction with **1** could be accurately described by a set of three interdependent first-order ordinary differential mole-balance equations. A mechanism-based rate-equation derived for bulky phosphite ligands was found to be consistent with the rate data (first-order in alkene and rhodium concentration, zero-order in hydrogen and negative order in carbon monoxide) over a wide alkene conversion range.

In terms of non-commercial Schiff base derived rhodium-based catalysts:

The performance of the monometallic rhodium-aryl (**4**) and heterobimetallic rhodium-ferrocenyl (**5**) Schiff base derived precatalysts bearing N'O chelate ligands were evaluated for the model reaction by varying operating conditions such as temperature (75-115°C), pressure (30-50 bar) and catalyst loading (7-tetradecene-to-precatalyst molar ratio from 1000:1 to 6000:1). It was found that the optimal reaction temperature for both **4** and **5** was 95°C (40 bar, $CO:H_2$, 1:1). Even though precatalysts **4** and **5** were less regioselective (40:60 split in favour of isomeric aldehydes) compared to the commercial catalyst systems, significantly higher turnover numbers (up to 4310) were recorded using the Schiff base derived precatalyst systems at lower rhodium loadings. Evidence of a cooperative effect by including the second metal (ferrocene) in the heterobimetallic catalyst system was also observed due to improved catalytic activity compared to the monometallic catalyst systems under low temperature conditions.

It was further found that the reaction kinetics of the model reaction with **5** could be accurately described by a set of four interdependent first-order ordinary differential mole-balance equations. A mechanism-derived rate equation derived for the hydroformylation using conventional monometallic rhodium-based catalyst was found to be consistent with the parametric influences of different reaction conditions affecting the reaction rate using the heterobimetallic precatalyst, with minor modification to account for observed fractional order dependence in precatalyst concentration. Thus, the rate of reaction was found to be first-order in alkene concentration, positive fractional-order in precatalyst concentration and first-order in both hydrogen and carbon monoxide.

OPSOMMING

Hierdie studie vorm deel van die algehele bestek van die RSA Olefiene Program vir die opgradering van lae-graad α-alkeen voermateriaal na hoër-waarde detergentreeksprodukte binne die Suid-Afrikaanse konteks. Die program word gemotiveer deur die unieke α-alkeenmarkposisie in Suid-Afrika, as 'n produseerder van beide onewe- en ewegetalle α-alkene via Fischer-Tropsch-omsetting van sintesegas. Gebaseer op beskikbare tegnologie tans, is die veredeling van hierdie lae-waarde kortketting α-alkene (C_5-C_9) via opeenvolgende oorgang-metaal-gekataliseerde alkeen metatesis en hidroformileringreaksies in oorweging in Suid-Afrika. Hierdie studie fokus op die evaluering van die hidroformileringsreaksie binne die bestek van die voorgestelde katalitiese veredelingsproses.

Die bydraes van die studie was dus tweevoudig deur eerstens die toepassing van kommersieel beskikbare rodium-gebaseerde katalisators en tweedens die toepassing van nie-kommersiële Schiff-basis afgeleide rodium-gebaseerde voorkatalisators vir die geïdentifiseerde model hidroformileringreaksie van die post-metatesis produk 7-tetradeseen. Vir beide stelle van katalisatorsisteme, het die studie beoog om i) die katalitiese vermoë van verskillende rodium-gebaseerde katalisators vir die model reaksie sisteme te verstaan, ii) die effek van proses kondisies op die hidroformilering vermoë te evalueer, en iii) die reaksiekinetika deur fenomenologiese tempo wet model ontwikkeling te evalueer en beskryf wat gebruik kan word in die reaksie ingenieurskonteks.

In terme van kommersiële rodium-gebaseerde katalise:

Die vermoë van drie kommersieel beskikbare katalisatorsisteme, Rh(2,4-ditertbutylphenyl)fosfiet (**1**), Rh-triphenylfosfien (**2**) en Rh-triphenylfosfiet (**3**) is gevalueer vir die modelreaksie deur verskeie bedryfskondisies soos temperatuur (60–90 °C) en druk (10–30 bar) te varieer. Katalisator vermoë is gekarakteriseer na aanleiding van die aktiwiteit (omset nommers) en selektiwiteit. Dit is bevind dat al drie kommersiële katalisators hidroformilering en isomerisasie gedrag gewys het wat grootliks temperatuur- en drukafhanklik was. Optimale kondisies is gevestig by 70 °C (30 bar, $CO:H_2$, 1:1) binne die nagevorste bestekke, waarvoor **1** die eksklusiewe hidroformilering-selektiewe was, terwyl **2** en **3** albei hidroformilering- en isomerisasie-selektief was. Oor die algemeen is dit gevind dat **1** die mees effektiewe kommersiële katalisatorsisteem in terme van beide aktiwiteit (TON van 980) en regioselektiwiteit na die mikpunt van uitgebreide aldehiedprodukt 2-heksielnonanal (>99%), is.

Dit is verder voorgestel en gevind dat die reaksiekinetika van die model reaksie met **1** akkuraat beskryf kon word deur 'n stel van drie interafhanklike eerste-orde gewone differensiële molbalans vergelykings. 'n Meganisme-gebaseerde tempovergelyking afgelei vir groot fosfiet ligande is bevind om in ooreenstemming met die tempo data (eerste-orde in alkeen en rodium konsentrasie, zero-orde in waterstof en negatief-orde in koolstofmonoksied) oor 'n wye alkeen omset bestek.

In terme van nie-kommersiële Schiff basis afgeleide rodium-gebaseerde katalisators:

Die vermoë van die monometaliese rodium-ariel (**4**) en heterobimetaliese rodium-ferroseniel (**5**) Schiff basis afgeleide prekatalisators wat N'O chelaat ligande dra, is geevalueer vir die model reaksie deur verskillende bedryfskondisies soos temperatuur (75–115 °C), druk (30–50 bar) en katalisator lading (7-tetradeseen-na-prekatalisator mol verhouding van 1000:1 tot 6000:1) te varieer. Dit is gevind dat die optimale reaksie temperatuur vir beide **4** en **5** 95 °C was (40 bar, $CO:H_2$, 1:1). Selfs al was **4** en **5** minder regioselektief (40:60 verdeel ten gunste van isometriese aldehiedes) in vergelyking met die kommersiële katalisatorsisteme, is beduidende hoër omset nommers (tot 4310) opgeteken deur die Schiff basis afgeleide prekatalisatorsisteme by laer rodium ladings, te gebruik. Bewyse van 'n samewerkende effek deur die insluiting van die tweede metaal (ferroseen) in die heterobimetaliese katalisatorsisteem is ook waargeneem as gevolg van die verbeterde katalitiese aktiwiteit in vergelyking met die monometaliese katalisatorsisteme onder lae temperatuurkondisies.

Dit is is verder gevind dat die reaksiekinetika van die model reaksie met **5** akkuraat beskryf kan word deur 'n stel van vier interafhanklike eerste-orde gewone differensiële molbalans vergelykings. 'n Meganisme-afgeleide tempo vergelyking afgelei vir die hidroformilering deur konvensionele monometaliese rodium-gebaseerde katalisators te gebruik, is gevind om konsekwent met die parametriese invloede van verskillende reaksiekondisies wat die reaksie tempo affekteer, deur die heterobimetaliese prekatalisator te gebruik, met mindere wysiging om vir waargenome breukorde afhanklikheid in prekatalisator konsentrasie te reken. Dus, die tempo van reaksie is gevind om eerste-orde in alkeenkonsentrasie te wees, positiewe breukorde in prekatalisatorkonsentrasie en eerste-orde in beide waterstof en koolstofmonoksied te wees.

ACKNOWLEDGEMENTS

The support of the DST-NRF Centre of Excellence (CoE) in Catalysis towards this research is hereby acknowledged. Opinions expressed and conclusions arrived at, are those of the author and are not necessarily to be attributed to the CoE. The author also wishes to thank the University of Stellenbosch and University of Cape Town for additional financial support towards this study.

PUBLICATIONS

The following international peer-reviewed publications resulted from the study presented in this dissertation:

- Breckwoldt, N. and Van der Gryp, P. 2018. Hydroformylation of post-metathesis product using commercial rhodium-based catalysts. Reaction Kinetics, Mechanisms and Catalysis. 125, 689-705.
- Breckwoldt, N., Goosen, N., Vosloo, H. and Van der Gryp, P. 2019. Kinetic evaluation of the hydroformylation of the post-metathesis product 7-tetradecene using bulky phosphite-modified rhodium catalyst. Reaction Chemistry and Engineering. 4, 695-704.
- Breckwoldt, N., Goosen, N., Van der Gryp, P. and Smith, G. 2019. Hydroformylation of the post-metathesis product 7-tetradecene using Schiff based derived rhodium(I) precatalysts. Applied Catalysis A: General. 573, 49-55.
- Breckwoldt, N., Smith, G., Van der Gryp, P. and Goosen, N. 2019. Kinetic evaluation of the hydroformylation of the post-metathesis product 7-tetradecene using a heterobimetallic rhodium-ferrocenyl Schiff base derived precatalyst. Reaction Kinetics, Mechanisms and Catalysis. 128, 333-347.

CONFERENCE PROCEEDINGS

The following conference proceedings resulted from the study presented in this dissertation:

- Breckwoldt, N, Vosloo, H., Smith, G. and Van der Gryp, P. Hydroformylation of post-metathesis internal olefins. Conference Proceedings of CATSA, Drakensberg, South Africa, November 2016.
- Breckwoldt, N. and Van der Gryp, P. Hydroformylation of post-metathesis olefins. Conferences Proceedings of Europacat, Florence, Italy, August 2017.

DECLARATION BY THE CANDIDATE

With regard to the chapters as detailed below, the nature and scope of my contribution were as follows:

Chapter	Pages	Nature of contribution	Extent of contribution (%)
4	46-67	Experimental planning and execution, data gathering and interpretation of results. Writing of manuscript and incorporating co-author feedback before submission of manuscript to journal.	80-90
5	68-89	Experimental planning and execution, data gathering, kinetic modelling and interpretation of results. Writing of manuscript and incorporating co-author feedback before submission of manuscript to journal.	80-90
6	90-106	Experimental planning and execution, data gathering and interpretation of results. Writing of manuscript and incorporating co-author feedback before submission of manuscript to journal.	80-90
7	107-126	Experimental planning and execution, data gathering, kinetic modelling and interpretation of results. Writing of manuscript and incorporating co-author feedback before submission of manuscript to journal.	80-90

The following co-authors have contributed to the following chapters:

Name	Email	Chapters	Nature of contribution	Extent of contribution (%)
Dr. N. Goosen	njgoosen@sun.ac.za	5,6,7	Supervisor/Co-supervisor to the candidate	5-10
Prof. P. Van der Gryp	Percy.VanderGryp@nwu.ac.za	4,5,6,7	Supervisor/Co-supervisor to the candidate	5-10
Prof. G. Smith	Gregory.Smith@uct.ac.za	6,7	Supervisor/Co-supervisor to the candidate	5-10

LIST OF TERMINOLOGIES

Bimetallic complex	A coordination complex containg two metals - metals can either be the same (homo-) or different (hetero-)
Chelate	A compound that contains two or more potential binding groups on the metal centre within a coordination complex
Chemoselectivity	Preference for producing one functional group over another
Ligand	An ion or molecule that binds to a central metal atom to form a coordination complex
Metallocene	A compound consisting of a metal 'sandwiched' between two cyclopentadienyl rings
Phosphine	An organophosphorus compound having the general formula $P(R_3)$
Phosphite	An organophosphorus compound having the general formula $P(OR)_3$
Precatalyst	A compound that is converted to an active catalyst during a catalytic reaction
Regioselectivity	Preference for bonding a functional group to one site over another
Schiff base	An imino compound having the genral formula RC=NR'

CONTENTS

CHAPTER 1: INTRODUCTION 1

1.1 Hydroformylation reaction 2

1.2 Study motivation 3

1.3 Aim and objectives 5

1.4 Study layout 6

1.5 Novel contributions 7

References 8

CHAPTER 2: LITERATURE STUDY 10

2.1 Transition metals in hydroformylation 11

2.2 Hydroformylation mechanism 12

2.3 Review of rhodium-catalysed internal alkene hydroformylation 14

2.3.1 Phosphine-modified catalysts 16

2.3.2 Phosphite-modified catalysts 21

2.3.3 Bimetallic catalysts 23

2.4 Review of kinetic modelling of the hydroformylation reaction 27

References 33

CHAPTER 3: EXPERIMENTAL 38

3.1 Materials 39

3.1.1 Catalysts used 39

3.1.2 Chemicals used 39

3.1.3 Synthesis of 7-tetradecene 40

3.2 Hydroformylation experiments 41

3.2.1 Experimental apparatus and methodology 41

3.2.2 Analytical methodology 42

3.2.3 Validation of equipment and method with literature 43

3.2.4 Uncertainty analysis 44

References 45

CHAPTER 4: MANUSCRIPT 1 46

Abstract 47

1. Introduction 48

2. Materials and methods 52

2.1 Chemicals used 52

2.2 Catalysts used 52

2.3 Synthesis of 7-tetradecene 53

2.4 Hydroformylation procedure 53

2.5 Analytical methods 53

3. Results and discussion 54

3.1 Reaction network: hydroformylation of 7-tetradecene 54

3.2 Screening of commercial catalysts 55

3.3 Hydroformylation of 7-tetradecene with (1)/[$Rh(CO)_2(acac)$] 57

4. Conclusions 63

Acknowledgements 64

References 64

CHAPTER 5: MANUSCRIPT 2 68

Abstract 69

1. Introduction 70

2. Materials and methods 72

2.1 Chemicals used 72

2.2 Experimental design 72

2.3 Hydroformylation procedure 73

2.4 Regression procedure and validation 74

2.5 Gas solubility 74

3. Results and discussion 75

3.1 Influence of temperature 75

3.2 Influence of catalyst concentration 79

3.3 Influence of hydrogen and carbon monoxide partial pressures 80

3.4 Modelling of the reaction rate 82
4. Conclusions 86
Conflicts of interest 86
Acknowledgements 86
References 87
CHAPTER 6: MANUSCRIPT 3 90
Abstract 91
1. Introduction 92
2. Experimental 94
2.1 Preparation of precatalysts 94
2.2 Chemicals used 94
2.3 Hydroformylation procedure 94
2.4 Lifetime studies 95
3. Results and discussion 95
3.1 Preliminary screening 95
3.2 Influence of reaction temperature 98
3.3 Influence of catalyst loading 99
3.4 Influence of pressure 101
3.5 Catalyst lifetime 102
4. Conclusions 103
Acknowledgements 104
References 104
CHAPTER 7: MANUSCRIPT 4 107
Abstract 108
1. Introduction 109
2. Materials and methods 110
2.1 Chemicals and precatalyst used 110
2.2 Reaction conditions for the kinetic study 111
2.3 Hydroformylation procedure 112

2.4 Methodology framework for describing the kinetics 112
3. Results and discussion 114
3.1 Typical product-distribution-time profiles 114
3.2 Influence of temperature 116
3.3 Influence of catalyst concentration 117
3.4 Influence of hydrogen and carbon monoxide partial pressures 118
3.5 Kinetic modelling of the reaction network 120
4. Conclusions 123
Acknowledgements 123
References 124
CHAPTER 8: CONCLUSIONS AND RECOMMENDATIONS 127
8.1 Conclusions 128
8.1.1 Overall aim 128
8.1.2 Hydroformylation with commercial rhodium catalysts 128
8.1.3 Hydroformylation with Schiff base derived rhodium precatalysts 129
8.2 Recommendations for future work 131
References 132
APPENDIX A: PERMISSIONS TO REPRODUCE PUBLISHED WORK 133
APPENDIX B: ANALYSIS OF UNCERTAINTY 138

CHAPTER 1

INTRODUCTION

In this chapter, a broad overview of the topic of study in this dissertation is presented. The chapter is divided into five sections. In the first section (Section 1.1), a brief introduction to the topic of hydroformylation is presented, followed by the motivation for the study in Section 1.2, which puts the relevance and potential industrial importance of the title reaction "hydroformylation of post-metathesis product" into perspective. Aims and objectives for the study are defined in Section 1.3, followed by the layout of the study in Section 1.4. The chapter ends with a summary of the novel contributions made within the study (Section 1.5)

1.1 Hydroformylation reaction

The hydroformylation reaction, or 'Oxo-process', represents one of the most important industrial applications of catalysis employing transition-metal-based complexes (Van Leeuwen and Claver, 2002). Otto Roelen discovered the reaction in the early 1930s during his investigation of oxygenated products that occur during Fischer-Tropsch reactions (Frey, 2013). Hydroformylation can be described as the metal-catalysed addition of hydrogen (H_2) and carbon monoxide (CO) across the double bond of an alkene to produce aldehydes (**Figure 1.1**). These aldehyde products contain a single carbon atom more than the starting alkene and are said to be formed in an atom-economical fashion since all of the reagents molecules (alkene, CO and H_2) appear in the final product.

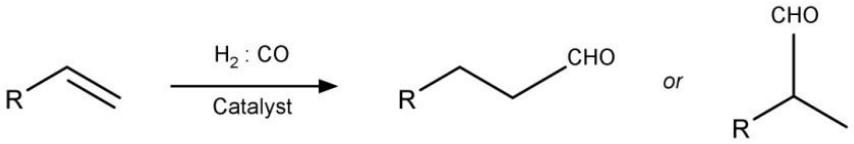

Figure 1.1: Transition-metal-catalysed hydroformylation reaction.

As an atom-efficient reaction, hydroformylation has enabled the targeting of a wide variety of molecules due to the synthetic versatility of the aldehyde functionality (Cornils and Hermann, 2002) (**Figure 1.2**). The largest volume of hydroformylation products are converted to alcohols for applications as detergents or plasticizers, while applications of the hydroformylation reaction also exist for fine-chemical synthesis, including the preparation of fragrances and pharmaceuticals. At the same time, multi-step catalytic reaction sequences involving the hydroformylation reaction are beginning to attract much interest in the field as a new and interesting avenue for organic synthesis (Chaudhari, 2012; Börner and Franke, 2016). The motivation for such multi-step catalytic sequences is in line with the ever-increasing industrial imperative to reduce raw material requirements, energy and undesired/waste products.

The research embarked upon within this dissertation lies within this domain of multi-step catalytic reactions in which the hydroformylation reaction step plays an important role.

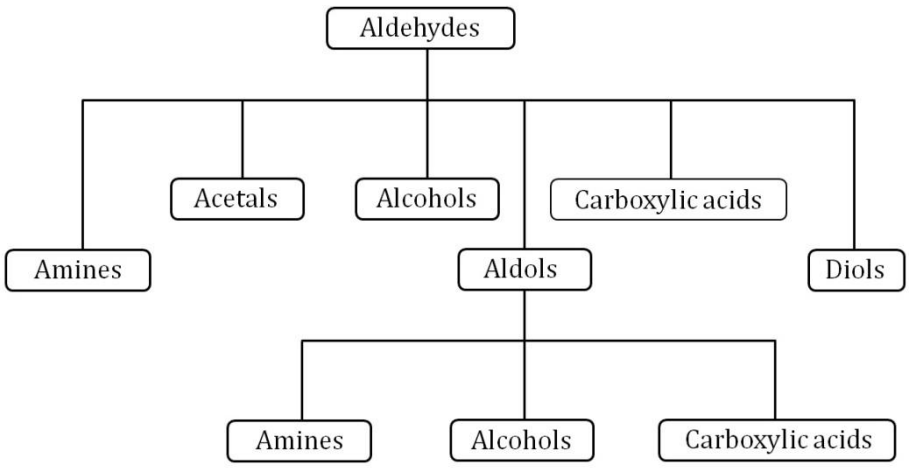

Figure 1.2: Different products that are accessible via the hydroformylation reaction. Adapted from Cornils and Hermann (2002).

1.2 Study motivation

The present study compliments previous and ongoing research within the RSA Olefins programme of the South African National Research Foundation-Department of Science and Technology's (DST-NRF) Centre of Excellence in Catalysis (c*Change) for evaluating the efficacy of transition-metal-catalysed reactions for the sequential upgrading of low-value α-alkene feedstocks. This programme is motivated by the unique α-alkene market situation in South Africa, as the country's major petrochemical company, Sasol Ltd., is the sole global producer of both odd and even-numbered α-alkenes via the Fischer-Tropsch process using syngas sourced from coal or natural gas (Dry, 2002; De Klerk, 2012). Due to the wide distribution of α-alkene products formed during such a process, several strategies have been identified in order to manipulate these product streams to meet targeted market opportunities. Based on currently available technologies, the beneficiation of low-value short-chain α-alkenes (C_5-C_9) via consecutive alkene metathesis and hydroformylation reactions is under consideration in South Africa (**Figure 1.3**).

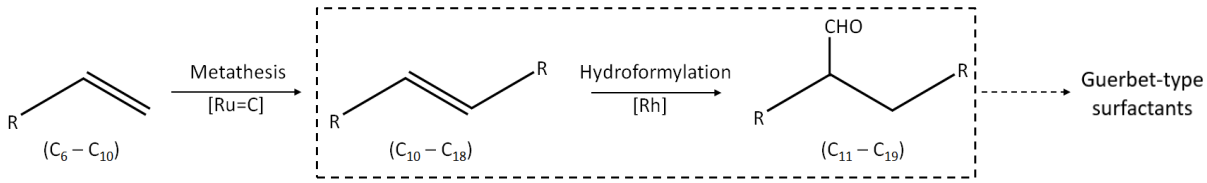

Figure 1.3: Beneficiation of low value α-alkenes as proposed by the RSA Olefins programme.

The first step in the proposed beneficiation scheme involves subjecting the short-chain α-alkene product streams to alkene metathesis reactions in order to increase the chain length to more synthetically desirable higher internal alkene products (C_{10}-C_{18}), i.e. post-metathesis products, with ethene (C_2) formed as a by-product. This is followed by hydroformylation of the post-metathesis product to yield corresponding alkyl-branched aldehydes (>C_{11}). Finally, the carbonyl function on the aldehyde can be hydrogenated to yield corresponding branched alcohols (i.e. 2-alkyl-1-alkanols) which are characteristic of the class of so-called Guerbet-type surfactant alcohols (O'Lenick, 2001). As surfactants, these branched Guerbet alcohols are characteristically more biodegradable as compared to their linear analogues; hence their application is attractive in meeting technological and environmental imperatives faced by detergent industries (Zoller, 2009). Moreover, these commodity alcohol products can be incorporated as feedstocks for many subsequent value-adding processes such as for the production of alkylphosphates, alkylpolyglycolethers, carboxylic acids and amines, among other valuable products.

To date, the metathesis of Fischer-Tropsch-type linear α-alkenes (C_5-C_9) has been studied extensively within the scope of the proposed beneficiation scheme (Jordaan et al., 2006; Jordaan et al., 2007; Van der Gryp et al., 2012; Du Toit et al., 2014; Du Toit et al., 2016). An example of such a process is the metathesis of readily available and inexpensive 1-octene (C_8) (**Figure 1.4**).

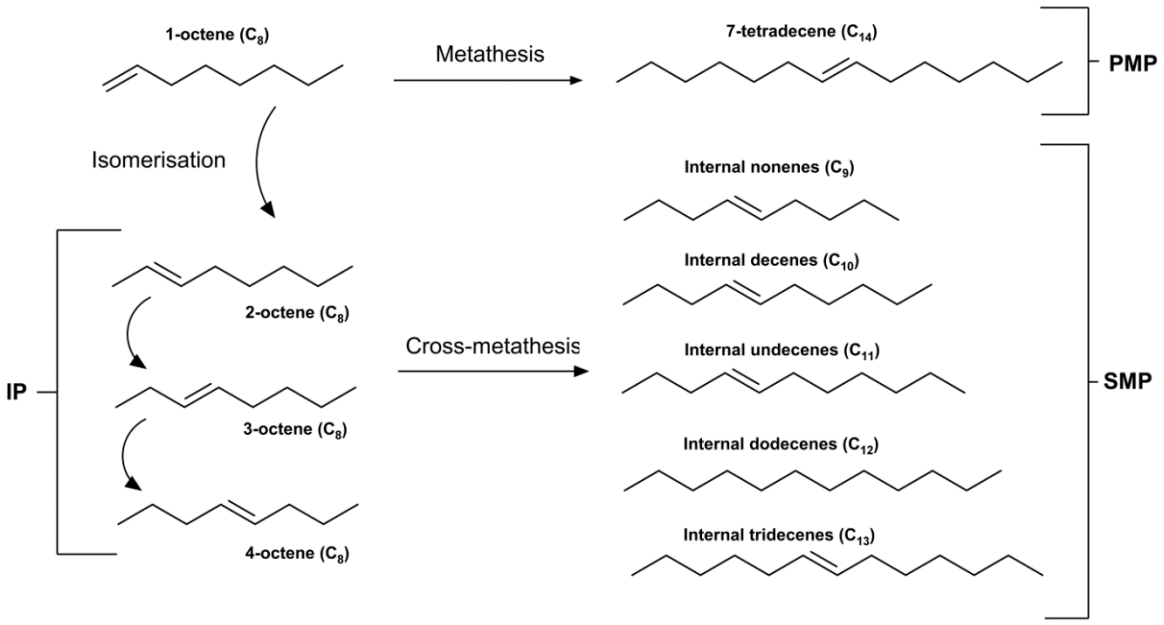

Figure 1.4: Product distribution during 1-octene metathesis.

A wide distribution of possible products is formed during 1-octene metathesis. These products can be more generally described as the primary metathesis product (PMP), isomerisation products (IPs) and secondary metathesis products (SMPs). The PMP refers to the higher internal alkene product 7-tetradecene (C_{14}) formed from the self-metathesis of 1-octene with ethene (C_2) formed as a by-product. IPs result from the double-bond isomerisation reaction of 1-octene yielding 2-, 3- and 4-octenes. SMPs are formed from the subsequent cross-metathesis of 1-octene with resulting IPs or the IPs with each another. IPs and SMPs are typically undesired side-products during the alkene metathesis reaction, while the PMP (7-tetradecene in the case of 1-octene metathesis) is the desired post-metathesis product.

While much progress contributing to the potential commercialization of such a beneficiation process (**Figure 1.3**) has been made in the field of metathesis, a detailed reaction engineering investigation of the hydroformylation of post-metathesis product to corresponding detergent-range series of aldehyde products still lacks in the literature. This study therefore aims to address this shortcoming.

1.3 Aim and objectives

The overall aim of this dissertation is to perform a detailed reaction engineering investigation of the rhodium-catalysed hydroformylation of the post-metathesis product with 7-tetradecene as a model substrate system. The objectives of the study were two-fold in terms of the application of both commercial and non-commercial catalyst systems for the model hydroformylation reaction as based on the shortcomings identified in the literature (see Chapter 2) as follows:

(i) Hydroformylation with commercial catalysts

(a) Understand the catalytic performances of different commercially available rhodium-based catalysts for the 7-tetradecene hydroformylation system.

(b) Evaluate the effect of different reaction conditions (temperature, catalyst loading, syngas pressure and ligand-to-metal ratios) on the catalytic performance.

(c) Evaluate and model the kinetic behaviour for 7-tetradecene hydroformylation.

(ii) Hydroformylation with non-commercial catalysts

(a) Understand the catalytic performances of monometallic and heterobimetallic Schiff base derived rhodium (I) precatalysts for the 7-tetradecene hydroformylation system.

(b) Evaluate the effect of different reaction conditions (temperature, catalyst loading and syngas pressure) on the catalytic performance.

(c) Evaluate and model the kinetic behaviour for 7-tetradecene hydroformylation.

The second broad objective of this dissertation forms part of a collaborative project with the Department of Chemistry at the University of Cape Town, South Africa.

1.4 Study layout

In order to address the objectives defined in the previous subsection (Section 1.3), this dissertation follows a layout consisting of eight chapters (this being Chapter 1).

Chapter 2 provides a survey of the pertinent hydroformylation literature that is of relevance to the present study. Overviews of the transition metals used in hydroformylation, the hydroformylation mechanism, rhodium-catalysed hydroformylation of internal alkenes and kinetic modelling of the hydroformylation reaction are presented.

In Chapter 3, a general account of the experimental framework used throughout this study is provided. Aspects concerning the experimental apparatus, experimental methodology, analysis and synthesis procedures are described.

The results of the study are reported in the form of four individual manuscripts, three of which have been published in international peer-reviewed journals at the time of writing this dissertation. The manuscripts are arranged according to the study of commercially available rhodium-based catalysts (Chapters 4 and 5) and non-commercial Schiff base derived rhodium precatalysts (Chapters 6 and 7). Where applicable, permissions to reproduce published work are available in Appendix A.

Lastly, in Chapter 8, the main findings and conclusions from the study are discussed along with recommendations for potential future work. It is the view of the author that the findings from the study contribute towards the field of hydroformylation as well as the broader understanding and advancement within the scope of the RSA Olefins Programme for the potential transition-metal-catalysed beneficiation of low value α-alkenes feedstocks to economically higher value products in the South African context.

1.5 Novel contributions

The following novel contributions with respect to the model hydroformylation reaction of the post-metathesis product 7-tetradecene are presented in this dissertation:

(i) The application of three commercially available rhodium catalyst systems: Rh-triphenylphosphine, Rh-triphenylphosphite and Rh-tris(2,4-ditertbutylphenyl)-phosphite, is demonstrated for the model hydroformylation reaction (Chapter 4). The influence of different operating conditons on the distribution of products and catalytic performance during the hydroformylation is investigated, the first such report demonstrating a systematic reaction engineering evaluation of the hydroformylation of post-metathesis product using homogeneous rhodium-based catalysts, to the best of the author's knowledge. This systematic evaluation resulted in unprecedented selectivity being found towards the targeted alkyl-branched aldehyde product 2-hexylnonanal, particulary when employing the Rh-tris(2,4-ditertbutyl-phenyl)-phosphite catalyst system.

(ii) A detailed reaction engineering kinetics evaluation of the model reaction using the commercially available Rh-tris(2,4-ditertbutylphenyl)phosphite catalyst system is presented (Chapter 5). A phenomenological mechanism-derived rate model is successfully applied and found to describe the influence of different operating conditions on the reaction rate, the first such study reported for the hydroformylation of post-metathesis product using the bulky phosphite-modified rhodium catalyst, to the best of the author's knowledge. The rate model is capable of accurately predicting the product-distribution trajectories over wide alkene conversion and operating condition range.

(iii) The application of non-commercialized monometallic rhodium and heterobimetallic rhodium-ferrocene precatalysts bearing hemilabile Schiff base-derived N'O chelate ligands is demonstrated for the model hydroformylation reaction (Chapter 6). The influence of different operating conditons on the distribution of products and catalytic performance during hydroformylation is investigated. It is the first report demonstrating the potential activity-enhancing effect when including a second metal in the design of such heterobimetallic Schiff base derived precatalysts, and also the first such report demonstrating the application of Schiff base derived rhodium precatalysts for the hydroformylation of higher internal alkenes of the post-metathesis type, to the best of the author's knowledge. Unprecedented activities are found for the class of

Schiff base derived rhodium precatalysts in hydroformylation, performing significantly better at lower catalyst loadings as compared to the investigated commercial catalyst systems.

(iv) It is demonstrated for the first time that the Schiff base derived monometallic and heterobimetallic precatalysts have the potential to be re-used over multiple reaction cycles with overall increase in total cumulative product turnovers (Chapter 6), thus enabling potential recycling strategies and re-use of these types of catalyst systems in the industrial context.

(v) A detailed reaction engineering kinetics evaluation of the model reaction using the heterobimetallic Schiff base derived rhodium-ferrocene precatalyst is presented (Chapter 7). A phenomenological mechanism-derived rate model is successfully applied and found to describe the influence of the different operating conditions on the reaction rate, the first such report using a heterobimetallic Schiff base derived rhodium precatalyst for the hydroformylation, to the best of the author's knowledge. The rate model is capable of accurately predicting the product-distribution trajectories over a wide alkene conversion and operating condition range.

(vi) Overall, the above contributions represent significant advancement made within the overall scope of the RSA Olefins programme for the upgrading of low-value α-alkene-containing streams to higher value surfactant range products in the South African context.

References

Börner, A. and Franke, R. 2016. Hydroformylation: Fundamentals, processes, and applications in organic dynthesis. Wiley-VCH.

Chaudhari, R. 2012. Homogeneous catalytic carbonylation and hydroformylation for synthesis of industrial chemicals. Topics in Catalysis. 55, 439-445.

Cornils, B. and Hermann, W. 2002. Applied homogeneous catalysis with organometallic compounds: a comprehensive handbook in three volumes. Wiley-VCH.

De Klerk, A. 2012. Fischer-Tropsch refining. John Wiley and Sons.

Dry, M. 2002. The Fischer–Tropsch process: 1950–2000. Catalysis Today. 7, 227-241.

Du Toit, J., Jordaan, M., Huijsmans, C., Jordaan, J., Van Sittert, C. and Vosloo, H. 2014. Improved metathesis lifetime: chelating pyridinyl-alcoholato ligands in the second generation Grubbs precatalyst. Molecules. 19, 5522-5537.

Du Toit, J., Van der Gryp, P., Loock, M., Tole, T., Marx, S., Jordaan, J. and Vosloo, H. 2016. Industrial viability of homogeneous olefin metathesis: Beneficiation of linear alpha olefins with the diphenyl-substituted pyridinyl alcoholato ruthenium carbene precatalyst. Catalysis Today. 275, 191-200.

Frey, G. 2014. 75 Years of oxo synthesis - The success story of a discovery at the OXEA site Ruhrchemie. Journal of Organometallic Chemistry. 754, 5-7.

Jordaan, M., Van Helden, P., Van Sittert, C. and Vosloo, H. 2006. Experimental and DFT investigation of the 1-octene metathesis reaction mechanism with the Grubbs 1 precatalyst. Journal of Molecular Catalysis A: Chemical. 254, 145-154.

Jordaan, M. and Vosloo, H. 2007. Ruthenium catalyst with a chelating pyridinyl-alcoholato ligand for application in linear alkene metathesis. Advanced Synthesis and Catalysis. 349, 184-192.

Mol, J. 2004. Industrial applications of olefin metathesis. Journal of Molecular Catalysis A: Chemical. 213, 39-45.

O'Lenick, A. 2001. Guerbet chemistry. Journal of Surfactants and Detergents. 4, 311-315.

Van der Gryp, P., Marx, S. and Vosloo, H. 2012. Experimental, DFT and kinetic study of 1-octene metathesis with Hoveyda-Grubbs second generation precatalyst. Journal of Molecular Catalysis A: Chemical. 355, 85-95.

Van Leeuwen, P. and Claver, C. (Eds.) 2002. Rhodium catalyzed hydroformylation (Vol. 22). Springer Science and Business Media.

Zoller, U. (Ed.) 2009. Handbook of detergents Part F: Production. CRC Press.

CHAPTER 2

LITERATURE STUDY

In this chapter, an overview of the relevant hydroformylation literature is presented. The chapter is divided into four sections, starting with Section 2.1 that briefly introduces the different transition metal catalysts used in hydroformylation. The hydroformylation mechanism is discussed in Section 2.2. Section 2.3 provides a state-of-the-art review of the rhodium-catalysed hydroformylation of internal alkenes. A review of kinetic modelling of the hydroformylation reaction using homogeneous rhodium-based catalysts is presented in Section 2.4.

2.1 Transition metals in hydroformylation

In principle, all transition metals can potentially catalyse the hydroformylation reaction, with the precondition that the metal atom is able to form the required metal carbonyl hydride complex $[HM(CO)_XL_Y]$, where M represents the transition metal and L represents one or more ligands (Franke et al., 2012). Hydroformylation processes are generally divided into either "modified" or "unmodified" processes. Modified hydroformylation process use ancillary organic ligands (L = phosphines, phosphites, etc.) to affect the desired activity and selectivity (regio- and chemo-) performance of the catalyst, whereas additional ancillary ligands are absent in the case of the unmodified process (L = CO) (Taddei and Mann, 2013).

Historically, the first industrial hydroformylation processes were catalysed using an unmodified cobalt complex. However, this catalyst was not very stable and necessitated the need for harsh reaction conditions (> 200 bar of syngas pressure) in order to avoid catalyst decomposition or deposition of metallic cobalt during the hydroformylation process (Van Leeuwen and Claver, 2002). A breakthrough in the field came when Wilkinson's group later introduced ligand-modified rhodium-based catalysts that were more active and selective under more mild reaction conditions as compared to the cobalt-based catalysts (Evans et al., 1968; Brown et al., 1970). These rhodium catalysts typically operate at low syngas pressures (20-60 bar) and temperatures ranging from 60-120°C. Other platinum-group metals, including ruthenium, palladium, iridium and osmium are less active in hydroformylation (Börner and Franke, 2016); the following order of activity of different metals has been found (in descending order):

$$Rh >> Co > Ru, Ir > Os > Pt > Pd >> Fe > Ni$$

The application of rhodium-based catalysts, especially, has therefore led to the widespread recognition of the hydroformylation reaction as a value-adding step in the chemical industry, accounting for approximately 70% of industrial hydroformylation capacity (Börner and Franke, 2016). For this reason, rhodium-based catalysts were considered exclusively for this investigation.

2.2 Hydroformylation mechanism

At the time of the discovery of the hydroformylation reaction by Roelen, the exact mechanistic details of the catalytic transformation were unknown. It was not until more than two decades later before a mechanism for the cobalt-catalysed hydroformylation reaction was proposed (Heck and Breslow, 1961). The rhodium-catalysed hydroformylation reaction follows the same fundamental mechanism, which is initiated via a dissociative pathway (**Figure 2.1**) (Evans et al., 1968; Brown and Wilkinson, 1970).

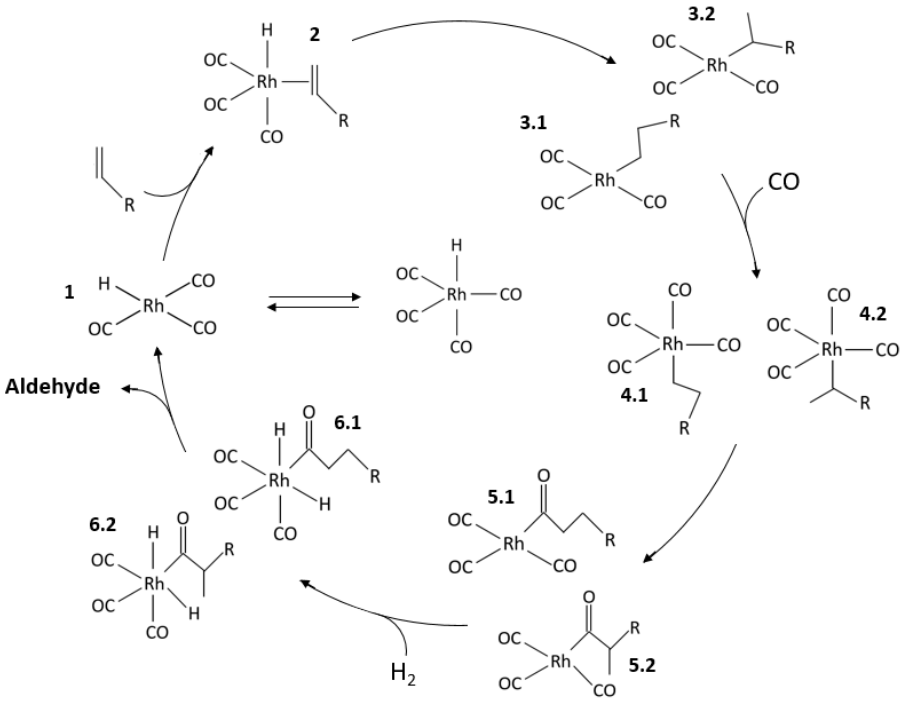

Figure 2.1: Reaction mechanism for rhodium-catalysed hydroformylation.

The mechanism begins with dissociation of a single carbonyl ligand from the metal-carbonyl hydride complex to yield the 16-electron, catalytically active metal-hydride complex **1**. This is followed by coordination of the alkene to a vacant site on the rhodium metal to yield the five-coordinated π-complex **2**. Regioselective migratory insertion of the alkene into the metal-hydride bond leads to the formation of either the linear (**3.1**) or branched (**3.2**) unsaturated rhodium alkyl species. Subsequent carbon monoxide coordination to the saturated alky species (**4.1** and **4.2**) and migratory insertion thereof yields corresponding acyl species (**5.1** and **5.2**). Oxidative dihydrogen addition to the acyl species yields **6.1** and **6.2**, which is followed by the irreversible reductive elimination of the aldehyde product and regeneration of the catalytically active rhodium-hydride complex **1**.

In general, it is widely accepted that the rate-determing step during hydroformylation will occur either at the i) coordination/insertion of the alkene to the carbonyl species **2** or ii) oxidative dihydrogen addition to the rhodium-acyl species **5**, as has been confirmed via several in situ spectroscopic studies (Van Rooy et al., 1995; Kamer et al., 2004; Zuidema et al., 2008). The relative rates of these reaction steps will depend on, among other factors, the ligand, the substrate and the operating conditions employed. For example, Van Rooy et al. (1995) showed that the rate determining step may vary for different substrates when employing the same catalyst, thus making general prediction of the rate-determining step for any given catalyst-substrate system challenging in the absence of sufficient system-specific rate data. The rate-determining step is expected to significantly influence the observed kinetic behaviour of the hydroformylation reaction for different catalyst-substrate systems; conversely observing the phenomenological response of the reaction rate to different operating conditions can often be rationalized based on the most plausible rate-determining step. Modelling of reaction kinetics with respect to mechanistic aspects of the hydroformylation reaction will be discussed in further detail in review of the kinetic modelling of the hydroformylation reaction (Section 2.4).

In addition to hydroformylation, alkene isomerisation and hydrogenation reactions may also proceed via the same catalyst under hydroformylation reaction conditions. Transition-metal-catalysed isomerisation, in general, can occur via one of two possible mechanisms, namely i) an alkyl mechanism involving consecutive metal-hydride addition-elimination reactions or ii) an allyl mechanism which proceeds via a π-allyl metal-hydride species (Vilches-Herrera et al., 2014). The possible isomerisation mechanisms are shown in **Figure 2.2**. The alkyl mechanism is the preferred isomerisation mechanism under hydroformylation conditions when employing rhodium-based catalysts, proceeding via the branched rhodium-alkyl species (**3.2**) (refer to **Figure 2.1**). The extent of hydrogenation of the alkene and aldehyde to corresponding alkane and alcohols, respectively, is usually minimal under hydroformylation conditions when employing rhodium-based catalysts.

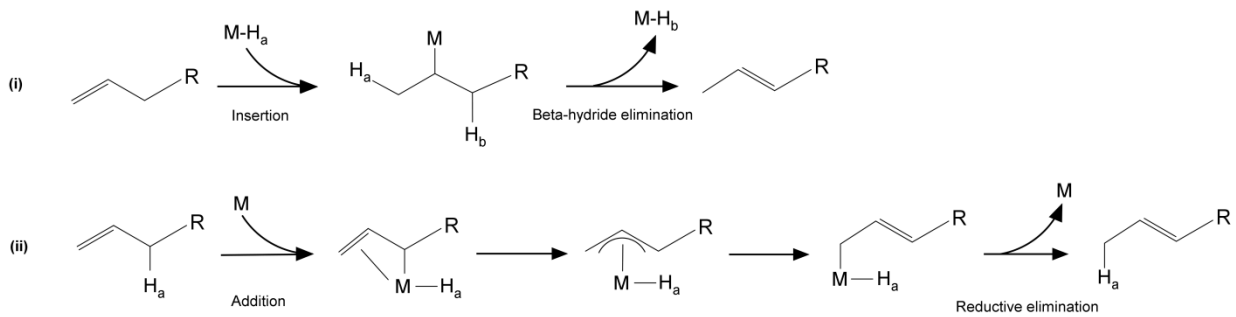

Figure 2.2: Isomerisation mechanisms using transition-metal complexes.

2.3 Review of rhodium-catalysed internal alkene hydroformylation

A wide range olefinic molecules, ranging from linear alkenes, dienes, functionalized alkenes, alkynes and even fatty acid compounds have been evaluated as substrates in the hydroformylation reaction (Franke et al., 2012). Commercially, the hydroformylation of unfunctionalized linear alkenes (propenes, butenes and higher alkenes) is however the most relevant. Although linear α-alkenes are the most frequently employed in industry, considerable research effort has also been devoted to the hydroformylation of linear internal alkenes due to the number of technically relevant olefinic streams that contain internal alkenes. These include, among others, Raffinates (mixtures of internal butenes or octenes derived from steam cracking processes), as well as Sasol's Fischer-Tropsch and Shell's Higher Olefins product streams (Van Leeuwen and Claver, 2002; Mol, 2004).

Principally, two different types of processes involving the hydroformylation of linear internal alkenes can be identified. The first type of process is the isomerisation-hydroformylation of internal alkenes, which is in line with the often important industrial imperative to produce linear aldehydes. A suitable catalyst for such a transformation is required to i) catalyse the isomerisation of the internal alkene to the terminal alkene, followed by ii) the selective activation of the terminal carbon atom once formed to produce the linear aldehyde (Carvajal et al., 2008). The isomerisation step, in this case, is especially challenging since isomerisation must overcome the greater thermodynamic preference for the internal double bond in order to reach the chain terminus. The second type of process involving the hydroformylation of internal alkenes is the branched-selective hydroformylation to corresponding branched aldehydes. The lower reactivity of the internal double bond as compared to the terminal bond makes this type of reaction quite challenging, since very few catalysts have been reported that will selectively discriminate and functionalize the internal double bond with high activity.

Several types of ligands have been evaluated together with rhodium within the scope of the above-described internal alkene hydroformylation processes. A summary of these different catalyst systems and their performances in the hydroformylation of internal alkenes is given in **Table 2.1**, and are discussed in more detail thereafter.

Table 2.1: Summary of internal alkene hydroformylation using rhodium-based catalysts.

Catalyst system	Alkene	Temp. (°C)	Press. (bar)	Sel.[a] (%)	Reference
Rh-Diphosphane	2-octene	120	2	90	(Van der Veen et al., 1999)
Rh-Triphenylphosphine	2-octene	120	2	46	
Rh-Diphosphane	4-octene	120	2	81	
Rh-Triphenyl phosphine	4-octene	120	2	23	
Rh/Ru – Phosphane-phosphite	2-butene	120	48	56	(Beller et al., 1999)
Rh-Phosphonite	1,2,3,4-octene	140	20	48	(Selent et al., 2000)
Rh-Phosphonite	1,2,3,4-octene	130	20	48	(Selent et al., 2001)
Rh-Diphosphite	1,2,3,4-octene	130	20	69	
Rh-Naphos	2-butene	120	10	91	(Klein et al., 2001)
Rh-Naphos	2-pentene	120	10	93	
Rh-Naphos	2-octene	120	10	91	
Rh-Naphos	4-octene	120	10	70	
Rh-Phosphabenzene	2-octene	90	10	76[b]	(Breit et al., 2001)
Rh-Pyrolylphosphane	2-pentene	120	25	33	(Jackstell et al., 2001)
Rh-Indolylphosphane	2-pentene	120	25	27	
Rh-Carbozolylphosphane	2-pentene	120	25	37	
Rh-TPPTS	7-tetradecene	100	100	77[b]	(Haumann et al., 2002)
Rh-Pyrolylamidite	2-octene	120	5	50	(Van der Slot et al., 2002)
Rh-Xantphos type	2-octene	120	3.6	89	(Bronger et al., 2003)
Rh-Biphephos	4-octene	125	20	89	(Behr et al., 2003)
Rh-Biphephos	2-pentene	100	30	99	(Vogl et al., 2005)
Rh-Tetraphosphoramidite	2-hexene	100	10	99	(Yan et al., 2006)
Rh-Tetraphosphoramidite	2-octene	100	10	98	
Rh-Phosphabarrelene	2-octene	70	10	98[b]	(Fuchs et al., 2006)
Rh-Phosphabenzene	2-octene	70	10	90[b]	
Rh-Triarylphosphite	2-octene	70	10	97[b]	
Rh-Triphenylphosphine	2-octene	70	10	95[b]	

[a]Selectivity for linear aldehydes, unless otherwise specified. [b]Selectivity for branched aldehydes.

Table 2.1: Summary of internal alkene hydroformylation using rhodium-based catalysts (continued).

Catalyst system	Alkene	Temp. (°C)	Press. (bar)	Sel.[a] (%)	Reference
Rh-(Meta-pyridyl)	2-octene	40	20	99[b]	(Kuil et al., 2006)
Rh-(Meta-pyridyl)	3-octene	40	20	99[b]	
Rh-(Meta-pyridyl)-Zn-tpp	2-octene	40	20	97[b]	
Rh-(Meta-pyridyl)-Zn-tpp	3-octene	40	20	97[b]	
Rh-Tetraphosphoramidite	2-octene	100	10	99	(Yu et al., 2008)
Rh-Diphosphite	1,2,3,4-octene	100	50	70	(Selent et al., 2011)
Rh-Biphephos	1,2,3,4-octene	100	50	93	
Rh-Dipyridyl-bis-Zn(II)(salphen)	3-hexene	25	20	-	(Gadzikwa et al., 2012)
Rh-Dipyridyl-bis-Zn(II)(salphen)	2-heptene	25	20	-	
Rh-Dipyridyl-bis-Zn(II)(salphen)	2-octene	25	20	-	
Rh-Dipyridyl-bis-Zn(II)(salphen)	2-nonene	25	20	-	
Rh-Triphosphoramidite	2-octene	100	10	98	(Chen et al., 2013)
Rh-Triphenylphosphite	2-decene	120	5	41	(Yuki et al., 2013)
Rh-Triphenylphosphine	2-decene	120	5	44	
Rh-Xantphos	2-decene	120	5	57	
Rh-Bisbi	2-decene	120	5	29	
Rh-Biphosphite	2-decene	120	5	95	
Rh-Biphosphite	2-octene	120	5	96	
Rh-Biphosphite	4-octene	120	5	94	
Rh-Biphosphite	2-tridecene	120	5	92	

[a]Selectivity for linear aldehydes, unless otherwise specified. [b]Selectivity for branched aldehydes.

2.3.1 Phosphine-modified catalysts

Phosphines are employed frequently as ligands in hydroformylation. Wilkson's group were the first to report that phosphine-modified rhodium carbonyl complexes resulted in active alkene hydroformylation catalysts under more mild conditions as compared to analogous cobalt carbonyl complexes (Evans et al., 1968; Brown and Wilkinson, 1970; Brown and Kent, 1987). Today, several phosphine ligands are commercially available as a quite inexpensive and air-stable ligand and find application in a variety of important industrial hydroformylation processes (Cornils and Hermann, 2002).

Van Leeuwen and co-workers (Van der Veen, et al., 1999) first demonstrated the successful application of homogeneous phosphine-modified rhodium catalysts for the hydroformylation of internal alkenes using dibenzophospholyl-(**1a**) and phenoxaphosphanyl (**1b**)-substituted diphosphine ligands of the Xantphos-type (**Figure 2.3**). Excellent n-regioselectivity toward the linear aldehyde product nonanal (90%) was observed for the hydroformylation of 2-octene. Bronger et al. (2003) later developed similar Xantphos-type phenoxaphosphanyl diphosphines (**2**), which show slightly improved n-regioselectivity performance (96%). Klein et al. (2001) also reported on the application of Naphos-type diphosphines bearing strong electron-withdrawing fluorinated substituent groups (**3b-d**) for the hydroformylation of 2-butene, 2-pentene, 2-octene and 4-octene, with n-regioselectivities of 91%, 93%, 91% and 70%, respectively.

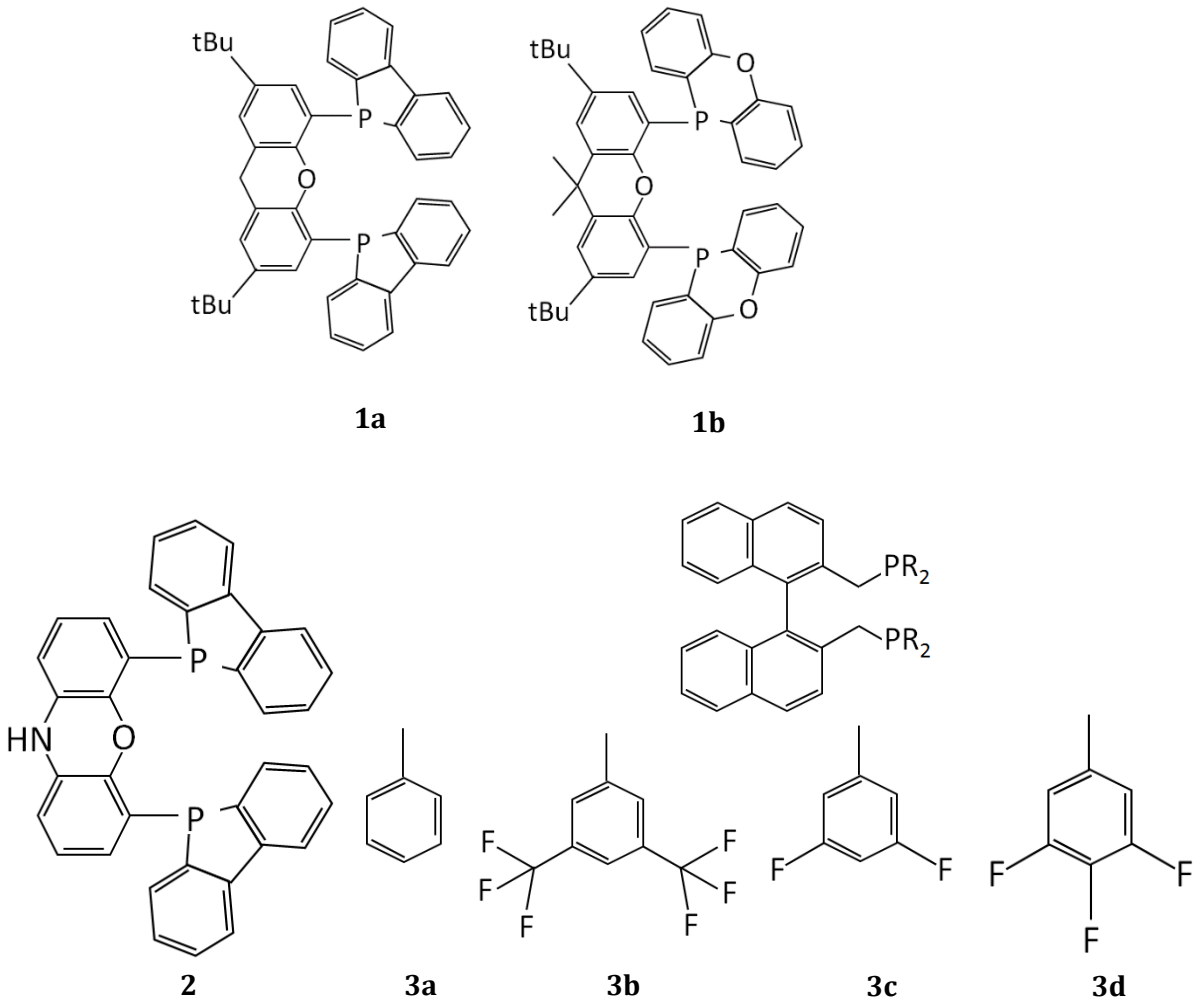

Figure 2.3: Diphosphine ligands evaluated for internal alkene hydroformylation.

Phosphabenzene ligands (**4**) (otherwise referred to as phosphinines) developed by Breit and co-workers (Breit et al., 2001), on the other hand, form very small amounts of linear aldehydes during the hydroformylation of internal alkenes, such as 2-octene (**Figure 2.4**). More reactive phosphabarrelene cages (**5**) based on the parent phosphabenzene ligand were later developed, yielding almost exclusively the corresponding branched aldehydes 2-methyloctanal (57.6%) and 2-ethylheptanal (35.7%) (Fuchs et al., 2006). Encapsulated rhodium catalysts based on the self-assembly of tris(meta-pyridyl)phosphine (**6**) and zinc(II) tetraphenylporphyrin (**7**) also show potential as branched-selective hydroformylation catalysts (Kuil et al., 2006). High branched selectivites were recorded in the hydroformylation of 2-octene (88% 2-ethylheptanal) and 3-octene (75% 2-propylhexanal). These self-assembling catalyst structures have also been employed for the combined regio- and stereo-selective hydroformylation of internal alkenes to yield entaniopure aldehydes (Gadzikwa et al., 2012).

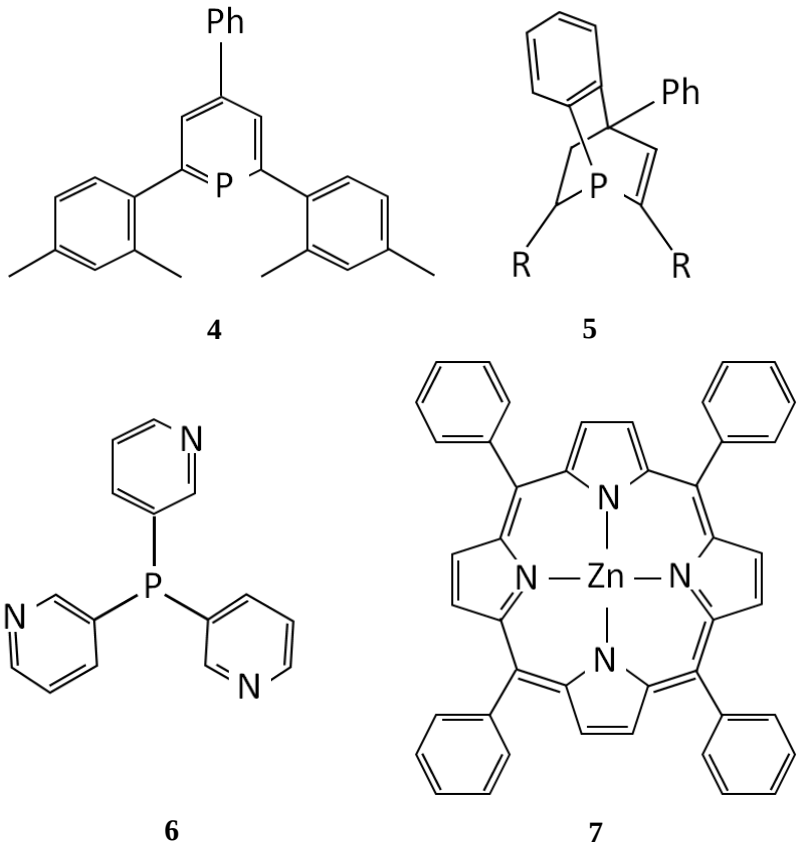

Figure 2.4: Phosphine derivative ligands evaluated for internal alkene hydroformylation.

Pyrrolyl- (**8, 11**), indolyl- (**9**) and carbazaolylphosphane (**10**) ligand systems (**Figure 2.5**) represent another interesting class of phosphine derivative (Jackstell et al. 2001; Van der Slot et al. 2002). However, these generally show quite low activity and n-regioselectivity performance in the hydroformylation reaction of internal alkenes. Poor selectivity and activity using pyrrolyl-based ligands was subsequently resolved in a later study by Yan et al. (2006) through the preparation of the tetraphosphorus ligand (**12a**) (**Figure 2.6**). The reason for this improvement was suggested to be due to the enhancement in chelating ability through multiple possible chelating modes of the tetraphosphorus ligand and hence an overall increase in the local phosphorus concentration at the metal centre. Thus, greater than 98% n-regioselectivity was observed for the hydroformylation of 2-octene. Varying substituents at the 3,3',5,5' positions of the biphenyl backbone (**12b-d**) could be employed to tailor the catalyst performance (Yu et al., 2008). In a more recent study, the application of a triphosphoramidite-modified system (**13**) was reported with high n-regioselectivity and activity in the hydroformylation of 2-octene (Chen et al., 2013).

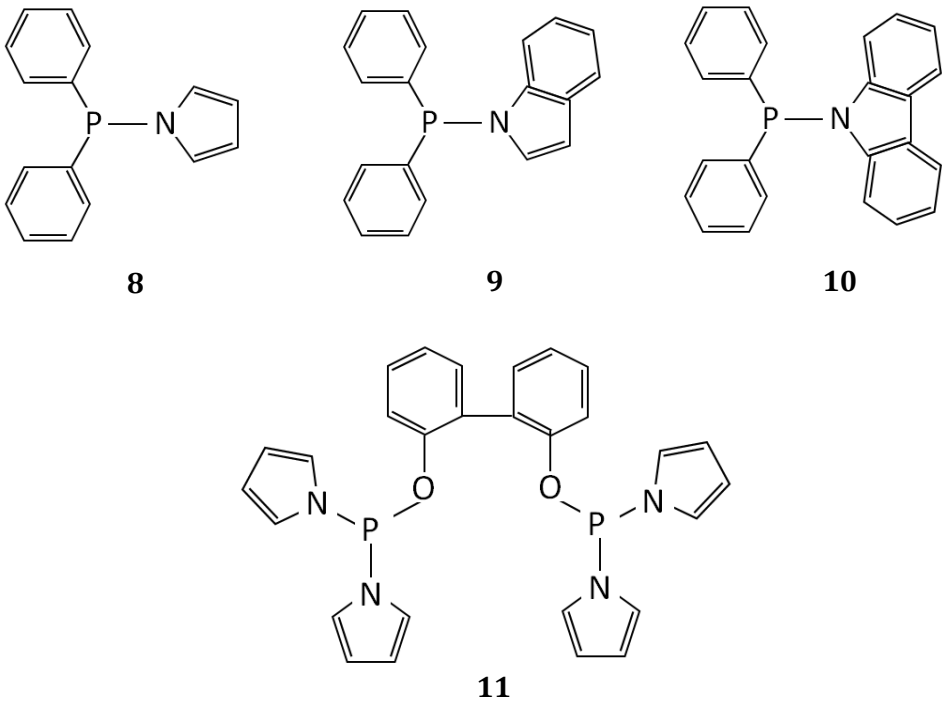

8 **9** **10**

11

Figure 2.5: Pyrrolyl-, indolyl- and carbazolylphosphane ligands evaluated for internal alkene hydroformylation.

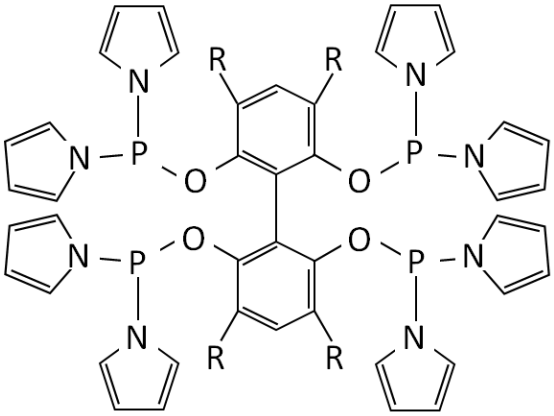

12a: R = H **12b:** R = methyl

12c: R = ethyl **12d:** R = phenyl

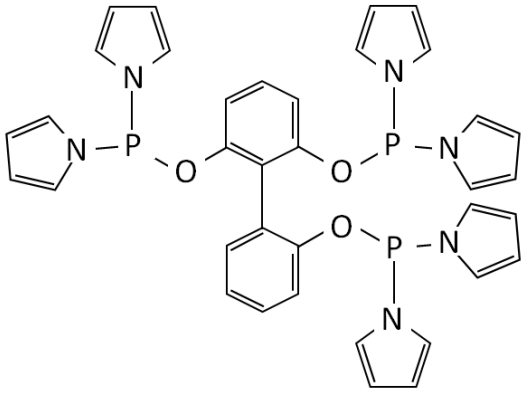

13

Figure 2.6: Tri- and tetra-pyrrolyl ligands evaluated for internal alkene hydroformylation.

To the best of the author's knowledge, only Haumann et al. (2002) previously evaluated the hydroformylation of any higher internal alkene of the post-metathesis-type. They used a water-soluble phosphine-rhodium catalyst (Rh-TPPTS) (**14**) (**Figure 2.7**) in an aqueous microemulsion. As a model reaction scheme, as is the focus of the present study, the hydroformylation of 7-tetradecene was considered in their investigation. Moderate to high activity was observed under harsh temperature and pressure conditions, with 77% selectivity achieved in favour of targeted aldehyde product 2-hexylnonanal.

14

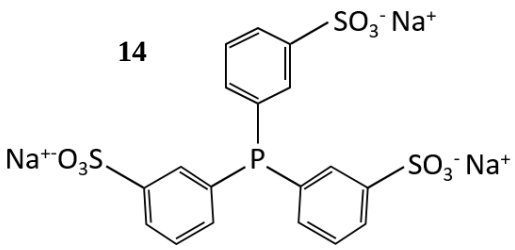

Figure 2.7: Water-soluble phosphine ligand for 7-tetradecene hydroformylation.

Even though Haumann and co-workers were successful in evaluating the rhodium-catalysed hydroformylation of 7-tetradecene using a water-soluble catalyst, there are still some major drawbacks, such as poor mass transfer and low reaction rates, which inhibit industrial-scale application of such biphasic processes for the hydroformylation of higher alkenes (Sharma and Jasra, 2015). Therefore, homogeneous catalyst systems are usually preferred because of the higher activity and better selectivity afforded by homogeneous catalysts, especially for the hydroformylation of higher alkenes.

2.3.2 Phosphite-modified catalysts

Much progress has been made using phosphite ligands for the rhodium-catalysed hydroformylation reaction. The use of phosphites ligands was first reported in the 1960s by Pruett and Smith (1967) and later expanded by Van Leeuwen's group (Van Leeuwen and Roobeek, 1983; Jongsma et al., 1991; Van Rooy et al., 1995; Van Rooy et al., 1996). Especially phosphite ligands with electron-withdrawing and bulky substituents at the ortho and para positions of the aryl rings give the most active hydroformylation catalysts. Due to strong π-electron acceptor properties, high activities are obtained for the hydroformylation of otherwise unreactive substrates when employing bulky phosphite ligands.

Selent et al. (2000) reported the use of phosphonite ligands (**15a-b**) (**Figure 2.8**) for the hydroformylation of a mixture of internal octenes. These catalyst systems were very active but formed low amounts of the linear aldehyde (48%). Modification with unsymmetrical diphosphites bearing acylphosphite moieties (**16a-f**) also yield very active hydroformylation catalysts; n-regioselectivity performance being slightly improved (up to 69%) when applied to the same internal octene mixture (Selent et al., 2001).

Behr et al. (2003) and Vogl et al. (2005) both investigated the performance of the commercially available diphosphite ligand, Biphephos (**17**). 2-Hexene hydroformylation gives almost exclusively the linear aldehyde (99%) when employing Rh-Biphephos as the catalyst. A series of diphosphites (**18a-c**) with structural resemblance to **17**, i.e. bearing typical 2,2'-dihydroxy-1,1'-biphenyl backbones, were later introduced (Selent et al., 2011). Up to 76% n-selectivity to nonanal was recorded for a mixture of internal octenes. In another reaction, 2-pentene was hydroformylated to hexanal with 99% selectivity.

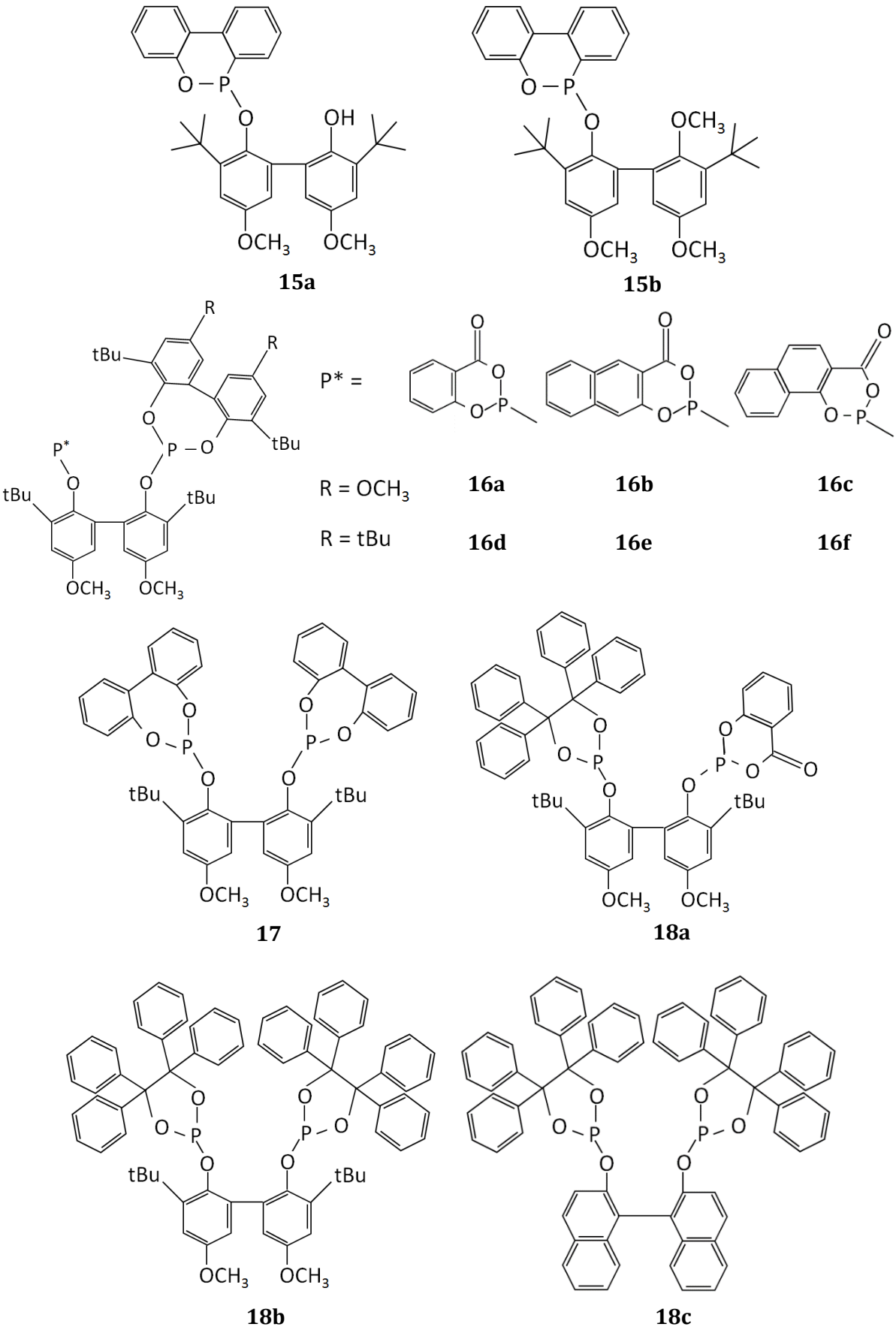

Figure 2.8: Phosphite ligands evaluated for internal alkene hydroformylation.

2.3.3 Bimetallic catalysts

Bimetallic complexes (complexes containing two metals) are becoming increasingly popular in terms of their applications for catalysing chemical transformations (Park and Hong, 2012; Van der Vlugt, 2012; Timerbulatova et al., 2013). This increased popularity is due to the realization of potential 'synergistic' interactions between two proximal metals that may lead to improved catalytic activity as compared to conventional monometallic analogues.

In general, bimetallic complexes can be classified according to the identities of the two metals: homobimetallic complexes contain two identical metals, while heterobimetallic complexes contain two different metals (Bratko and Gómez, 2013). Heterobimetallic complexes can potentially offer a more diverse application as a catalyst, whereby each metal is responsible for performing a different function. For example, one of the metals can act as the catalytically active site, while the second metal may be responsible for increasing or decreasing the electron density around the active metal during the catalytic cycle (Van den Beuken and Feringa, 1998). Alternatively, both metal sites may participate in the reaction leading to the desired product that would otherwise not be accessible using the monometallic catalyst system alone. Overall, both strategies could potentially lead to more active and selective catalyst systems.

Very few heterobimetallic systems have been evaluated as internal alkene hydroformylation catalysts. Beller et al. (1999) evaluated the hydroformylation of 2-butene using a phosphane-phosphite ligand (**19**) of the Binaphos-type (**Figure 2.9**) together with Ru_3CO_{12} as an isomerisation catalyst. Remarkably, the addition of the ruthenium-based complex resulted in improved n-regioselectivity and five-fold enhancement in the activity as compared to the rhodium-based monometallic catalyst. More recently, Yuki et al. (2013) proposed a dual rhodium-ruthenium catalyst system based on the combination of the rhodium-biphosphite (**20**) and Shvo's ruthenium-based catalyst (**21**). For the hydroformylation of 2-tridecene, near complete chemoselectivity to the linear alcohol was achieved, with n-regioselectivity (with respect to alcohols) of around 83%.

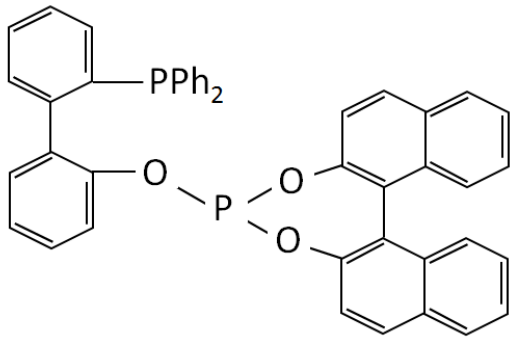

19

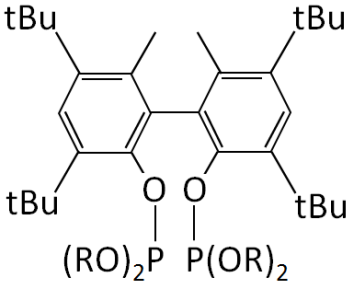

20

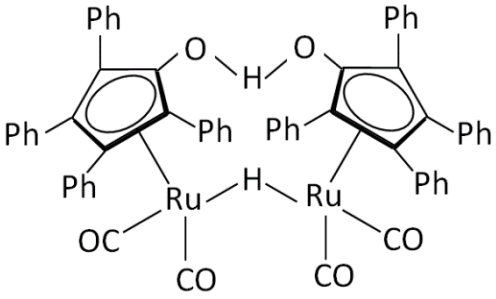

21

Figure 2.9: Bimetallic catalyst-ligand systems evaluated for internal alkene hydroformylation.

Metallocenes constitute another very important class of organometallic compound. Due to the synthetic versatility, redox activity and electron transfer ability of ferrocene especially, organometallic compounds containing ferrocene units have become particularly prominent in catalysis (Atkinson et al., 2004). Apart from the ability to fine-tune the catalytic behaviour of the catalyst complex by means of the ferrocene unit, the inherent air and thermal stability associated with ferrocene is also very attractive in terms of catalyst design (Larik et al., 2016).

A number of rhodium-ferrocene complexes have been reported as heterobimetallic precatalysts for hydroformylation (Lally et al., 2000; Hierso et al., 2004; Trzeciak et al., 2005; Peng et al., 2008; Kühnert et al., 2008; Bebbington et al., 2010; Madalska et al., 2014; Stockmann et al., 2014). These rhodium-ferrocene catalyst systems predominantly make use of phosphorus donor sites in order to affect the desired electronic and steric modification by the ferrocene unit. Very little is documented on hydroformylation catalysts containing metallocene groups other than ferrocene (Bianchini et al., 2005). An overview of rhodium-ferrocene complexes and their performances in the hydroformylation reaction is summarized in **Table 2.2**. In some cases,

an improvement in the catalytic performance of rhodium was observed by including the ferrocene unit to yield the heterobimetallic catalyst system.

More recently, a novel approach for designing heterobimetallic rhodium-ferrocene complexes bearing Schiff base derived N'O donor ligands was also reported and evaluated for hydroformylation (Siangwata et al.,2015; Siangwata et al., 2016) (**22** and **23**) (**Figure 2.10**). These Schiff base derived N'O ligands form part of a larger group of ligands termed 'hemilabile' or 'chelating' ligands, i.e. that contain two electronically different donor atom groups, thus facilitating opening/closing of a vacant site on the metal through temporary release/coordination of the more weakly bound donor atom (Braunstein et al., 2001). This property is often attributed to better stabilization of the active catalytic intermediates and potentially improved catalytic activity performance (Braunstein et al., 2001). In this regard, the reported Schiff base derived chelate complexes were shown to be very active in the hydroformylation reaction with high conversions (>99%) of 1-octene and show a preference towards forming branched aldehydes (Siangwata et al.,2015; Siangwata et al., 2016). In general, these types of Schiff base derived metal complexes demonstrate excellent thermal stability under high temperature conditions and are stable in the presence of air and moisture (Gupta and Sutar, 2008); thus making the potential application of this family of compounds very attractive as hydroformylation precatalysts in an industrial context.

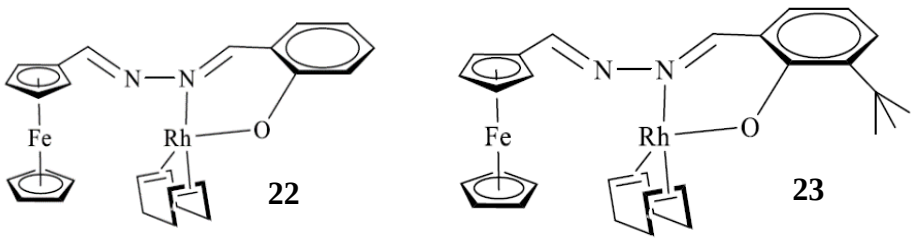

Figure 2.10: Novel series of heterobimetallic rhodium-ferrocene precatalysts bearing Schiff base derived N'O chelate ligands.

Table 2.2: Summary of hydroformylation using heterobimetallic rhodium-ferrocene precatalysts.

Catalyst system	Alkene	Temperature (°C)	Pressure (bar)	Conversion (%)	Selectivity[a] (%)	Reference
Rh-(Ferroncenyl-1-phosphonite- 1'-phosphine)	1-octene	80	10	30	52	Lally et al. (2000)
Rh-(Phosphine-menthyl-phosphonite ferrocenediyl)	1-octene	-	-	100	80	Hierso et al. (2004)
Rh-(1'-Diphenylphosphino ferrocene-carboxylic acid)	1-hexene	80	10	100	71	Trzeciak et al. (2005)
Rh-(Ferrocenyl bidentate phosphonite)	Vinyl acetate	60	40	64	93[b]	Peng et al. (2008)
Rh-(Ferrocenyl bidentate phosphonite)	Styrene	60	40	83	92[b]	Peng et al. (2008)
Rh-(Ph_2P - 1,1' ferrocenyl-$BMes_2$)	1-octene	90	40	100	72	Bebbington et al. (2010)
Rh-(1-(1,3,2-Dioxaphosphorinan-2-yl)-2-N,N-dimethylaminomethyl ferrocene)	Methyl acrylate	50	20	~100	-	Stockmann et al. (2014)
Rh-[Fe(1-PPh_2(thienylene)-2-$NMe_2CH_2C_5H_3$)(C_5H_5)]	1-hexene	50	50	-	64	Madalska et al. (2014)
Rh-(N,O-bidentate ferrocenyl)	1-octene	95	40	>99.9	43	Siangwata et al. (2016)

[a]Selectivity for linear aldehydes. [b]Enateoselectivity.

2.4 Review of kinetic modelling of the hydroformylation reaction

Kinetic modelling of homogeneous catalytic reactions forms an integral part of understanding the rate behaviour of such reaction systems and in some instances, insight into the reaction mechanism can also be gained through study of the reaction kinetcs (Chaudhari et al., 2001). While extensive study of the catalysis and product distribution/selectivity aspects in hydroformylation reactions has been reported in general, a relatively lesser amount of literature deals with the kinetic modelling aspect of the homogeneously catalysed hydroformylation reaction. An overview of some of the different kinetic models using homogeneous rhodium-based catalysts is summarised in **Table 2.3**. Excellent reviews on the topic of the kinetics of the hydroformylation reaction, and homogeneous catalytic reactions in general, are also available (Chaudhari et al., 2001; Van Leeuwen and Claver, 2002; Cornils and Hermann, 2002).

Kinetic modelling studies were reported for a variety of substrates, including linear (Deshpande and Chaudhari, 1988; Bhanage et al., 1997; Deshpande et al., 1998; Kiss et al., 1999; Srivastava et al., 2005; Rosales et al., 2007; Rosales et al., 2007; Bernas et al., 2008; Rosales et al., 2008; Rush et al., 2008; Salmi et al., 2009; Murzin et al., 2012; Rosales et al., 2016; Li et al., 2017), substituted (Deshpande et al., 1989; Deshpande et al., 1989; Nair et al., 1999; Bergounhou et al., 2004; Carilho et al., 2012) and cyclic alkenes (Güven et al., 2014). These kinetic models can be classified as either empirical- or mechanism-based. Empirical-based rate equations usually follow a power law expression as a function of the different operating conditions (catalyst, alkene, carbon monoxide and hydrogen concentrations) affecting the overall reaction rate. However, these empirical models do not provide much of a mechanistic understanding of the reaction conditions affecting the overall reaction rate (Chaudhari et al., 2001). Therefore, mechanism-based rate equation models derived from the most plausible rate-determining step in the hydroformylation reaction mechanism (aspects concerning the hydroformylation mechanism were discussed in Section 2.2) is becoming a more common approach for modelling the kinetics of the hydroformylation reaction.

In general, describing the kinetics of the hydroformylation reaction using a mechanism-based rate model can be simplified to fit one of two classical cases depending on the rate-determining step. The first case is consistent with a rate-determining step that occurs early in the mechanistic cycle, leading to a first-order dependence of the overall reaction rate with respect to the substrate and hydrogen independence (referred to as Type I kinetics):

$$\text{rate} = \frac{\text{k[Rh][Alkene]}}{1 + \text{K[CO]}} \quad \text{(Type I kinetics)}$$

Either the alkene insertion or coordination step determines the rate in this case, although it still remains unclear as to which of these is the true rate-determining step (Zuidema et al., 2008). In terms of mechanistic rate-model development, however, the resulting rate equation is independent of whether alkene insertion or coordination is rate-determining, as both assume a first-order dependence in the alkene during model derivation.

On the other hand, the second classical case for describing the kinetics of the hydroformylation reaction using a mecahism-based rate model is consistent with oxidative dihydrogen addition of the rhodium-acyl species as the rate-determining step, which leads to independence of the overall reaction rate with respect to the substrate, but first-order dependence in hydrogen (referred to as Type II kinetics) (Zuidema et al., 2008):

$$\text{rate} = \frac{\text{k[Rh][H}_2\text{]}}{\text{[CO]}} \quad \text{(Type II kinetics)}$$

As an 'extension' of the classical Type II kinetic behaviour, treating alkene insertion/coordination as a rate-contributing pre-equilibrium step prior to the dihydrogen addition step leads to a more complex rate expression with first-order dependence in both the alkene and hydrogen expected (Shahuran et al., 2010):

$$\text{rate} = \frac{\text{k[Rh][alkene][H}_2\text{][CO]}}{1 + \text{K[CO]}} \quad \text{(Type II kinetics extension)}$$

The rate of hydroformylation is usually inhibited by carbon monoxide, in accordance with the pre-equilibrium carbon monoxide dissociative step to form the active catalyst, as well as due to the formation of inactive saturated rhodium-acyl species at high carbon monoxide pressures (not necessarilyl accounted for by the rate model).

Almost all of the reviewed mechanism-based models show characteristics of these different classical cases; the exact form of the rate equation often depending on the treatment of the equilibria between different species involved in the mechanism and the assumptions made in order to simplify development of the resulting rate equation. Moreover, mechanism-based rate modelling studies reported thus far in the literature using homogeneous rhodium-based catalysts focus on the hydroformylation of lower alkenes (< C_{10}), while none have been reported for the hydroformylation of higher (internal) alkenes of the post-metathesis type, to the best of the author's knowledge.

Table 2.3: Summary of kinetic modelling of the hydroformylation reaction using homogeneous rhodium-based catalyst.

Alkene	Ligand (Solvent)	Temp. (°C)	P_{H2} (bar)	P_{CO} (bar)	C_{Alkene} (M)	C_{Rh} (mM)	Rate model	Reference
Linear alkenes								
Ethene	Triphenylphosphine (Toluene)	60-80	4.1-27.6	4.1-27.6	-	0.5-4.0	$\frac{k[Alkene][CO][H_2]^{1.5}}{(1+K_1[CO])^2(1+K_2[Alkene])^2}$	Deshpande et al. (1998)
	Triphenylphosphine (Tetraglyme)	80-110	2.9-7.5	0.1-5.6	-	0.1-0.9	$\frac{k\frac{[Alkene]}{[L]}}{1+K_1\frac{[CO]}{[L]}+K_2\frac{[L]}{[CO]}}$	Kiss et al. (1999)
Propene	Cyclohexyl diphenylphosphine (2,2,4-Trimethyl-1,3 pentane-diol monoisobutyrate)	75-115	4.0-7.5	4.0-7.5	-	0.2-1.0	$\frac{k[H_2][CO][RH][Alkene]}{L^x}$	Bernas et al. (2008)
	Triphenylphosphine (2,2,4-Trimethyl-1,3 pentane-diol monoisobutyrate)	75-115	4.0-7.5	4.0-7.5	-	0.2-1.0	$\frac{k[H_2][CO][RH][Alkene]}{L^x}$	Bernas et al. (2008)
	2,2'-Bis[(1,1'-diphenyl-2,2'-diyl)-phos-phito]-3,3',5,5'-tetra-tert-butyl-1,1'-diphenyl (*p*-Xylene)	90	0.5-28	0.5-28	0.37-5.95	0.3	$\frac{kP_{H2}[Alkene]}{P_{H2}+K_1P_{H2}P_{CO}+K_2[Alkene]}$	Rush et al. (2008)
	Cyclohexyl diphenylphosphine (2,2,4-Trimethyl-1,3-pentanediol monoisobutyrate)	85-115	0.5-7.5	0.5-7.5	-	0.9	$\frac{(kK_1+K_2[L]^{0.5})[Alkene][Rh][H_2][CO]}{1+K_3[L]^{0.5}+K_4[L]}$	Murzin et al. (2012)

Table 2.3: Summary of kinetic modelling of the hydroformylation reaction using homogeneous rhodium-based catalyst (continued).

Alkene	Ligand (Solvent)	Temp. (°C)	P_{H2} (bar)	P_{CO} (bar)	C_{Alkene} (M)	C_{Rh} (mM)	Rate model	Reference
Linear alkenes (continued)								
1-Butene	Triphenylphosphine (2,2,4-Trimethyl-1,3 pentane-diol monoisobutyrate)	70-100	5.0-15.0	5.0-15.0	-	0.1-0.2	$\frac{k[Alkene][Rh]}{[L]^{\alpha}}$	Salmi et al. (2009)
	Triphenylphosphine (Valeraldehyde)	90-120	6.5-19.9	0.6-3.5	3.9-4.8	0.6-1.2	$\frac{kP_{H2}^{a}P_{CO}^{b}[Rh]^{c}[Alkene]^{d}}{\exp(P_{CO})}$	Li et al. (2017)
1-Hexene	Triphenylphosphine (Ethanol)	30-50	0.7-16.9	6.1-16.9	0.2-1.6	0.3-1.2	$\frac{k[H_2][CO][Alkene][Rh-Rh_c]}{(1+K_1[CO])^{2.5}(1+K_2[alkene])^{2.1}}$	Deshpande et al. (1988)
	Triphenylphosphine (Benzene)	60-100	5.0-30.0	2.0-25.0	0.3-1.9	0.05-0.5	$\frac{k[H_2]^{0.75}[CO][Rh]^{0.35}[Alkene]}{(1+K_1[CO]+K_2[Alkene])^{3}[Alkene]}$	Srivastava et al. (2005)
	1,2-Bis(diphenylphosphino)ethane (Toluene)	80	1.0-7.0	1.0-7.0	0.1-0.7	0.6-3.2	$\frac{kK_1K_2K_3[Rh][CO][Alkene]}{[CO]+K_1K_2[Alkene]}$	Rosales et al. (2007a)
	Triphenylphosphine (Toluene)	60	0.7-2.7	0.3-4.5	2.2-6.6	0.6-2.1	$\frac{kK_1K_2K_3[Rh][Alkene][H_2][CO]}{K_1[CO]^3[H_2]+K_1K_2K_3[Alkene][H_2]}$	Rosales et al. (2007b)

Table 2.3: Summary of kinetic modelling of the hydroformylation reaction using homogeneous rhodium-based catalyst (continued).

Alkene	Ligand (Solvent)	Temp. (°C)	P_{H2} (bar)	P_{CO} (bar)	C_{Alkene} (M)	C_{Rh} (mM)	Rate model	Reference
Linear alkenes (continued)								
1-Hexene	1,1,1-Tris(diphenylphosphinomethyl)ethane (Toluene)	80	1.4-5.5	1.4-5.5	0.2-0.6	1.7-3.4	$\frac{kK_1K_2K_3[Rh][CO][Alkene]}{1+K_1+K_1K_2[CO]+K_1K_3[Alkene]}$	Rosales et al. (2008)
	1,2-Bis(diphenylphosphino)ethane (1,4-Dioxane)	80-130	N/A (CH_2O)	N/A (CH_2O)	0.5-0.8	1.0-4.1	$\frac{k[Rh][Alkene][CH_2O]}{K_1+K_2[CH_2O]}$	Rosales et al. (2016)
1-Dodecene	Triphenylphosphine (Toluene)	50-70	6.8-17	1.7-20.4	0.2-2.2	1.0-8.0	$\frac{k[H_2][CO][catalyst][alkene]}{(1+K_1[CO])^2(1+K_2[alkene])}$	Bhanage et al. (1997)
Substituted alkenes								
Vinyl acetate	Triphenylphosphine (Ethanol)	50-70	13.6-34	3.4-34	0.5-2.9	0.3-1	$\frac{k[H_2][CO][Rh][Alkene]}{(1+K_1[CO])^3(1+K_2[Alkene])^2}$	Deshpande et al. (1989a)
Allyl alcohol	Triphenylphosphine (Ethanol)	60-80	13.6-38.5	3.5-40.8	0.4-0.7	1-4	$\frac{k[H_2]^{1.5}[CO][Rh][Alkene]}{(1+K_1[B])^3(1+K_2[Alkene])^2}$	Deshpande et al. (1989b)
Styrene	Triphenylphosphine (Toluene)	60-80	10.3-41.2	3.0-41.2	0.1-1.0	0.9-6.9	$\frac{kK_1K_2[H_2][CO][Rh][Alkene]}{1+K_1[CO]+K_1K_2[CO][alkene]+K_1K_2[CO][Alkene]+K_1K_2K_3[CO]^2[alkene]+K_1K_2K_3K_4[CO]^3[alkene]}$	Nair et al. (1999)

Table 2.3: Summary of kinetic modelling of the hydroformylation reaction using homogeneous rhodium-based catalyst (continued).

Alkene	Ligand (Solvent)	Temp. (°C)	P_{H2} (bar)	P_{CO} (bar)	C_{Alkene} (M)	C_{Rh} (mM)	Rate model	Reference
Substituted alkenes (continued)								
Styrene	1,2,5-Triphenyl-1H-phosphole (Toluene)	31-60	5-15	5-15	0.2-0.7	0.4-1.6	$\frac{k[H_2][Rh][Alkene]}{K_1(1+K_2[Ald]+K_3[CO])+[Alkene]\left(1+\frac{K_4+k[CO]}{K_5[CO]}+K_6[CO]\right)}$	Bergounhou et al. (2004)
Phenylpropene	Tris[(R)-20 -benzyloxy-1,10 -binaphthyl-2-yl]phosphite (Toluene)	50-90	10-30	10-25	0.03-0.3	0.2-0.6	$\frac{k[RH][Alkene][H_2]}{[CO]^{0.3}[L]^{0.3}}$	Carilho et al. (2012)
Cyclic alkenes								
Cyclohexene	Tris(2,4-ditertbutylphenyl)phosphite (Toluene)	60-80	22.5-45	15-25	2.24-3.35	0.18-0.36	$\frac{k[Rh][Alkene]}{1+KCO}$	Güven et al. (2014)

References

Atkinson, R., Gibson, V. and Long, N. 2004. The syntheses and catalytic applications of unsymmetrical ferrocene ligands. Chemical Society Reviews. 33, 313-328.

Bebbington, M., Bontemps, S., Bouhadir, G., Hanton, M., Tooze, R., van Rensburg, H. and Bourissou, D. 2010. A 1,1′-ferrocenyl phosphine-borane: synthesis, structure and evaluation in Rh-catalyzed hydroformylation. New Journal of Chemistry. 34, 1556-1559.

Behr, A., Obst, D., Schulte, C., and Schosser, T. 2003. Highly selective tandem isomerization–hydroformylation reaction of trans-4-octene to n-nonanal with rhodium-biphephos catalysis. Journal of Molecular Catalysis A: Chemical. 206, 179-184.

Beller, M., Zimmermann, B. and Geissler, H. 1999. Dual catalytic systems for consecutive isomerization–hydroformylation reactions. Chemistry-A European Journal. 5, 1301-1305.

Bergounhou, C., Neibecker, D. and Mathieu, R. 2004. Kinetics and mechanism of the hydroformylation of styrene catalysed by the rhodium/TPP system (TPP= 1, 2, 5-triphenyl-1H-phosphole). Journal of Molecular Catalysis A: Chemical. 220, 167-182.

Bernas, A., Maki-Arvela, P., Lehtonen, J., Salmi, T. and Murzin, D. 2008. Kinetic modeling of propene hydroformylation with Rh/TPP and RH/CHDPP catalysts. Industrial and Engineering Chemistry Research. 47, 4317-4324.

Bhanage, B., Divekar, S., Deshpande, R. and Chaudhari, R. 1997. Kinetics of hydroformylation of l-dodecene using homogeneous HRh(CO)(PPh3)3 catalyst. Journal of Molecular Catalysis A: Chemical. 115, 247-257.

Bianchini, C., Oberhauser, W., Orlandini, A., Giannelli, C. and Frediani, P. 2005. Operando high-pressure NMR and IR study of the hydroformylation of 1-hexene by 1,1‘-bis (diarylphosphino) metallocene-modified rhodium (I) catalysts. Organometallics. 24, 3692-3702.

Börner, A. and Franke, R. 2016. Hydroformylation: Fundamentals, processes, and applications in organic synthesis. Wiley-VCH.

Bratko, I. and Gómez, M. 2013. Polymetallic complexes linked to a single-frame ligand: cooperative effects in catalysis. Dalton Transactions. 42, 10664-10681.

Braunstein, P. and Naud, F. 2001. Hemilability of hybrid ligands and the coordination chemistry of oxazoline-based systems. Angewandte Chemie International Edition. 40, 680-699.

Breit, B., Winde, R., Mackewitz, T., Paciello, R. and Harms, K. 2001. Phosphabenzenes as monodentate π-acceptor ligands for rhodium-catalyzed hydroformylation. Chemistry - A European Journal. 7, 3106-3121.

Bronger, R., Kamer, P. and van Leeuwen, P. 2003. Influence of the bite angle on the hydroformylation of internal olefins to linear aldehydes. Organometallics. 22, 5358-5369.

Brown, C. and Wilkinson, G. 1970. Homogeneous hydroformylation of alkenes with hydridocarbonyltris-(triphenylphosphine) rhodium (I) as catalyst. Journal of the Chemical Society A: Inorganic, Physical, Theoretical. 2753-2764.

Brown, J. and Kent, A. 1987. Structural characterisation in solution of intermediates in rhodium-catalysed hydroformylation and their interconversion pathways. Journal of the Chemical Society, Perkin Transactions. 2, 1597-1607.

Carrilho, R., Neves, A., Lourenço, M., Abreu, A., Rosado, M., Abreu, P., Eusébio, M., Kollár, L., Bayón, J. and Pereira, M. 2012. Rhodium/tris-binaphthyl chiral monophosphite complexes: Efficient catalysts for the hydroformylation of disubstituted aryl olefins. Journal of Organometallic Chemistry. 698, 28-34.

Carvajal, M., Kozuch, S. and Shaik, S. 2009. Factors controlling the selective hydroformylation of internal alkenes to linear aldehydes. 1. The isomerization step. Organometallics. 28, 3656-3665.

Chaudhari, R., Seayad, A. and Jayasree, S. 2001. Kinetic modeling of homogeneous catalytic processes. Catalysis Today. 66, 371-380.

Chen, C., Qiao, Y., Geng, H. and Zhang, X. 2013. A novel triphosphoramidite ligand for highly regioselective linear hydroformylation of terminal and internal olefins. Organic Letters. 15, 1048-1051.

Cornils, B., and Hermmann, W. 2002. Applied homogeneous catalysis with organometallic compounds: A comprehensive handbook in three volumes. Wiley-VCH.

Deshpande, R. and Chaudhari, R. 1989. Hydroformylation of allyl alcohol using homogeneous HRh (CO)(PPh3)3 Catalyst: A kinetic study. Journal of Catalysis. 115, 326-336.

Deshpande, R. and Chaudhari, R. 1989. Hydroformylation of vinyl acetate using homogeneous HRh (CO)(PPh3) 3 catalyst: A kinetic study. Journal of Molecular Catalysis. 57, 177-191.

Deshpande, R. and Chaudhari, R. 1988. Kinetics of hydroformylation of 1-hexene using homogeneous HRh(CO)(PPh3) 3 complex catalyst. Industrial and Engineering Chemistry Research. 27, 1996-2002.

Deshpande, R., Bhanage, B.M.; Divekar, S., Kanagasabapathy, S., Chaudhari, R. 1998. Kinetics of hydroformylation of ethylene in a homogeneous medium: comparison in organic and aqueous systems. Industrial and Engineering Chemistry Research. 37, 2391–2396.

Evans, D., Osborn, J. and Wilkinson, G. 1968. Hydroformylation of alkenes by use of rhodium complex catalysts. Journal of the Chemical Society A: Inorganic, Physical, Theoretical. 11, 3133-3142.

Franke, R., Selent, D. and Börner, A. 2012. Applied hydroformylation. Chemical Reviews. 112, 5675-5732.

Fuchs, E., Keller, M., and Breit, B. 2006. Phosphabarrelenes as ligands in rhodium-catalyzed hydroformylation of internal alkenes essentially free of alkene isomerization. Chemistry - A European Journal. 12, 6930-6939.

Gadzikwa, T., Bellini, R., Dekker, H. and Reek, J. 2012. Self-assembly of a confined rhodium catalyst for asymmetric hydroformylation of unfunctionalized internal alkenes. Journal of the American Chemical Society. 134, 2860-2863.

Gupta, K. and Sutar, A. 2008. Catalytic activities of Schiff base transition metal complexes. Coordination Chemistry Reviews. 252, 1420-1450.

Güven, S., Hamers, B., Franke, R., Priske, M., Becker, M. and Vogt, D. 2014. Kinetics of cyclooctene hydroformylation for continuous homogeneous catalysis. Catalysis Science and Technology. 4, 524-530.

Haumann, M., Yildiz, H., Koch, H. and Schomacker, R. 2002. Hydroformylation of 7-tetradecene using Rh-TPPTS in a microemulsion. Applied Catalysis A: General. 236, 173-178.

Heck, R. and Breslow, D. 1961. The reaction of cobalt hydrotetracarbonyl with olefins. Journal of the American Chemical Society. 83 , 4023-4027.

Hierso, J., Lacassin, F., Broussier, R., Amardeil, R. and Meunier, P. 2004. Synthesis and characterisation of a new class of phosphine-phosphonite ferrocenediyl dinuclear rhodium complexes. Journal of Organometallic Chemistry. 689, 766-769.

Jackstell, R., Klein, H., Beller, M., Wiese, K. and Roettger, D. 2001. Synthesis of pyrrolyl-, indolyl-, and carbazolylphosphanes and their catalytic application as ligands in the hydroformylation of 2-pentene. European Journal of Organic Chemistry. 2001, 3871-3877.

Jongsma, T., Challa, G. and Van Leeuwen, P. 1991. A mechanistic study of rhodium tri(o-t-butylphenyl) phosphite complexes as hydroformylation catalysts. Journal of Organometallic Chemistry. 421, 121-128.

Kamer, P., van Rooy, A., Schoemaker, G. and van Leeuwen, P. 2004. In situ mechanistic studies in rhodium catalyzed hydroformylation of alkenes. Coordination Chemistry Reviews. 248, 2409-2424.

Kiss, G., Mozeleski, E., Nadler, K. VanDriessche, E. and DeRoover, C. 1999. Hydroformylation of ethene with triphenylphosphine modified rhodium catalyst: kinetic and mechanistic studies. Journal of Molecular Catalysis A: Chemical. 138, 155-176.

Klein, H., Jackstell, R., Wiese, K., Borgmann, C. and Beller, M. 2001. Highly selective catalyst systems for the hydroformylation of internal olefins to linear aldehydes. Angewandte Chemie International Edition. 40, 3408-3411.

Kühnert, J., Ecorchard, P. and Lang, H. 2008. Heterometallic transition-metal complexes based on 1-carboxy-1′-(diphenylphosphanyl) ferrocene,(tmeda/pmdta) zinc (II), and gold (I) units. European Journal of Inorganic Chemistry. 32, 5125-5137.

Kuil, M., Soltner, T., Van Leeuwen, P. and Reek, J. 2006. High-precision catalysts: regioselective hydroformylation of internal alkenes by encapsulated rhodium complexes. Journal of the American Chemical Society. 128, 11344-11345.

Lally, M., Broussier, R. and Gautheron, B. 2000. Ferrocene-based phosphonite–phosphine ligands, Pd and Rh complexes. Tetrahedron Letters. 41, 1183-1185.

Larik, F., Saeed, A., Fattah, T., Muqadar, U. and Channar, P. 2017. Recent advances in the synthesis, biological activities and various applications of ferrocene derivatives. Applied Organometallic Chemistry. 31, e3664.

Li, X., Zhang, K., Qin, L. and Ma, H. 2017. Kinetic studies of hydroformylation of 1-butene using homogeneous Rh/PPh3 complex catalyst. Molecular Catalysis. 443, 270-279.

Madalska, M., Lönnecke, P. and Hey-Hawkins, E. 2014. Aryl-based ferrocenyl phosphine ligands in the rhodium (I)-catalyzed hydroformylation of olefins. Journal of Molecular Catalysis A: Chemical. 383, 137-142.

Mol, J. 2004. Industrial applications of olefin metathesis. Journal of Molecular Catalysis A: Chemical. 213, 39-45.

Murzin, D., Bernas, A. and Salmi, T. 2012. Mechanistic model for kinetics of propene hydroformylation with Rh catalyst. AIChE Journal. 58, 2192-2201.

Nair, V., Mathew, S. and Chaudhari, R. 1999. Kinetics of hydroformylation of styrene using homogeneous rhodium complex catalyst. Journal of Molecular Catalysis A: Chemical. 143, 99-110.

Park, J. and Hong, S. 2012. Cooperative bimetallic catalysis in asymmetric transformations. Chemical Society Reviews. 41, 6931-6943.

Peng, X., Wang, Z., Xia, C. and Ding, K. 2008. Ferrocene-based bidentate phosphonite ligands for rhodium (I)-catalyzed enantioselective hydroformylation. Tetrahedron Letters. 49, 4862-4864.

Pruett, R. and Smith, J. 1969. Low-pressure system for producing normal aldehydes by hydroformylation of alpha-olefins. The Journal of Organic Chemistry. 34, 327-330.

Rosales, M., Chacon, G., Gonzalez, A., Pacheco, I., Baricelli, P. and Melean, L. 2008. Kinetics and mechanisms of homogeneous catalytic reactions Part 9. Hydroformylation of 1-hexene catalyzed by a rhodium system containing a tridentated phosphine. Journal of Molecular Catalysis A: Chemical. 287, 110-114.

Rosales, M., Durán, J., González, Á., Pacheco, I. and Sánchez-Delgado, R. 2007. Kinetics and mechanisms of homogeneous catalytic reactions: Part 7. Hydroformylation of 1-hexene catalyzed by cationic complexes of rhodium and iridium containing PPh3. Journal of Molecular Catalysis A: Chemical. 270, 250-256.

Rosales, M., Gonzalez, A., Guerrero, Y., Pacheco, I. and Sanchez-Delgado, R. 2007. Kinetics and mechanisms of homogeneous catalytic reactions Part 6. Hydroformylation of 1-hexene by use of

Rh(acac)(CO)2/dppe [dppe = 1,2-bis(diphenylphosphino)ethane] as the precatalyst. Journal of Molecular Catalysis A: Chemical. 270, 241-249.

Rosales, M., Pérez, H., Arrieta, F., Izquierdo, R., Moratinos, C. and Baricelli, P. 2016. Kinetics and mechanisms of homogeneous catalytic reactions. Part 14. Hydroformylation of 1-hexene with formaldehyde catalyzed by a cationic bis (diphosphine) rhodium complex. Journal of Molecular Catalysis A: Chemical. 421, 122-130.

Rush, S., Noskov, Y., Kron, T. and Korneeva, G. 2009. Kinetics and mechanism of propene hydroformylation catalyzed by rhodium complexes with a diphosphite ligand. Kinetics and Catalysis. 50, 557-566.

Salmi, T., Ahlkvist, J., Bernas, A., Warna, J., Makai-Arvela, P., Still, C., Lehtonen, J. and Murzin, D. 2009. Hydroformylation of 1-butene on Rh Catalyst. Industrial Engineering Chemistry Research. 48, 1325-1331.

Selent, D., Franke, R., Kubis, C., Spannenberg, A., Baumann, W., Kreidler, B. and Börner, A. 2011. A new diphosphite promoting highly regioselective rhodium-catalyzed hydroformylation. Organometallics. 30, 4509-4514.

Selent, D., Hess, D., Wiese, K., Rottger, D., Kunze, C. and Börner, A. 2001. New phosphorus ligands for the rhodium-catalyzed isomerization/hydroformylation of internal octenes. Angewandte Chemie International Edition. 40, 1696-1698.

Selent, D., Wiese, K.., Rottger, D., and Börner, A. 2000. Novel oxyfunctionalized phosphonite ligands for the hydroformylation of isomeric n-olefins. Angewandte Chemie International Edition. 39, 1639-1641.

Shaharun, B. Dutta, H. Mukhtar and S. Maitr. 2010. Hydroformylation of 1-octene using rhodium-phosphite catalyst in a thermomorphic solvent system. Chemical Engineering Science. 65, 273-281.

Sharma, S. and Jasra, R. 2015. Aqueous phase catalytic hydroformylation reactions of alkenes. Catalysis Today. 247, 70-81.

Siangwata, S., Baartzes, N., Makhubela, B. and Smith, G. 2015. Synthesis, characterisation and reactivity of water-soluble ferrocenylimine-Rh(I) complexes as aqueous-biphasic hydroformylation catalyst precursors. Journal of Organometallic Chemistry. 769, 26-32.

Siangwata, S., Chulu, S., Oliver, C. and Smith, G. 2016. Rhodium-catalysed hydroformylation of 1-octene using aryl and ferrocenyl Schiff base-derived ligands. Applied Organometallic Chemistry. 1-9.

Srivastava, V., Sharma, S., Shukla, R., Subrahmanyam, N. and Jasra, R. 2005. Kinetic studies on the hydroformylation of 1-hexene using RhCl (AsPh3)3 as a catalyst. Industrial and Engineering Chemistry Research. 44, 1764-1771.

Stockmann, S., Lönnecke, P., Bauer, S. and Hey-Hawkins, E. 2014. Heterobimetallic complexes with ferrocenyl-substituted phosphaheterocycles. Journal of Organometallic Chemistry. 751, 670-677.

Taddei, M. and Mann, A. 2013. Hydroformylation for organic synthesis. Wiley-VCH.

Timerbulatova, M., Gatus, M., Vuong, K., Bhadbhade, M., Algarra, A., Macgregor, S. and Messerle, B. 2013. Bimetallic complexes for enhancing catalyst efficiency: probing the relationship between activity and intermetallic distance. Organometallics. 32, 5071-5081.

Trzeciak, A., Štěpnička, P., Mieczyńska, E. and Ziółkowski, J. 2005. Rhodium (I) complexes with 1′-(diphenylphosphino) ferrocenecarboxylic acid as active and recyclable catalysts for 1-hexene hydroformylation. Journal of Organometallic Chemistry. 690, 3260-3267.

Van den Beuken, E. and Feringa, B. 1998. Bimetallic catalysis by late transition metal complexes. Tetrahedron. 54, 12985-13011.

Van der Slot, S., Duran, J., Luten, J., Kamer, P. and Van Leeuwen, P. 2002. Rhodium-catalyzed hydroformylation and deuterioformylation with pyrrolyl-based phosphorus amidite ligands: influence of electronic ligand properties. Organometallics. 21, 3873-3883.

Van der Veen, L., Kamer, P. and Van Leeuwen, P. 1999. Hydroformylation of internal olefins to linear aldehydes with novel rhodium catalysts. Angewandte Chemie International Edition. 38, 336-338.

Van der Vlugt, J. 2012. Cooperative catalysis with first-row late transition metals. European Journal of Inorganic Chemistry. 3, 363-375.

Van Leeuwen, P. and Claver, C. (Eds.). 2002. Rhodium catalyzed hydroformylation (Vol. 22). Springer Science & Business Media.

Van Leeuwen, P. and Roobeek, C. 1983. Hydroformylation of less reactive olefins with modified rhodium catalysts. Journal of Organometallic Chemistry. 258, 343-350.

Van Rooy, A., de Bruijn, J., Roobeek, K., Kamer, P. and Van Leeuwen, P. 1996. Rhodium-catalysed hydroformylation of branched 1-alkenes; bulky phosphite vs. triphenylphosphine as modifying ligand. Journal of Organometallic Chemistry. 507, 69-73.

Van Rooy, A., Orij, E., Kamer, P. and van Leeuwen, P. 1995. Hydroformylation with a rhodium/bulky phosphite modified catalyst. A comparison of the catalyst behavior for Oct-1-ene, Cyclohexene, and Styrene. Organometallics. 14, 34-43.

Vilches-Herrera, M., Domke, L. and Börner, A. 2014. Isomerization-hydroformylation tandem reactions. ACS Catalysis. 4, 1706-1724.

Vogl, C., Paetzold, E., Fischer, C. and Kragl, U. 2005. Highly selective hydroformylation of internal and terminal olefins to terminal aldehydes using a rhodium-biphephos-catalyst system. Journal of Molecular Catalysis. A: Chemical. 232, 41-44.

Yan, Y., Zhang, X. and Zhang, X. 2006. A tetraphosphorus ligand for highly regioselective isomerization-hydroformylation of internal olefins. Journal of the American Chemical Society. 128, 16058-16061.

Yu, S., Chie, Y., Guan, Z. and Zhang, X. 2008. Highly regioselective isomerization-hydroformylation of internal olefins to linear aldehyde using rh complexes with tetraphosphorus ligands. Organic Letters. 10, 3469-3472.

Yuki, Y., Takahashi, K., Tanaka, Y. and Nozaki, K. 2013. Tandem isomerization/hydroformylation/hydrogenation of internal alkenes to n-alcohols using Rh/Ru dual- or ternary-catalyst systems. Journal of the American Chemical Society. 135, 17393-17400.

Zuidema, E., Escorihuela, L., Eichelsheim, T., Carbó, J., Bo, C., Kamer, P. and Van Leeuwen, P. 2008. The rate-determining step in the rhodium-xantphos-catalysed hydroformylation of 1-octene. Chemistry-A European Journal. 14, 1843-1853.

CHAPTER 3

EXPERIMENTAL

In this chapter, details of the materials, methods and procedures followed in the experimental component of this study are presented. The chapter is divided into two sections. Section 3.1 covers the details of the chemicals and catalyst materials used, as well as the synthesis details of 7-tetradecene. In Section 3.2, details on the hydroformylation experiments are provided, including standard apparatus, experimental methodology, analytical techniques and uncertainty analysis.

3.1 Materials

3.1.1 Catalysts used

Table 3.1 lists the commercially available rhodium catalyst precursor and phosphorus ligands used for the study. All components were used as is from the suppliers without further purification. The non-commercialized Schiff-base derived precatalysts were prepared as reported previously Siangwata et al. (2016), using standard reagents and procedures described therein.

Table 3.1: List of ligands and rhodium catalyst precursor used.

Chemical name	Purity	Supplier
Rhodium precursor		
(Acetylacetonato)dicarbonylrhodium(I)	98%	Sigma-Aldrich
Ligands		
Triphenylphosphine	99%	Sigma-Aldrich
Triphenylphosphite	97%	Sigma-Aldrich
Tris(2,4-ditertbutylphenyl)phosphite	98%	Sigma-Aldrich

3.1.2 Chemicals used

A list of chemicals used in the hydroformylation reaction experiments is given in **Table 3.2**. All components were used as is from the suppliers without further purification.

Table 3.2: List of chemicals used for hydroformylation experiments.

Chemical name	Purity	Supplier
Toluene	>99%	ACE Chemicals
7-Tetradecene	>98%	Self-synthesized[a]
$CO:H_2$ mix	50:50	Afrox
Hydrogen	>99.999	Afrox
Carbon monoxide	>99.3	Afrox

[a]Synthesis procedure described in Section 3.1.3

3.1.3 Synthesis of 7-tetradecene

A list of the chemicals used in the synthesis procedure of 7-tetradecene is given in **Table 3.3**. All components were used as is from the suppliers without further purification.

Table 3.3 Chemicals used for 7-tetradcene synthesis.

Chemical name	Purity	Supplier
1-Octene	98%	Sigma-Aldrich
Hoveyda-Grubbs 2nd Generation Precatalyst	97%	Sigma-Aldrich

7-Tetradecene was synthesized and purified according to three steps: i) metathesis reaction of 1-octene, ii) catalyst separation and ii) 7-tetradecene fractionation.

1-Octene metathesis was performed using Hoveyda-Grubbs 2nd Generation Precatalyst (HGr2). Metathesis reactions were conducted in a stirred flat-bottom beaker (open to atmosphere) to allow evolution of ethene and drive the reaction towards near-complete conversion of 1-octene. The beaker was initially charged with 20 mL 1-octene and heated to 50°C. HGr2 (13 mg) was then added to the reaction mixture and metathesis was allowed to proceed for at least 5 hrs at constant temperature conditions with stirring. At the end of the reaction time, the post-metathesis mixture containing 1-octene, 7-tetradecene and HGr2 was collected. The above procedure was repeated multiple times until sufficient volume of product mixture had been recovered.

HGr2 was subsequently separated from the collected post-metathesis mixture via organic solvent nanofiltration (OSN) according to the same methodology reported previously (Van der Gryp et al., 2010). OSN separations were thus conducted batch-wise using a stainless steel dead-end cell. The cell was pressurized with ultra-high purity nitrogen gas and the catalyst-free permeate was collected through Duramem® 280 membrane. Following removal of HGr2 to yield a clear mixture containing 1-octene and 7-tetradecene, 1-octene (normal boiling point: 121°C) was fractionated from 7-tetradecene (normal boiling point: 250°C) via one-pot batch distillation to yield 7-tetradecene with purity >98%, as monitored by GC. Formation of 7-tetradecene was also verified via GC-MS experiments.

3.2 Hydroformylation experiments

3.2.1 Experimental apparatus and methodology

Hydroformylation experiments were performed using a 100ml stainless steel batch-reactor setup, as shown schematically in **Figure 3.1**. The reactor was fitted with thermocouple to regulate the reaction temperature, bourdon pressure gauge to control the reactor pressure and a magnetic stirrer to provide agitation/mixing during the reaction. A pre-determined quantity of toluene, rhodium precatalyst, modifying ligand (where applicable) and the alkene was used for each experiment. The exact quantities were however dependent on the particular study and will therefore not be discussed here. Rather, details of these quantities can be found as part of results chapters (Chapters 4 to 7) where applicable. Once all required reagents/solvents had been charged to the reactor vessel, the reactor was placed into an oil bath and heated to the controlled temperature set-point, where after the vessel was pressurized with syngas to the desired operating pressure. The operating pressure was kept constant during the course of the reaction. After the reaction had proceeded for the desired length of time, the reactor vessel was de-pressurized of syngas and sampled.

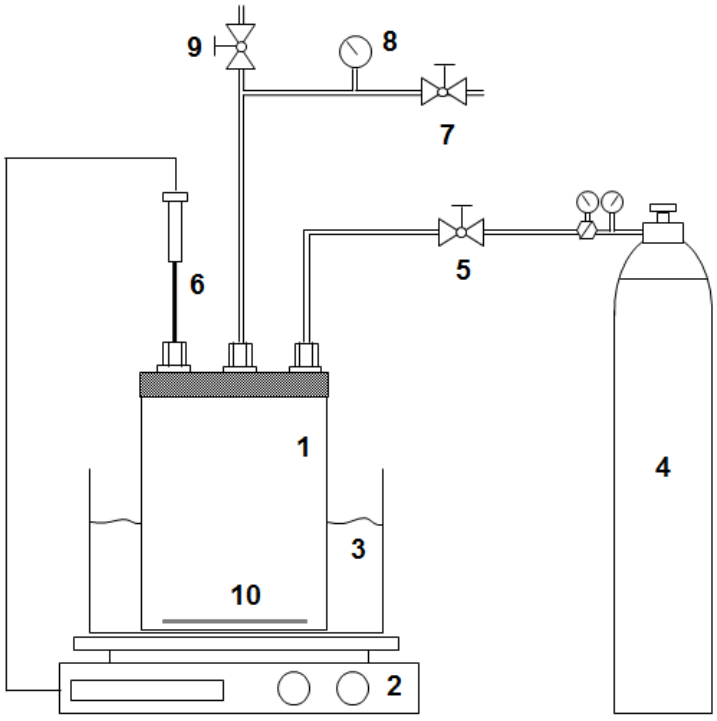

Figure 3.1: Schematic of hydroformylation reactor setup (**1** = Stainless steel reaction, **2** = Magnetic stirrer/heating plate, **3** = Oil bath, **4** = Syngas cylinder, **5** = Syngas feed valve, **6** = Thermocouple, **7** = Safety pressure-relief valve, **8** = Reactor pressure gauge, **9** = Reactor depressurisation valve, **10** = Magnetic stirrer bar).

3.2.2 Analytical methodology

Quantification of the product distributions was determined by means of GC-MS analysis using an Agilent 7890A GC, Zebron ZB-1701 capillary column (60m x 250µm x 0.25µm) and Agilent 5975C single quadrupole mass detector. The GC analysis programme was as follows: column pressure 23.787 psi (He); split ratio 25:1; oven programmed to 45°C for 1 min, 45-250°C at 10°C/min for 20 min; detector temperature 280°C.

A list of the chemicals used in the analytical procedure is given in **Table 3.4**. All components were used as is from the suppliers without further purification.

Table 3.4: List of chemicals used for analytical procedures.

Chemical name	Purity	Supplier
Dichloromethane	>99%	ACE Chemicals
Dodecane	>99%	Sigma-Aldrich

For preparation of the samples for analysis by GC-MS, 100 uL of dodecane (external standard) was pipetted into the 1 mL post-reaction sample obtained from the reactor, and then diluted with dichloromethane to a suitable concentration before injection into the GC-MS.

Quantification of the relative volume of each component (V_i) in the sample was calculated using **Equation 3.1**, which relates the volume of dodecane ($V_{dodecane}$), the peak response area of dodecane ($A_{dodecane}$) and the peak response area of the component (A_i) to V_i. RF represents the linear proportionality constant (response factor) relating these quantities. V_i was then converted to a molar basis (N_i) using **Equation 3.2**, where ρ_i and MW_i represent the mass density and molecular mass of the component, respectively.

$$V_i = V_{dodeccane} \times \left(\frac{A_i}{A_{dodecane}}\right) \times (RF) \qquad (3.1)$$

$$N_i = \frac{\rho_i \times V_i}{MW_i} \qquad (3.2)$$

The response factors were determined by generating calibration curves for the different components (alkenes and aldehydes), as shown in **Figure 3.2**. Calibration curves were generated by measuring the response of several standard samples with known amounts of analyte component species and external standard (100 uL). The gradient of the linear calibration curve represents the response factor of for each component. Due to lack of available

standards for every component, the assumption was made that all components of the same type (i.e. alkenes or aldehydes) will respond similarly.

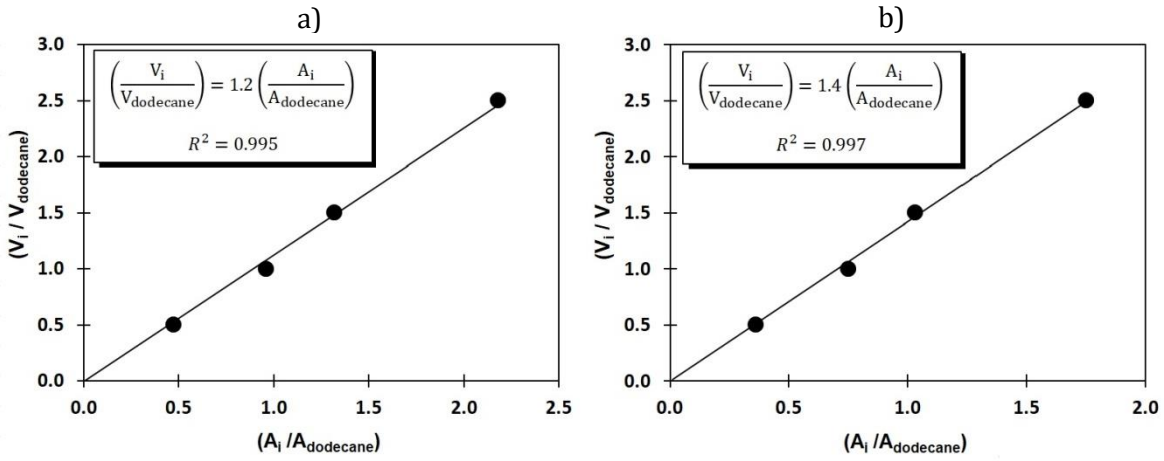

Figure 3.2: Calibration curves used in determining response factors for a) alkenes and b) aldehydes.

3.2.3 Validation of equipment and method with literature

In order to validate the equipment and methodologies employed for this study (Section 3.2.1 and 3.2.2) the hydroformylation of 1-octene was performed as a validation experiment. The validation experiment was performed using the Rh-triphenylphosphine catalyst under identical reaction conditions (80°C and 20 bar, $CO:H_2$ = 1:1) reported previously in the literature (Buhling et al., 1995; Van der Veen et al., 1999). Comparison of the results generated with those obtained in the literature is summarised in **Figure 3.3**. It is clear that the hydroformylation results are reproducible with literature (less than 1% error at a 95% confidence level).

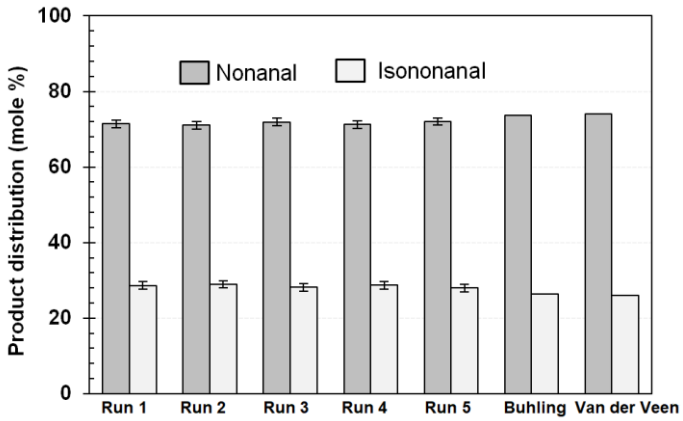

Figure 3.3: Validation of experimental procedure for 1-octene hydroformylation.

3.2.4 Uncertainty analysis

In order to evaluate the experimental uncertainty, a detailed uncertainty analysis of the experimental procedure was performed as per guidelines described in Evaluation of measurement data - Guide to the expression of uncertainty in measurement document produced by Working Group 1 of the Joint Committee for Guides in Metrology (JCGM/WG 1). Based on this uncertainty analysis procedure, the experimental error with respect to product formations (7-tetradecene, isoalkenes, 2-hexylnonanal and isoaldehdyes) was estimated to be ± 1 mole %. Details of the uncertainty analysis methodology can be found in the Appendices (Appendix B).

In order to further corroborate the results determined from the uncertainty analysis, additional hydroformylation experiments were performed in triplicate at arbitrary reaction conditions (70°C and 30 bar, $CO:H_2$ = 1:1 for 2h) using the Rh-tris(2,4-ditertbutylphenyl)-phosphite catalyst system. Product distribution results for the different experimental runs are summarised in **Table 3.5**. The error for the different product formations determined from the uncertainty analysis and those determined from replicate measurements where expected to be quite similar, which indeed they are.

Table 3.5: Replicate experiments for 7-tetradecene hydroformylation.

Experiments	Isoalkenes (%)	Isoaldehydes (%)	2-hexylnonanal (%)
Experiment 1	1.2	93.9	4.9
Experiment 2	2.0	93.9	4.0
Experiment 3	1.4	94.7	3.9
Mean	1.5	94.2	4.3
Standard deviation	0.5	0.4	0.5
Error (95% confidence)	1.1	1.1	1.3

References

Buhling, A., Kamer, P. and van Leeuwen, P. 1995. Rhodium catalysed hydroformylation of higher alkenes using amphiphilic ligands. Journal of Molecular Catalysis A: Chemical. 98, 69-80.

Siangwata, S., Chulu, S., Oliver, C. and Smith, G. 2016. Rhodium-catalysed hydroformylation of 1-octene using aryl and ferrocenyl Schiff base-derived ligands. Applied Organometallic Chemistry. 1-9.

Van der Gryp, P., Barnard, A., Cronje, J., de Vlieger, D., Marx, S. and Vosloo, H. 2010. Separation of different metathesis Grubbs-type catalysts using organic solvent nanofiltration. Journal of Membrane Science. 35, 70-77.

Van der Veen, L. , Kamer, P. and Van Leeuwen, P. 1999. Hydroformylation of internal olefins to linear aldehydes with novel rhodium catalysts. Angewandte Chemie International Edition. 38, 336-338.

CHAPTER 4

MANUSCRIPT 1

Hydroformylation of post-metathesis product using commercial rhodium-based catalysts

Nicholas C.C. Breckwoldt[1] and Percy van der Gryp[1,2]

[1]Department of Process Engineering, University of Stellenbosch, Private Bag X1, Matieland 7602, South Africa

[2]School of Chemical and Minerals Engineering, Research Focus Area for Chemical Resource Beneficiation, North-West University, Hoffmann Street, Potchefstroom, 2522, South Africa

This chapter has been published in the form of a journal article:

Breckwoldt, N. and Van der Gryp, P. 2018. Hydroformylation of post-metathesis product using commercial rhodium-based catalysts. Reaction Kinetics, Mechanisms and Catalysis. 125, 689-705.

Abstract

The hydroformylation of the post-metathesis product 7-tetradecene using different commercially available homogeneous rhodium-based catalysts has been investigated. The influences of different reaction conditions such as temperature (60-90°C), pressure (10-30 bar), ligand-to-metal ratio (0-30) and unwanted impurities in the reaction environment were found to have significant effect on resulting product distributions and catalyst performance parameters such as the turnover number and selectivity. The two main reactions observed were hydroformylation of 7-tetradecene to target aldehyde product 2-hexylnonanal over the entire temperature range and isomerisation above 70°C. Selectivities as high as 99% toward target product 2-hexylnonanal were observed with turnover numbers up to 980 (mol product. mol Rh^{-1}). A comparative study with different post-metathesis products also shows preferred selectivity (67-85%) toward corresponding branched aldehydes which is advantageous in the industrial context in which mixed post-metathesis feedstocks might be expected.

1. Introduction

The hydroformylation reaction (or oxo-process) represents one of the most important industrial applications of homogeneous catalysis (Cornils and Hermann, 2002; Börner and Franke, 2016). During the course of the reaction involving an alkene and a suitable transition-metal based complex, a new carbon-carbon bond is formed, while simultaneously introducing the synthetically versatile formyl group (-CHO) in the form of either linear or branched aldehydes (Van Leeuwen, 2002). Since catalyst systems that give a high selectivity to desired product are attractive in the industrial context, controlling the selectivity of the reaction remains one of the most important challenges, especially when internal alkenes are employed as feedstock (Vilches-Herrera et al., 2014). Regarding the variation of the different hydroformylation processes involving internal alkenes that have been reported, two process types can be distinguished. These are i) isomerisation-hydroformylation of internal alkenes in order to obtain the linear product (Van der Veen et al., 1999; Beller et al., 1999; Selent et al., 2000; Selent et al., 2001; Klein et al., 2001; Jackstell et al., 2001; Van der Slot et al., 2002; Bronger et al., 2003; Behr et al., 2003; Vogl et al., 2005; Yan et al., 2006; Yu et al., 2008; Selent et al., 2011; Chen et al., 2013 and Yuki et al., 2013) and ii) the selective hydroformylation of internal alkenes to corresponding branched aldehydes (Breit et al., 2001; Haumann et al., 2002; Fuchs et al., 2006 and Kuil et al., 2006). The industrial relevance of the first group can be exemplified by the production of *n*-pentanal from industrially important feedstocks such as raffinate-II (a mixture of isomeric butenes derived through steam cracking) for which the subsequent downstream conversion to the C10 plasticizer alcohol, 2-propylheptanol, is of interest (Van Leeuwen, 2002). Also important is the *n*-selective hydroformylation of internal octenes for incorporation into high performance plasticizers such as diiso-nonyl phthalate (Taddei and Mann, 2013). The preparation of polyols and certain plasticizers can be distinguished as examples for which the branched-selective hydroformylation has gained attention recently (Reinius et al., 2001; Riihimaki et al., 2003 and Riihimaki et al., 2003). A summary of catalyst performances in the hydroformylation of linear internal alkenes using rhodium-based catalysts is given in **Table 1**.

Table 1: Summary of the hydroformylation of internal alkenes using rhodium-based catalysts.

Catalyst system	Alkene	Temp. (°C)	Press. (bar)	Sel.[a] (%)	Reference
Rh-Diphosphane	2-octene	120	2	90	(Van der Veen et al., 1999)
Rh-Triphenylphosphine	2-octene	120	2	46	
Rh-Diphosphane	4-octene	120	2	81	
Rh-Triphenyl phosphine	4-octene	120	2	23	
Rh/Ru – Phosphane-phosphite	2-butene	120	48	56	(Beller et al., 1999)
Rh-Phosphonite	1,2,3,4-octene	140	20	48	(Selent et al., 2000)
Rh-Phosphonite	1,2,3,4-octene	130	20	48	(Selent et al., 2001)
Rh-Diphosphite	1,2,3,4-octene	130	20	69	
Rh-Naphos	2-butene	120	10	91	(Klein et al., 2001)
Rh-Naphos	2-pentene	120	10	93	
Rh-Naphos	2-octene	120	10	91	
Rh-Naphos	4-octene	120	10	70	
Rh-Phosphabenzene	2-octene	90	10	76[b]	(Breit et al., 2001)
Rh-Pyrolylphosphane	2-pentene	120	25	33	(Jackstell et al., 2001)
Rh-Indolylphosphane	2-pentene	120	25	27	
Rh-Carbozolylphosphane	2-pentene	120	25	37	
Rh-TPPTS	7-tetradecene	100	100	77[b]	(Haumann et al., 2002)
Rh-Pyrolylamidite	2-octene	120	5	50	(Van der Slot et al., 2002)
Rh-Xantphos type	2-octene	120	3.6	89	(Bronger et al., 2003)
Rh-Biphephos	4-octene	125	20	89	(Behr et al., 2003)
Rh-Biphephos	2-pentene	100	30	99	(Vogl et al., 2005)
Rh-Tetraphosphoramidite	2-hexene	100	10	99	(Yan et al., 2006)
Rh-Tetraphosphoramidite	2-octene	100	10	98	
Rh-Phosphabarrelene	2-octene	70	10	98[b]	(Fuchs et al., 2006)
Rh-Phosphabenzene	2-octene	70	10	90[b]	
Rh-Triarylphosphite	2-octene	70	10	97[b]	
Rh-Triphenylphosphine	2-octene	70	10	95[b]	
Rh-(Meta-pyridyl)	2-octene	40	20	99[b]	(Kuil et al., 2006)
Rh-(Meta-pyridyl)	3-octene	40	20	99[b]	
Rh-(Meta-pyridyl)-Zn-tpp	2-octene	40	20	97[b]	
Rh-(Meta-pyridyl)-Zn-tpp	3-octene	40	20	97[b]	
Rh-Tetraphosphoramidite	2-octene	100	10	99	(Yu et al., 2008)
Rh-Diphosphite	1,2,3,4-octene	100	50	70	(Selent et al., 2011)
Rh-Biphephos	1,2,3,4-octene	100	50	93	

[a]Selectivity to linear aldehydes, unless stated otherwise. [b]Selecitivity to branched aldehydes.

Table 1: Summary of the hydroformylation of internal alkenes using rhodium-based catalysts (continued).

Catalyst system	Alkene	Temp. (°C)	Press. (bar)	Sel.[a] (%)	Reference
Rh-Dipyridyl-bis-Zn(II)(salphen)	3-hexene	25	20	-	(Gadzikwa et al., 2012)
Rh-Dipyridyl-bis-Zn(II)(salphen)	2-heptene	25	20	-	
Rh-Dipyridyl-bis-Zn(II)(salphen)	2-octene	25	20	-	
Rh-Dipyridyl-bis-Zn(II)(salphen)	2-nonene	25	20	-	
Rh-Triphosphoramidite	2-octene	100	10	98	(Chen et al., 2013)
Rh-Triphenylphosphite	2-decene	120	5	41	(Yuki et al., 2013)
Rh-Triphenylphosphine	2-decene	120	5	44	
Rh-Xantphos	2-decene	120	5	57	
Rh-Bisbi	2-decene	120	5	29	
Rh-Biphosphite	2-decene	120	5	95	
Rh-Biphosphite	2-octene	120	5	96	
Rh-Biphosphite	4-octene	120	5	94	
Rh-Biphosphite	2-tridecene	120	5	92	

[a]Selectivity to linear aldehydes, unless stated otherwise. [b]Selecitivity to branched aldehydes.

The RSA Olefins programme of the Department of Science and Technology National Research Foundation's (DST-NRF) Centre of Excellence in Catalysis (c*Change) aims to investigate the beneficiation of low-value alkene feedstocks to inter alia higher value products in the surfactant range (Du Toit et al., 2016; Peddie et a., 2017). The motivation being that there is a relatively untapped potential supply of these high-value commodity products in the form of low-value linear α-alkenes (C_5-C_9) feedstocks produced by South African-based petrochemical company, Sasol Ltd, through world-renowned Fischer-Tropsch processes (Dry, 2002; De Klerk and Furimsky, 2010). The proposed beneficiation scheme, as shown in **Figure 1**, involves alkene metathesis of α-alkenes (C_5-C_9) to higher internal alkenes of the post-metathesis type (C_{10}-C_{18}), followed by functionalization thereof through hydroformylation to corresponding branched aldehydes. These branched aldehyde products can be recovered and converted downstream to beta-branched surfactant alcohols of the Guerbet-type (O'Lenick, 2001) which are attractive due to their improved biodegradability and surface acting properties as compared to corresponding linear analogues (Zoller, 2009).

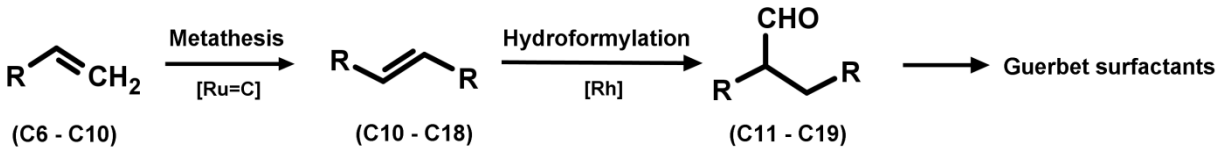

Figure 1: Beneficiation of α-alkene feedstock proposed by the RSA Olefins programme.

As a case study for the metathesis of linear α-alkene feedstocks promoting the industrialization of the proposed process, the metathesis of 1-octene to post-metathesis product 7-tetradecene has been explored recently (Du Toit et al., 2016; Jordaan et al., 2006; Jordaan et al., 2007; Van der Gryp et al., 2012). Only few reports, however, have appeared on the hydroformylation of post-metathesis product using rhodium-based catalyst (Arhancet et al., 1991; Haumann et al., 2002). These studies report aqueous-phase processes with either poor conversion (ca. 5%) to products (Arhancet et al., 1991) or progress under severe reaction conditions (ca. 100 bar) (Haumann et al., 2002). As concerns the hydroformylation of post-metathesis product using homogeneous rhodium-based catalysts which are commercially available, to our knowledge, no attempts have been reported. However, the hydroformylation of post-metathesis product using homogeneous catalysts is attractive because the application of these catalysts systems is well-established on an industrial scale due to the high selectivity and reactivities which can be achieved under relatively mild reaction conditions (Franke et al., 2012). Furthermore, the hydroformylation of post-metathesis product could reduce the number of steps currently employed in the preparation of Guerbet-type surfactant alcohols by conventional synthetic routes (O' Lenick, 2001).

In view of our longstanding industrial interest in the beneficiation of α-alkene feedstocks to inter alia higher value products in the surfactant and detergent range, we report herein an evaluation of the rhodium-catalysed hydroformylation of post-metathesis product 7-tetradecene using different homogeneous catalysts systems which are commercially available.

It is therefore the aim of this publication to characterise the performances of the different commercially available rhodium-based catalysts in the hydroformylation of post-metathesis product and to describe the hydroformylation system from a reaction engineering viewpoint.

2. Materials and methods

2.1 Chemicals used

The chemicals used for the hydroformylation reactions were the post-metathesis product 7-tetradcene (prepared as per details provided in Section 2.3) and toluene (>99%, ACE Chemicals) as solvent. For analytical analyses by gas chromatography (GC), dichloromethane (>99%) (Sigma-Aldrich) was used to increase sample volumes, with dodecane (99%) (Sigma-Aldrich) used as external standard. Synthesis gas (CO/H_2, 1:1) was supplied by Afrox. All chemicals were used without any further purification.

2.2 Catalysts used

As rhodium catalyst precursor, $[Rh(CO)_2(acac)]$ (acac = acetylacetonato) (98%) was used as received from Sigma. Tris(2,4-di-tertbutylphenyl)phosphite (97%) (Sigma-Aldrich), triphenylphosphine (97%) (Sigma-Aldrich) and triphenlyphosphite (97%) (Sigma-Aldrich) were used as phosphorus modifying ligands together with rhodium catalyst precursor to prepare the catalyst in situ. The commercially available monodenate phosphorus ligands: tris(2,4-di-tertbutylphenyl)phosphite (**1**), triphenylphosphine (**2**) and triphenylphosphite (**3**) that were used in this study are shown in **Figure 2**.

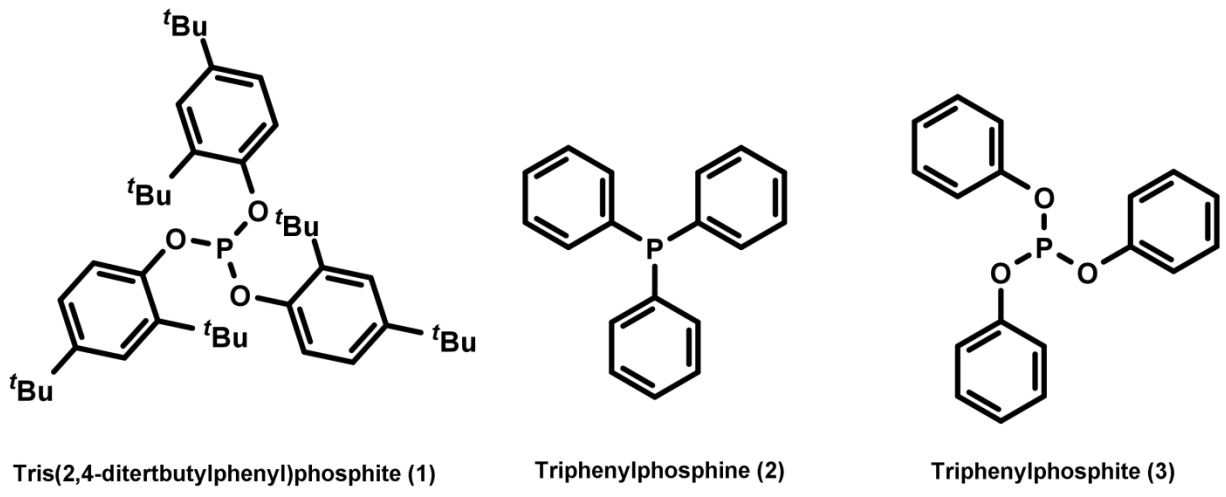

Figure 2: Commercially available monodentate phosphorus ligands used in this study.

2.3 Synthesis of 7-tetradecene

7-Tetradecene was synthesized according to the self-metathesis reaction of 1-octene (98%) (Sigma-Aldrich) with commercially available Hoveyda-Grubbs second generation precatalyst, $RuCl_2(=CH\text{-}o\text{-}OPrC_6H_4)(H_2IMes)$ (98%) (Sigma-Aldrich) as reported previously (Van der Gryp et al., 2012). The metathesis catalyst was removed from the post-metathesis reaction mixture using nanofiltration according to published methods (Van der Gryp et al., 2010). Unreacted 1-octene was then boiled off under a fume hood and monitored by GC to yield 7-tetradecene in high (> 98%) purity.

2.4 Hydroformylation procedure

Hydroformylation reactions were performed in a 100 mL stainless steel pressure cell fitted with teflon insert, thermocouple, pressure gauge and magnetic stirring. In a typical experiment, toluene (8.5 mL), $[Rh(CO)_2(acac)]$ (0.012 mmol) and phosphorus ligand (0.24 mmol) were together transferred to the reactor following procedures suggested previously (Breit et al., 2001). 7-Tetradecene (3 mL) was then added to the reactor, which was then sealed and heated in an oil bath to the desired temperature set-point. The reactor was pressurized with syngas ($CO:H_2$, 1:1) and the reaction allowed to proceed at fixed reaction conditions. At the end of the reaction, the reactor was depressurised, sampled (1 mL) and prepared for analysis by GC-MS. The average error (mole %) with respect to the product formations in this study was determined by repeating selected experiments in triplicate. Using the triplicate measurements, the average error for each species was calculated to be ±1% (at 95% confidence level assuming normal distribution of 7-tetradecene, isoalkenes, isoaldehydes and 2-hexylnonanal).

2.5 Analytical methods

Dodecane (0.1 mL) was added as external standard to the sample and diluted with dichloromethane before injection into GC-MS. For analysis by GC-MS, an Agilent 7890A GC, Zebron ZB-1701 capillary column (60m x 250µm x 0.25µm) and Agilent 5975C single quadrupole mass detector was used. The GC analysis programme used was as follows: column pressure 23.787 psi (He); split ratio 25:1; oven programmed to 45°C for 1 min, 45-250°C at 10°C/min for 20 min; detector temperature 280°C.

3. Results and discussion

3.1 Reaction network: hydroformylation of 7-tetradecene

Hydroformylation of alkenes are accompanied often by isomerisation reactions that can lead to a wide product distribution (Vilches-Herrera et al., 2014; Hentschel et al., 2015). In addition to target aldehyde(s), the final product mixture often contains a combination of both isomeric alkenes and isomeric aldehyde products which increases the complexity of the reaction network. In order to more conveniently describe the reaction network of interest, the use of lumped pseudo-component terms "isoalkene" and "isoaldehyde" were suggested previously to represent the two types of isomeric products which may form (Kiedorf et al., 2014; Hentschel et al., 2015). These definitions were therefore adopted in this study for the hydroformylation of post-metathesis product 7-tetradecene, as shown in **Figure 3**. Thus from **Figure 3**, three major groups of products can be identified, namely: 2-hexylnonanal, isoalkenes and isoaldehydes. 2-Hexylnonanal refers to the target hydroformylation product of 7-tetradecene. Isoalkenes refer to the double bond isomerisation products of 7-tetradecene (6-tetradecene, 5-tetradecene, etc.), which may in turn undergo hydroformylation to corresponding isoaldehydes (2-pentydecanal, 2-butyldecanal, etc.). These product groups (2-hexylnonanal, isoalkenes and isoaldehydes) were therefore used to describe the product distribution for the hydroformylation of post-metathesis product 7-tetradecene using different rhodium-based catalysts. The catalytic performance was further described according to the productivity and selectivity of the catalysts. Selectivity is defined as the ability of the catalyst to preferentially favour the formation of target aldehyde product (2-hexylnonanal), while minimizing the formation of isomerisation products (isoalkenes and isoaldehydes) (Van der Veen et al., 1999). The turnover number (TON) can be used to describe the productivity of the catalyst (Bligaard et al., 2016). The definition of TON adopted in this study indicates the number of moles of target aldehyde formed per mole of rhodium present (mol product.mol Rh^{-1}) over the reaction time.

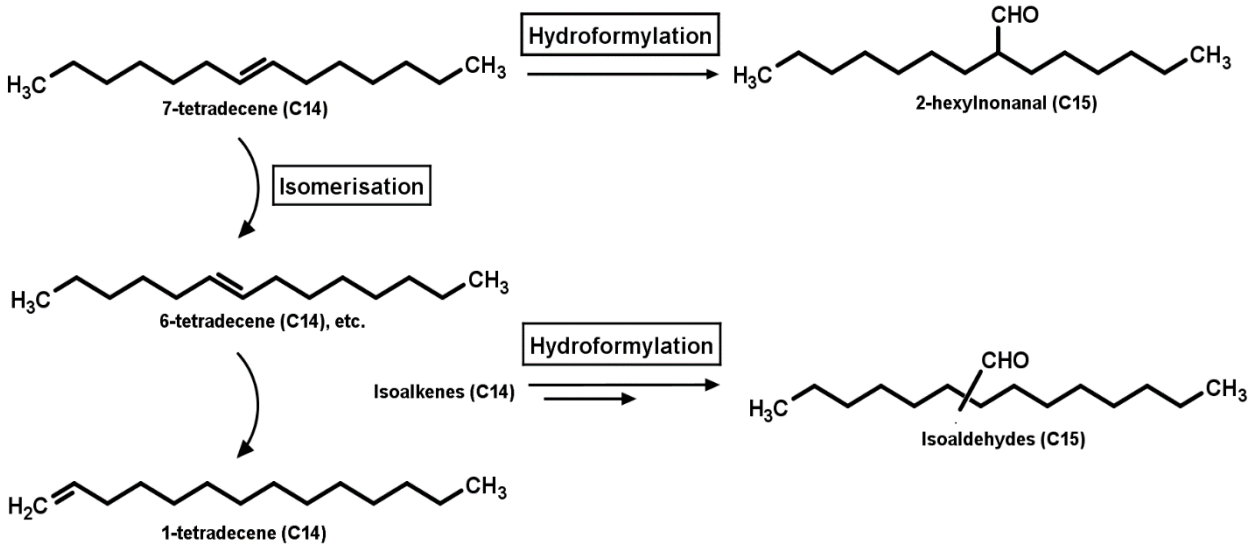

Figure 3: Reaction network for the hydroformylation of post-metathesis product 7-tetradecene.

3.2 Screening of commercial catalysts

For comparison, the catalytic performance of rhodium-based catalysts generated in situ from $[RhCO)_2(acac)]$ and commercially available phosphorus ligands (**1**-**3**) were evaluated in the hydroformylation reaction of post-metathesis product 7-tetradecene. In each reaction, toluene was used as solvent and reactions were allowed to progress over 5 h under fixed reaction conditions: temperatures (60-90°C) and applied pressures of 30 bar, which are comparable to those typically employed within industrial operations (Van Leeuwen, 2002). Screening results for the different catalyst systems (**1**-**3**)/$[RhCO)_2(acac)]$ are presented in **Table 2**. From the results it is clear that the presence of different phosphorus ligands has a significant influence on the catalyst selectivity and activity performance. The sterically bulky phosphite-modified catalyst (**1**)/$[Rh(CO)_2(acac)]$ displayed excellent conversion of 7-tetradecene to products (> 91%) under all reaction conditions. The TON and selectivity toward target branched aldehyde product 2-hexylnonanal after 5 hours were in the ranges 817-980 (mol product. mol Rh^{-1}) and 90-99%, respectively. These values are markedly higher than those obtained by employing phosphine-modified (**2**)/$[Rh(CO)_2(acac)]$ (224-441, S = 53-100%) and smaller phosphite (**3**)/$[Rh(CO)_2(acac)]$ catalyst system (48-334 , S = 33-98%) under the range of operating conditions tested.

The TON of the different catalyst systems were thus found to increase in the order: (**1**)/[$Rh(CO)_2(acac)$] > (**2**)/[$Rh(CO)_2(acac)$] > (**3**)/[$Rh(CO)_2(acac)$] and correlates well with previous findings [44, 45]. Tricas et al. [45] similarly observed improved hydroformylation reactivity by employing bulky phosphites ligands such as (**1**) as compared to phosphine-modified system. This clearly demonstrates the excellent suitability of strong π-acceptor ligands for present reaction and can be explained by the strong π-acceptor capacity of bulky phosphite ligand (**1**) which promotes more facile dissociation of carbonyl ligand during catalysis, which in turn, results in greater reactivity with (**1**)/[$Rh(CO)_2(acac)$] catalyst system (Van Rooy et al., 1996). The high selectivity to corresponding branched aldehyde product in the case of (**1**)/[$Rh(CO)_2(acac)$] catalyst system may be explained by the formation of mono-ligated rhodium complex, $HRh(CO)_3L$ (L = bulky phosphite ligand **1**) due to the large cone angle (Jongsma et al., 1991). Consequently, dissociation of a carbonyl group from the $HRh(CO)_3L$ complex during the reaction mechanism yields a sterically less hindered complex compared to the di-substituted $HRh(CO)_2L_2$ complexes that are preferred when employing smaller phosphine (**2**) and phosphite (**3**) ligands. The sterically less hindered complex favours the formation of the secondary alkyl-rhodium species and hence the corresponding branched aldehyde (Dabbawala et al., 2011). Given the excellent aldehyde turnovers and favourable selectivity performance towards target branched aldehyde in the hydroformylation of post-metathesis product, (**1**)/[$Rh(CO)_2(acac)$] catalyst system was selected for further evaluations.

Table 2: Screening of commercial catalysts for the hydroformylation of 7-tetradecene[a].

Ent	Catalyst system	Temp. (°C)	Pres. (bar)	Conv.	S (%)	TON
1	(**1**)/[$RhCO)_2(acac)$]	60	30	91.2	89.6	817
2	(**2**)/[$RhCO)_2(acac)$]	60	30	22.4	100	224
3	(**3**)/[$RhCO)_2(acac)$]	60	30	4.9	97.7	48
4	(**1**)/[$RhCO)_2(acac)$]	70	30	98.9	99.1	980
5	(**2**)/[$RhCO)_2(acac)$]	70	30	46.7	83.6	391
6	(**3**)/[$RhCO)_2(acac)$]	70	30	47.6	62.1	296
7	(**1**)/[$RhCO)_2(acac)$]	80	30	99.6	89.5	892
8	(**2**)/[$RhCO)_2(acac)$]	80	30	67.9	65.0	441
9	(**3**)/[$RhCO)_2(acac)$]	80	30	75.9	44.0	334
10	(**1**)/[$RhCO)_2(acac)$]	90	30	99.5	84.9	845
11	(**2**)/[$RhCO)_2(acac)$]	90	30	77.0	52.5	404
12	(**3**)/[$RhCO)_2(acac)$]	90	30	88.4	32.8	290

[a]Reactions were performed under the conditions: [Rh] = 1mM, $[7\text{-tetradecene}]_0$ = 1 M, P/Rh = 20 in toluene (6.97 M).

3.3 Hydroformylation of 7-tetradecene with (1)/[$Rh(CO)_2(acac)$]

3.3.1 Influence of reaction temperature and pressure

In order to determine the ideal reaction conditions for the hydroformylation of 7-tetradecene using (**1**)/[$Rh(CO)_2(acac)$] catalyst system, temperature and pressure were varied in the range 60-90°C and 10-30 bar ($CO:H_2$,1:1), respectively. Hydroformylation results with toluene as solvent are summarized in **Table 3**. From the results it is clear that temperature and pressure have a significant effect on the catalytic performance of (**1**)/[$RhCO)_2(acac)$] catalyst system. By operating under the mild reaction conditions (60°C, 10 bar), product formation towards 2-hexylnonanal reaches 43% and isomerisation products (isoalkenes and isoaldehydes) remain relatively insignificant (less than 1%). As the temperature increases from 60 to 90°C at constant low pressure, isoalkenes (less than 1% at 60°C to 22% at 90°C) and isoaldehydes (0% at 60°C to 18% at 90°C) increase, while 2-hexylnonanal product formation varies in the range 39% to 46%.

These results indicate the presence of two competing reaction pathways which are present, as is shown in **Figure 3**. The first pathway is toward the formation of target aldehyde (2-hexylnonanal) and is active across the whole temperature range. The second pathway, starting at a temperature of ~70°C, becomes productive toward the formation of isoalkenes (isomerisation) that are readily converted to corresponding isoaldehydes. Similar results with regard to the formation of isomerisation products using rhodium-based catalysts were reported previously (Hanson et al., 1987; Van Rooy et al., 1995). Van Rooy et al. (1995) also found that significant isomerisation products begin to form above 70°C using a similar bulky phosphite-modified rhodium catalyst for 1-octene hydroformylation. The formation of isomerisation products, specifically the double bond migrations to yield 6-,5-tetradecenes, etc., are most likely the result of a β-hydride elimination reaction of rhodium alkyl species generated during the hydroformylation reaction cycle (Pino et al., 1980).

Table 3: Hydroformylation of 7-tetradecene with (1)/[$Rh(CO)_2(acac)$] catalyst system[a].

Temp. (°C)	Pres.(bar)	7-tetradecene (%)	Isoalkenes (%)	Isoaldehydes (%)	2-Hexylnonanal (%)	TON
60	10	56.9	0.6	0.0	42.5	425
60	20	29.7	3.6	5.4	61.2	612
60	30	8.8	1.4	8.1	81.7	817
70	10	40.7	9.4	3.6	46.4	464
70	20	3.9	3.8	9.8	82.4	824
70[b]	30	92.5	0.3	0.2	7.0	70
70[c]	30	39.7	9.0	15.1	36.2	362
70	30	1.1	0.3	0.6	98.0	980
70[d]	30	3.6	0.0	2.9	93.5	935
80	10	30.1	25.5	5.4	39.0	390
80	20	2.3	3.1	14.9	79.7	797
80	30	0.4	1.2	9.2	89.2	892
90	10	17.2	21.8	17.9	43.2	432
90	20	5.3	7.1	22.7	64.9	649
90	30	0.5	1.7	13.4	84.5	845

[a]Reactions were performed under the conditions: [Rh] = 1mM, $[7\text{-tetradecene}]_0$ = 1 M, P/Rh = 20 in toluene (6.97 M) for 5 hours; [b]P/Rh = 0, [c]P/Rh = 10; [d]P/Rh = 30.

Upon increasing the reaction pressure from 10 to 30 bar at low temperature conditions (60°C), 2-hexylnonanal product formation is improved from 42 to 82%, while isomerisation product formations (isoalkenes and isoaldehydes combined) become significant (around 10%). At both elevated temperature and pressure conditions (90°C, 30 bar) 2-hexylnonanal product formation is 85%, with simultaneous increase in isomerisation product formations (15%); al beit lower still than total observed isomerization product formations (40%) under low pressure conditions. This shows that the hydroformylation of 7-tetradeccene with (**1**)/[$Rh(CO)_2(acac)$] catalyst systems should be preferably operated at higher pressure conditions.

According to Fogler (2014), "the economic success of a chemical plant is the minimization of undesired side reactions that occur along with desired reaction". For the hydroformylation of 7-tetradecene with (**1**)/[$Rh(CO)_2(acac)$] catalyst system, it is thus clear that the reactor design objective must be selection of process conditions (temperature and pressure) which maximizes the selectivity of 2-hexylnonanal relative to isomerisation products (isoalkenes and isoaldehydes), while also maintaining the highest possible productivity (TON). High selectivity is not only important from a synthetic point of view, but also important due to the difficulty in separating close-boiling point isomeric aldehydes downstream. The influence of reaction

temperature on these two performance parameters (selectivity, TON) at maximum operating pressure (30 bar) is shown in **Figure 4**. The selectivity towards target aldehyde product 2-hexylnonanal increases to a maximum (99%) between 60 and 70° and then decreases to 85%. This indicates that the reaction should be preferentially operated at low temperature conditions (70°C) to favour a high selectivity. The TON similarly increases between 60 and 70° to a maximum of 980 (mol product. mol Rh^{-1}) and then decreases thereafter. This result further suggests that that ideal conditions with (**1**)/[$Rh(CO)_2(acac)$] are achieved at 70°C and 30 bar, as these reaction conditions gave the highest combined selectivity and reactivity performance.

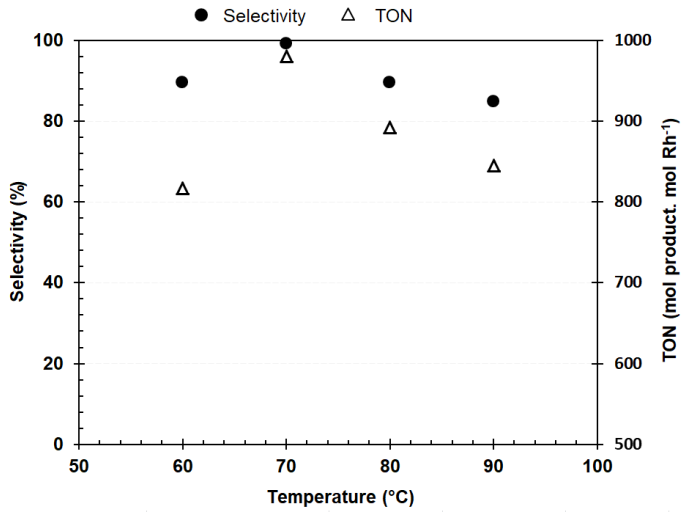

Figure 4: Influence of temperature on selectivity and productivity (TON) performance with (1)/[$Rh(CO)_2(acac)$] catalyst after 5 hours. Reactions were performed under conditions: [Rh] = 1 mM, $[7\text{-tetradecene}]_0$ = 1 M, P/Rh = 20 and P = 30 bar in toluene (6.97 M).

3.3.2 Influence of phosphorus to rhodium molar ratio

From an industrial perspective, hydroformylation catalysts are extremely expensive to use due to their rare rhodium metal content. An excess of ligand is therefore required to maintain the catalytic activity of rhodium in the long-term. Too large an excess of ligand, however, may decrease the activity of the catalyst through steric hindrance of the interaction between substrate and metal or alternatively stabilisation of catalyst species which prevents necessary dissociation of ligands during catalytic cycle. It is therefore purpose of this section to investigate the influence of phosphorus-to-metal ratio (P/Rh) in the hydroformylation of post-metathesis product with (**1**)/[Rh(CO)2(acac)] catalyst system. The P/Rh was varied in the range 0 to 30 under conditions found to be optimal (70°C, 30 bar) and the results are presented in **Figure 5**. It

is clear that an increase in P/Rh had a significant influence on the TON, mostly beneficial. As the P/Rh ratio increases from 0 to 20, the TON increases from 70 to 980 (mol product.mol Rh^{-1}). However, as the P/Rh increase above 20, it appears that the TON stabilises or even decreases slightly. As a plausible explanation for the low TON observed at low P/Rh ratio, Jongsma et al. (1991) proposed that the rhodium precursor may not be completely converted to active rhodium-hydride species. It can, therefore, be concluded that a P/Rh ratio of at least 20 is required to ensure that rhodium is effectively converted catalytically active hydride species during the hydroformylation of 7-tetradecene with (**1**)/[$Rh(CO)_2(acac)$] and was considered the optimal P/Rh ratio in all subsequent reactions.

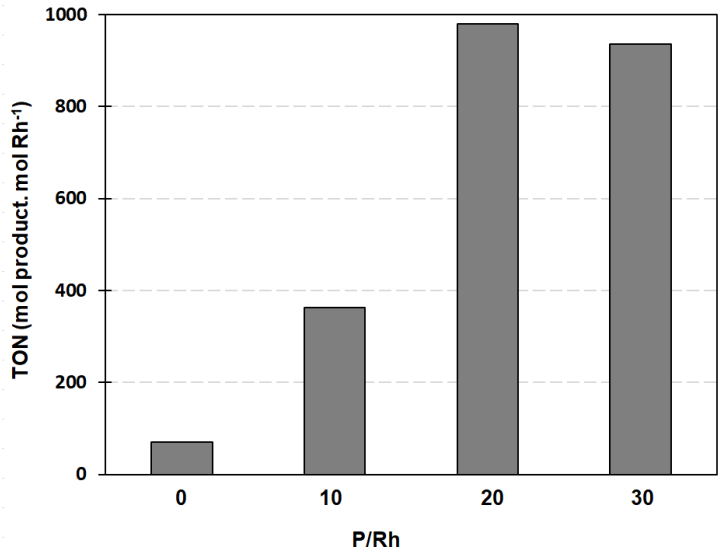

Figure 5: Influence of P/Rh on the TON for the hydroformylation of 7-tetradecene with (1)/[$Rh(CO)_2(acac)$] catalyst system after 5 hours. Reactions were performed under conditions: [Rh] = 1 mM, $[7\text{-tetradecene}]_0$ = 1 M, T =70°C, P = 30 bar in toluene (6.97 M).

3.3.3 Influence of unrecovered metathesis catalyst

The metathesis of α-alkenes to produce corresponding post-metathesis products (i.e. metathesis of 1-octene to 7-tetradecene) relies prevalently on the use of ruthenium-based catalysts, most notably ruthenium carbenes of the Grubbs-type (Du Toit et al., 2016; Jordaan et al., 2006; Jordaan et al., 2007 and Van der Gryp et al., 2012). These are often homogeneous in nature and therefore often challenging to separate from their post-reaction mixtures. Recently it has been shown that Grubbs-type catalysts can be recovered from their post-reaction mixtures to levels below 9 ppm using nanofiltration (Van der Gryp et al., 2010). Other methods have been found to reduce the catalyst content within the range 200-1200 ppm (Maynard et al., 1999;

Paquette et al., 2000; Ahn et al., 2001 and Westhus et al., 2004). The presence of possible undesired impurities such as ruthenium-based metathesis catalyst, for example Hoveyda-Grubbs Second Generation Precatalyst (**HGr2**), on downstream hydroformylation performance is therefore of interest. In order to determine the influence of ruthenium-based Grubbs-type catalyst on hydroformylation performance, concentrations of **HGr2** were varied in the range 0-800 ppm relative to 7-tetradecene under optimized reaction conditions. 800 ppm represents typical maximum catalyst load expected for 1-octene metathesis using **HGr2** (Van der Gryp et al., 2010). Hydroformylation results are summarised in **Figure 6**. Several authors have reported interactive effects between rhodium- and ruthenium-based complexes under hydroformylation conditions (Beller et al., 1999; Yuki et al., 2013). However, variation in the concentration of ruthenium-based metathesis precatalyst present during the reaction had no notable effect on the hydroformylation performance with (**1**)/[$Rh(CO)_2(acac)$] system. This can be seen from **Figure 6** with relatively constant 2-hexylnonanal product formation (99%) over the precatalyst concentration range. Studies have shown (Galan et al., 2009; Poater et al., 2012) that Grubbs-based catalysts may decompose via a carbon monoxide-induced ylidene attack of the aromatic ring of the n-heterocyclic carbene and may account for the lack of interactive effects between the two metals. It is furthermore well known that Grubbs-based catalysts are temperature sensitive (Lehman et al., 2003) and may decompose under the typically higher temperatures employed during the hydroformylation as compared to metathesis.

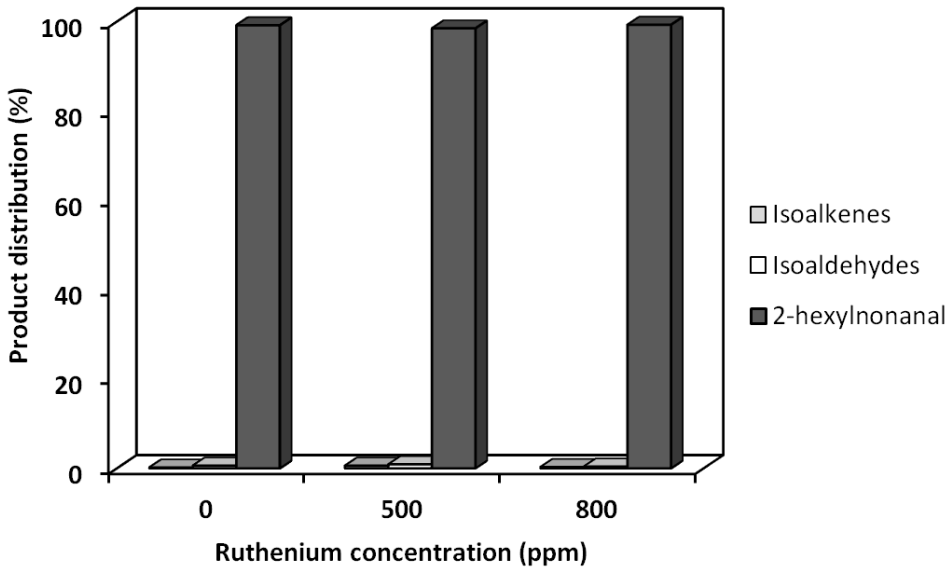

Figure 6: Influence of unrecovered ruthenium-based metathesis catalyst on the product distribution in the hydroformylation of 7-tetradecene with (1)/[$Rh(CO)_2(acac)$] catalyst system. Reactions were performed under conditions: [Rh] = 1 mM, $[7\text{-tetradecene}]_0$ = 1 M, T =70°C, P = 30 bar in toluene (6.97 M).

3.3.4 Hydroformylation of different post-metathesis products

Encouraged by the high catalytic activities and selectivity afforded by (**1**)/[$Rh(CO)_2(acac)$] catalyst system for the hydroformylation of post-metathesis product 7-tetradecene, the hydroformylation of different post-metathesis products (4-octene and 5-decene) were also evaluated. Reactions were performed under conditions found to be optimal for 7-tetradecene, and therefore hydroformylation with different post-metathesis product are not necessarily optimised. Hydroformylation results are shown in **Figure 7**.

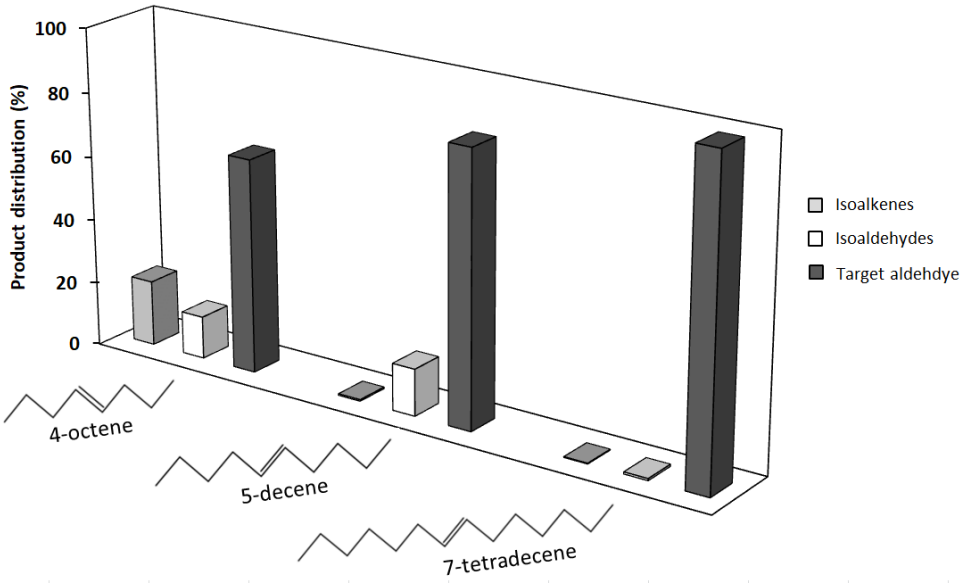

Figure 7: Hydroformylation of different post-metathesis products using (1)/[$Rh(CO)_2(acac)$] catalyst system. Reactions were performed under conditions: [Rh] = 1 mM, $[alkene]_0$ = 1 M, T= 70°C, P = 30 bar and P/Rh = 20 in toluene (6.97 M).

From the results it is evident that (**1**)/[$Rh(CO)_2(acac)$] affords moderate to excellent selectivity in the hydroformylation of the different post-metathesis products which were evaluated. For the hydroformylation of 4-octene, the major product observed at the end of the reaction is 2-propylhexanal in ~67% selectivity. Previous studies involving the hydroformylation of post-metathesis product such as 4-octene using diphosphite-modified rhodium-based catalysts yield selectively the linear aldehyde (Behr et al., 2003; Yuki et al., 2013). The hydroformylation of 5-decene with (**1**)/[$Rh(CO)_2(acac)$] also yields the preferred branched aldehyde product 2-butylheptanal in high selectivity (85%). There is a notable decrease in isomerisation product formation with increasing chain length of post-metathesis product, i.e. C8 (30%) < C10 (10%) < C14 (less than 1%). This could be attributed to changes in the structure of intermediate species

formed during the catalysis due to varied steric hindrance caused by the position of the double bond. Klein and co-workers (Klein et al., 2001) have reported that internal alkenes are thermodynamically favoured as compared to terminal alkene analogues and may account for the observed resistance to isomerisation behaviour with an increase in chain length.

4. Conclusions

In this study, the catalytic performance of commercially available rhodium-based catalysts (**1**-**3**)/[Rh(acac)$(CO)_2$] were evaluated in the model hydroformylation of post-metathesis product 7-tetradecene to target branched aldehyde product 2-hexylnonanal. It was found that the influence of reaction temperature (60-90°C) and pressure (10-30, CO/H_2 = 1:1) on the product distribution, selectivity and catalyst activity was significant due to competing hydroformylation and isomerisation reactions. Mainly hydroformylation of post-metathesis product was observed at low temperatures, typically below 70°C, while at higher temperatures, isomerisation products were also significant. By employing (**1**)/[Rh(acac)$(CO)_2$] catalyst system, selectivities as high as 99% could be achieved under optimized conditions (70°C, 30 bar). (**1**)/[Rh(acac)$(CO)_2$] is therefore the most effective commerical catalyst for the investigated system. The broader value in the industrial context for post-metathesis product hydroformylation reactions has also been demonstrated by employing different post-metathesis products, 4-octene and 5-decene and show similar preferred selectivity towards corresponding target branched aldehydes 2-propylhexanal and 2-butylheptanal, respectively, for the different post-metathesis products. The reaction was found to be unaffected by the presence of possible unwanted impurities in the reaction environment such as unrecovered ruthenium-based metathesis catalyst (up to 800 ppm) which are typically challenging to remove from their post-metathesis-reaction mixtures. Thus, the hydroformylation of post-metathesis product might be achieved in the industrial context by employing commercially available homogeneous rhodium-based catalysts such as (**1**)[Rh(acac)$(CO)_2$]. In the next step of our investigations concerning the hydroformylation of post-metathesis product, we aim to study the reaction engineering kinetics and modelling of the reaction in order to describe the reaction from a reactor design perspective.

Acknowledgements

The support of the DST-NRF Centre of Excellence in Catalysis (CoE) towards this research is hereby acknowledged. Opinions expressed and conclusions arrived at, are those of the author and are not necessarily to be attributed to the CoE. The authors also wish to thank the Department of Process Engineering, University of Stellenbosch for financial support.

References

Ahn, Y., Yang, K. and Georg, G. 2001. A convenient method for the efficient removal of ruthenium byproducts generated during olefin metathesis reactions. Organic Letters. 3, 1411-1413.

Arhancet, J. Davis, M. and Hanson, B. 1991. Supported aqueous-phase, rhodium hydroformylation catalysts II: Hydroformylation of linear, terminal and internal olefins. Journal of Catalysis. 129, 100-105.

Behr, A., Obst, D., Schulte, C. and Schosser, T. 2003. Highly selective tandem isomerization–hydroformylation reaction of trans-4-octene to n-nonanal with rhodium-biphephos catalysis. Journal of Molecular Catalysis A: Chemical. 206, 179-184.

Beller, M., Zimmermann, B. and Geissler, H. 1999. Dual catalytic systems for consecutive isomerization–hydroformylation reactions. Chemistry - A European Journal. 5, 1301-1305.

Bligaard, T., Bullock, R., Campbell, C., Chen, J., Gates, B., Gorte, R., Jones, C., Jones, W., Kitchin, J. and Scott, S. 2016. Toward benchmarking in catalysis science: best practices, challenges, and opportunities. ACS Catalysis. 6, 2590-2602.

Börner, A. and Franke, R. 2016. Hydroformylation: Fundamentals, processes, and applications in organic synthesis. Wiley-VCH.

Breit, B., Winde, R., Mackewitz, T., Paciello, R. and Harns, K. 2001. Phosphabenzenes as monodentate π-acceptor ligands for rhodium-catalyzed hydroformylation. Chemistry - A European Journal. 3106-3121.

Bronger, R., Kamer, P. and Van Leeuwen, P. 2003. Influence of the bite angle on the hydroformylation of internal olefins to linear aldehydes. Organometallics. 22, 5358-5369.

Chen, C., Qiao, Y., Geng, H. and Zhang, X. 2013. A novel triphosphoramidite ligand for highly regioselective linear hydroformylation of terminal and internal olefins. Organic Letters. 15, 1048-1051.

Cornils, B. and Hermann, W. 2002. Applied homogeneous catalysis with organometallic compounds: a comprehensive handbook in three volumes. Wiley-VCH.

Dabbawala, A., Jasra, R. and Bajaj, H. 2011. Selective hydroformylation of 1-hexene to branched aldehydes using rhodium complex of modified bulky phosphine and phosphite ligands. Catalysis Communications. 12, 403-407.

De Klerk, A. and Furimsky, E. 2010. Catalysis in the refining of Fischer-Tropsch syncrude. Wiley-VCH.

Dry, M. 2002. The Fischer-Tropsch process: 1950–2000. Catalysis Today. 71, 227-241.

Du Toit, J., Van der Gryp, P., Loock, M., Tole, T., Marx, S., Jordaan, J. and Vosloo, H. 2016. Industrial viability of homogeneous olefin metathesis: Beneficiation of linear alpha olefins with the diphenyl-substituted pyridinyl alcoholato ruthenium carbene precatalyst. Catalysis Today. 275, 191-200.

Fogler, H. 2014. Elements of chemical reaction engineering. Pearson Education.

Franke, R., Selent, D. and Börner, A. 2012. Applied hydroformylation. Chemical Reviews. 112, 5675-5732.

Fuchs, E., Keller, M. and Breit, B. 2006. Phosphabarrelenes as ligands in rhodium-catalyzed hydroformylation of internal alkenes essentially free of alkene isomerization. Chemistry - A European Journal. 12, 6930-6939.

Gadzikwa, T., Bellini, R., Dekker, H. and Reek, J. 2012. Self-assembly of a confined rhodium catalyst for asymmetric hydroformylation of unfunctionalized internal alkenes. Journal of the American Chemical Society. 134, 2860-2863.

Galan, B., Pitak, M., Gembicky, M., Keister, J. and Diver, S. 2009. Ligand-promoted carbene insertion into the aryl substituent of an N-heterocyclic carbene ligand in ruthenium-based metathesis catalysts. Journal of the American Chemical Society. 131, 6822-6832.

Hanson, B. and Davis, M. 1987. Hydroformylation of 1-hexene utilizing homogeneous rhodium catalysts: Regioselectivity as a function of conversion. Journal of Chemical Education. 64, 928-930.

Haumann, M., Yildiz, H., Koch, H. and Schomacker, R. 2002. Hydroformylation of 7-tetradecene using Rh-TPPTS in a microemulsion. Applied Catalysis A: General. 236, 173-178.

Hentschel, B., Kiedorf, G., Gerlach, M., Hamel, C., Seidel-Morgenstern, A., Freund, H. and Sundmacher, K. 2015. Model-based identification and experimental validation of the optimal reaction route for the hydroformylation of 1-dodecene. Industrial and Engineering Chemistry Research. 54, 1755-1765.

Jackstell, R., Klein, H., Beller, M., Wiese, K. and Roettger, D. 2001. Synthesis of pyrrolyl-, indolyl, and carbazolylphosphanes and their catalytic application as ligands in the hydroformylation of 2-pentene. European Journal of Organic Chemistry. 2001, 3871-3877.

Jongsma, T. and Challa, G. 1991. A mechanistic study of rhodium tri(o-t-butylphenyl)phosphite complexes as hydroformylation catalyst. Journal of Organometallic Chemistry. 421, 121-128.

Jordaan, M. and Vosloo, H. 2007. Ruthenium catalyst with a chelating pyridinyl-alcoholato ligand for application in linear alkene metathesis. Advanced Synthesis and Catalysis. 349, 184-192.

Jordaan, M., Van Helden, P., Van Sittert, C. and Vosloo, H. 2006. Experimental and DFT investigation of the 1-octene metathesis reaction mechanism with the Grubbs 1 precatalyst. Journal of Molecular Catalysis A: Chemical. 254, 145-154.

Kiedorf, G., Hoang, D., Müller, A., Jörke, A., Markert, J., Arellano-Garcia, H., Seidel-Morgenstern, A. and Hamel, C. 2014. Kinetics of 1-dodecene hydroformylation in a thermomorphic solvent system using a rhodium-biphephos catalyst. Chemical Engineering Science. 115, 31-48.

Klein, H., Jackstell. R., Wiese, K., Borgmann, C. and Beller, M. 2001. Highly selective catalyst systems for the hydroformylation of internal olefins to linear aldehydes. Angewandte Chemie International Edition. 40, 3408-3411.

Kuil, M., Soltner, T., Van Leeuwen, P. and Reek, J. 2006. High-precision catalysts: regioselective hydroformylation of internal alkenes by encapsulated rhodium complexes. Journal of the American Chemical Society. 128, 11344-11345.

Lehman, S., Schwendeman, J., O'Donell, P. and Wagener, K. 2003. Olefin isomerization promoted by olefin metathesis catalysts. Inorganical Chimica Acta. 345, 190-198.

Maynard, H. and Grubbs, R. 1999. Purification technique for the removal of ruthenium from olefin metathesis reaction products. Tetrahedron Letters. 40, 4137–4140.

O'Lenick, A. 2001. Guerbet chemistry. Journal of Surfactants and Detergents. 4, 311-315.

Paquette, L., Schloss, J., Efremove, I., Fabris, F., Gallou, F., Mendez-Andino, J. and Yang, J. 2000. A convenient method for removing all highly-colored byproducts generated during olefin metathesis reactions. Organic Letters. 2, 1259-1261.

Peddie, W., Van Rensburg, J., Vosloo, M., and Van Der Gryp, P. 2017. Technological evaluation of organic solvent nanofiltration for the recovery of homogeneous hydroformylation catalysts. Chemical Engineering Research and Design. 121, 219-232.

Pino, P. 1980. Hydroformylation of olefinic hydrocarbons with rhodium and cobalt catalysts: Analogies and dissimilarities. Journal of Organometallic Chemistry. 200, 223-242.

Poater, A. and Cavallo, L. 2012. Deactivation of Ru-benzylidene Grubbs catalysts active in olefin metathesis. Theoretical Chemistry Accounts. 131, 1155-1160.

Reinius, H., Suomalainen, P., Riihimaki, H., Karvinen, E., Pursiainen J. and Krause, A. 2001. o-Alkyl-substituted triphenyl phosphines: activity and regioselectivity in rhodium-catalysed propene hydroformylation. Journal of Catalysis. 199, 302–308.

Riihimaki, H., Kangas, T., Suomalainen, P., Reinius, H., Jaaskelainen, S., Haukka, M., Krause, A., Pakkanen, T. and Pursiainen, J. 2003. Synthesis of new o-alkyl substituted arylalkylphosphanes: study of their molecular structure and influence on rhodium-catalyzed propene and 1-hexene hydroformylation. Journal of Molecular Catalysis A: Chemical. 200, 81–94.

Riihimaki, H., Suomalainen, P., Reinius, H., Suutari, J., Jaaskelainen, S., Krause, A., Pakkanen, T. and Pursianen, J. 2003. o-Alkyl-substituted aromatic phosphanes for hydroformylation studies: synthesis, spectroscopic characterization and ab initio investigations. Journal of Molecular Catalysis A: Chemical. 200, 69-79.

Selent, D., Hess, D., Wiese, K., Rottger, D., Kunze, C. and Börner, A. 2001. New Phosphorus Ligands for the Rhodium-Catalyzed Isomerization/hydroformylation of internal octenes. Angewandte Chemie International Edition. 40, 1696-1698.

Selent, D., Kubis, C., Spannenberg, A., Baumann, W., Börner, A., Franke, R. and Kreidler, B. 2011. A new diphosphite promoting highly regioselective rhodium-catalyzed hdroformylation. Organometallics. 30, 4509-4514.

Selent, D., Wiese, K., Rottger, D. and Börner, A. 2000. Novel oxyfunctionalized phosphonite ligands for the hydroformylation of isomeric n-olefins. Angewandte Chemie International Edition. 39, 1639-1641.

Taddei, M. and Mann, A. (Eds.). 2013. Hydroformylation for organic synthesis. Springer.

Tricas, H., Diebolt, O. and Van Leeuwen, P. 2013. Bulky monophosphate ligands for ethene hydroformylation. Journal of Catalysis. 298, 198-205.

Van der Gryp, P., Barnard, A., Cronje, J., De Vlieger, D., Marx, S. and Vosloo, H. 2010. Separation of different metathesis Grubbs-type catalysts using organic solvent nanofiltration. Journal of Membrane Science. 353, 70-77.

Van der Gryp, P., Marx, S. and Vosloo, H. 2012. Experimental, DFT and kinetic study of 1-octene metathesis with Hoveyda-Grubbs second generation precatalyst. Journal of Molecular Catalysis A: Chemical. 355, 85-95.

Van der Slot, S., Duran, J., Luten, J., Kamer, P. and Van Leeuwen P. 2002. Rhodium-catalyzed hydroformylation and deuterioformylation with pyrrolyl-based phosphorus amidite ligands: influence of electronic ligand properties. Organometallics. 21, 3873-3883.

Van der Veen, L., Kamer, P., Van Leeuwen, P. 1999. Hydroformylation of internal olefins to linear aldehydes with novel rhodium catalysts. Angewandte Chemie International Edition. 38, 336-338.

Van Leeuwen, P. and Claver, C. (Eds.) 2002. Rhodium catalyzed hydroformylation (Vol. 22). Springer Science and Business Media.

Van Rooy, A., de Bruijn, J., Roobek, K., Kamer, P. and Van Leeuwen, P. 1996. Rhodium-catalysed hydroformylation of branched 1-alkenes; bulky phosphite vs. triphenylphosphine as modifying ligand. Journal of Organometallic Chemistry. 507, 69-73.

Van Rooy, A., Orij, E., Kamer, P. and Van Leeuwen, P. 1995. Hydroformylation with a rhodium /bulky phosphite modified catalyst. Catalyst comparision for oct-1-ene, cyclochexene, and styrene. Organometallics. 14, 34-43.

Vilches-Herrera, M., Domke, L. and Börner, A. 2014. Isomerization-hydroformylation tandem reactions. ACS Catalysis. 4, 1706-1724.

Vogl, C., Paetzold, E., Fischer, C., Kragl, U. 2005. Highly selective hydroformylation of internal and terminal olefins to terminal aldehydes using a rhodium-biphephos-catalyst system. Journal of Molecular Catalysis A: Chemical. 232, 41-44.

Westhus, M., Gonthier, E., Brohm, D., Breinbauer, R. 2004. An efficient and inexpensive scavenger resin for Grubbs' catalyst. Tetrahedron Letters. 45, 3141-3142.

Yan, Y., Zhang, X. and Zhang, X. 2006. A tetraphosphorus ligand for highly regioselective isomerization-hydroformylation of internal olefins. Journal of the American Chemical Society. 128, 16058-16061.

Yu, S., Chie, Y., Guan, Z. and Zhang, X. 2008. Highly regioselective isomerization-hydroformylation of internal olefins to linear aldehyde using Rh complexes with tetraphosphorus ligands. Organic Letters. 10, 3469-3472.

Yuki, Y., Takahashi, K., Tanaka, Y. and Nozaki, K. 2013. Tandem isomerization/hydroformylation/hydrogenation of internal alkenes to n-alcohols using Rh/Ru dual- or ternary-catalyst systems. Journal of the American Chemical Society. 135, 17393-17400.

Zoller, U. (Ed.) 2009. Handbook of detergents Part F: Production. CRC Press.

CHAPTER 5

MANUSCRIPT 2

Kinetic evaluation of the hydroformylation of post-metathesis product 7-tetradecene using bulky phosphite-modified rhodium catalyst

Nicholas C.C. Breckwoldt[1], Neill J. Goosen[1], Hermanus C.M. Vosloo[2] and Percy Van der Gryp[3]

[1]Department of Process Engineering, University of Stellenbosch, Private Bag X1, Matieland 7602, South Africa.

[2]Research Focus Area for Chemical Resource Beneficiation, Catalysis and Synthesis Research Group, North-West University, Hoffmann Street, Potchefstroom, 2522, South Africa.

[3]School of Chemical and Minerals Engineering, Research Focus Area for Chemical Resource Beneficiation, North-West University, Hoffmann Street, Potchefstroom 2522, South Africa.

This chapter has been published in the form of a journal article:

Breckwoldt, N., Goosen, N., Vosloo, H. and Van der Gryp, P. 2019. Kinetic evaluation of the hydroformylation of the post-metathesis product 7-tetradecene using bulky phosphite-modified rhodium catalyst. Reaction Chemistry and Engineering. 4, 695-704.

Abstract

Reaction engineering kinetics for the hydroformylation of the post-metathesis product 7-tetradecene using bulky phosphite-modified rhodium catalyst Rh-tris(2,4-di-tertbutylphenyl)phosphite were evaluated. The reaction was performed at different temperatures (60 to 90°C), catalyst concentrations (0.5 to 1 mM), hydrogen partial pressures (15 to 25 bar) and carbon monoxide partial pressures (15 to 25 bar). The reaction system is well described by three interdependent mole balance equations in combination with a phenomenological mechanism-based rate law equation derived for bulky phosphite ligand coordinated to rhodium. The kinetics were thus found to be first-order in alkene and catalyst concentrations (above a critical concentration), negative-order in carbon monoxide and zero-order in hydrogen. Activation energy for the hydroformylation reaction was calculated as 68 $kJ.mol^{-1}$.

1. Introduction

Hydroformylation is one of the most important examples of homogeneous catalytic processes in industry (Cornils and Hermann, 2002; Van Leeuwen and Claver, 2002). During the course of the hydroformylation reaction, aldehydes are produced via the activation of alkenes with syngas (H_2/CO) and the principle metals used to catalyze the reaction are either rhodium or cobalt. The advantages of rhodium-based catalysts are a higher activity and selectivity under mild process conditions and therefore much of the current research on the hydroformylation reaction has focused on the application and elucidation of the different rhodium-ligand catalyst systems (Franke et al., 2012).

Phosphite ligands have been applied extensively in the rhodium-catalysed hydroformylation of alkenes since the first report thereof in the late 1960s by Pruett and Smith (1969) and later by the group of Van Leeuwen (Van Leeuwen and Roobeek, 1983). Especially phosphite ligands with electron-withdrawing and bulky substituents at the ortho and para positions of the aryl rings are known to give the most active hydroformylation catalysts (Jongsma et al., 1991). The latter feature not only leads to high reaction rates, but bulky phosphites are also more resistant to hydrolysis which adds to their attractiveness in the industrial context (Van Leeuwen and Claver, 2002).

The rhodium-catalysed hydroformylation reaction depends on several factors such as temperature, applied syngas pressure and most notably, the type of alkene substrate used. In general, reaction kinetics describing the reaction can be classified into one of two extreme cases depending on the substrate dependence: i) the rate-determining step occurs early in the mechanistic cycle and reaction rate is first-order with respect to the substrate (Type I kinetics) or ii) hydrogenolysis of the rhodium-acyl species is rate-determining and consequently reaction rate is independent of the substrate but first-order in hydrogen (Type II kinetics) (Zuidema et al. 2008). In the exceptional case, fractional order dependencies may also be observed (Kamer et al., 2004). It is therefore clear that the rate equation may be unique for any given substrate-catalyst system and knowledge thereof, as well as estimation of the kinetic parameters, is necessary for the reactor design (Fogler, 2014).

Several kinetic investigations have been reported in the literature for the rhodium-catalysed hydroformylation reaction using bulky phosphite ligands and different rate equations have been proposed (Van Rooy et al., 1995; Van Rooy et al., 1996; Kubis et al., 2012; Kubis et al., 2014; Guven et al., 2014). In the hydroformylation of 1-octene, for example, very high reaction rates are observed and hydrogenolysis of the rhodium-acyl species is rate-determining; thus the alkene does not appear in the rate equation (Type II kinetics) (Van Rooy et al., 1995). This has

been supported recently via in situ IR experiments which point to the existence of rhodium-acyl species as the preferred resting species present during the reaction of 1-alkenes (Kamer et al., 2004). On the other hand, the rate equation proposed for more sterically hindered alkenes such as cyclohexene and 3,3-dimethyl-1-butene is linear in the alkene since the hydrogenolysis step no longer controls the reaction rate as the rate-determining step now occurs earlier in the mechanistic cycle (Type I kinetics). This case was also confirmed via in situ IR experiments which show that the hydrido complex $HRh(CO)_3L$ (L = bulky phosphite) remains unchanged following alkene addition (Kamer et al., 2004). However, while these studies reveal much for our mechanistic understanding of the different operating conditions appearing in the mechanistic rate equations, current literature on the application and complete kinetic parameter estimation of a mechanism-derived rate equation using bulky phosphite-modified catalyst remains limited (Guven et al., 2014), especially for substrate systems which are of potential commercial interest. It was therefore the overarching goal of this study demonstrate such an application.

Regarding the choice of substrate system, the hydroformylation of higher linear internal alkenes (> C_{10}) has become increasingly important over the last few years for the preparation of alkyl-branched surfactant alcohols which have been requested by detergent industries in order to meet ever-growing environmental and technological imperatives such as improved biodegradability and surface-acting properties (Zoller, 2009). In an industrial context, large-scale processes such as the Shell Higher Olefins Process (SHOP) incorporate alkene metathesis in order to produce vast quantities of these higher linear internal alkenes, which can in turn, be functionalized downstream via the hydroformylation process (Mol, 2004). In South Africa, the prominent petrochemical company Sasol Ltd. is a major producer of short chain alkenes, especially α-alkenes (Dry, 2002) which can be subjected to metathesis reactions in order to produce longer internal alkenes for downstream functionalization (Jordaan et al., 2007; Van der Gryp et al., 2012; Du Toit et al., 2014; Du Toit et al., 2016).

Recently our group evaluated the hydroformylation of the post-metathesis product 7-tetradecene as a model higher internal alkene substrate system using different phosphorus-modified rhodium catalysts (Breckwoldt and Van der Gryp, 2018). Of the various catalyst systems investigated, the commercially available Rh-tris(2,4-di-tertbutylphenyl)phosphite catalyst was found to be the most effective and gave excellent selectivities (>99%) towards corresponding target branched aldehyde product 2-hexylnonanal under mild reaction conditions.

It is therefore the aim of this study to investigate and describe the reaction engineering kinetics for the hydroformylation of the post-metathesis product 7-tetradecene using the bulky phosphite-modified rhodium catalyst over a range of operating conditions. A phenomenological mechanism-based rate equation consistent with the rate data is derived and kinetic parameters are estimated in order that the rate equation can be used in a reaction-engineering context.

2. Materials and methods

2.1 Chemicals used

7-Tetradecene was prepared via the metathesis of 1-octene using Hoveyda-Grubbs Second Generation precatalyst, as reported by Van der Gryp et al. (2012). Following the metathesis step, 7-tetradecene was purified by removing the metathesis catalyst via organic solvent nanofiltration and unreacted 1-octene was boiled off under fumehood to yield 7-tetradecene in high purity (>98%). Toluene (>99%, ACE Chemicals) was used as solvent for all hydroformylation experiments. Carbon monoxide and hydrogen gas were supplied by Afrox Ltd. Rhodium catalyst precursor (acetylacetonato)dicarbonyl-rhodium(I) (98%) and bulky phosphite ligand tris(2,4-diterbutylphenyl)phosphite (98%) were used as received from Sigma-Aldrich.

2.2 Experimental design

The kinetic investigations in this study were performed under the following standard reaction conditions as conducted in toluene as solvent: reaction temperature = 70°C, initial 7-tetradecene molar concentration = 1 $mol.L^{-1}$, catalyst molar concentration = 1 $mmol.L^{-1}$, ligand-to-metal molar ratio = 20, partial pressure of carbon monoxide (P_{CO}) = 15 bar and partial pressure of hydrogen (P_{H2}) = 15 bar. The influence of temperature, catalyst concentration, carbon monoxide and hydrogen partial pressures on the kinetics of the reaction was evaluated under the range of conditions given in **Table 1**. The kinetic data were generated over several hours so as to ensure that interpretation of the results were applicable over a wide alkene conversion range.

Table 1: Ranges of operating conditions investigated in this study.

Parameter (Units)	Parameter Range
Catalyst concentration (mol.L^{-1})	0.5 – 1.0 (10^{-3})
Carbon monoxide partial pressure (bar)	15 – 25
Hydrogen partial pressure (bar)	15 – 25
Temperature (°C)	60 – 90
Reaction volume (L)	8.5 (10^{-3})

2.3 Hydroformylation procedure

Hydroformylation experiments were performed in 100 mL stainless steel pressure reactor fitted with temperature-feedback and pressure-regulated control. For each experiment, 0.012 mmol (3 mg) rhodium precursor and 0.233 mmol (150 mg) phosphite ligand were added to 8.5 mL toluene in the reactor and stirred at room temperature according to the catalyst preformation method proposed by Breit and co-workers (Breit et al., 2001) before adding the alkene. 11.6 mmol (2.28 g) of 7-tetradecene was then added and reactor was heated to the desired reaction temperature before pressurizing with syngas which marked the start (time zero) of the reaction. Subsequent kinetic data showed clearly the rapid formation of an active hydroformylation catalyst in the absence of any induction period. The total syngas pressure was maintained constant over the complete alkene conversion range. All standard experiments were performed with an equimolar syngas feed (H_2:CO, 1:1). However, where the influence of hydrogen and carbon monoxide partial pressures on the reaction kinetics was of interest, the equimolar syngas feed was replaced with two separate hydrogen and carbon monoxide feed cylinders. The hydrogen and carbon monoxide gases were loaded separately into two separate sample cylinders (150 mL, received from Swagelok) and measured gravimetrically in order to provide the desired H_2:CO molar ratio. The high pressure gases were then connected and sufficient mixing time was allowed to ensure that the gases were well mixed prior to conducting the kinetic experiments. The procedure for preparing unequal H_2:CO molar ratios was validated by preparing an equimolar feed which gave the same results to the previously reported procedure with equimolar feed purchased from Afrox. Separate hydroformylation experiments were conducted for all consecutive data points, changing only the reaction time at constant reaction conditions in order to generate the product-time series. Samples were taken at the end of each run and were prepared and analysed via GC-MS according to previous methods (Breckwoldt and Van der Gryp, 2018). GC-MS programming was the following: Agilent 7890A GC, Zebron ZB-1701 capillary column (60 m 9 250 lm 9 0.25 lm) and Agilent 5975C single

quadrupole mass detector; column pressure 23.787 psi (He); split ratio 25:1; oven temperature 45°C for 1 min, 45–250°C at 10 °C.min^{-1} for 20 min; detector temperature of 280°C.

2.4 Regression procedure and validation

Regression of the observed hydroformylation rate data was performed in Matlab® using built-in least squares regression function (lsqnonlin.m) which applies the 'Levenberg- Marquardt' algorithm to minimize the objective function, as reported by Koeken et al. (2011). Modelled ordinary differential mole balance equations were solved numerically using 4th order Runga-Kutta integral method and confidence intervals of the regression coefficients were estimated using the bootstrap method (Fox, 2015). Validation of the regression procedure was confirmed using kinetic rate data available in the literature (Deshpande et al., 2011) and thereafter deemed satisfactory for application in this study.

2.5 Gas solubility

The solubility of carbon monoxide and hydrogen gas in toluene were estimated in this study using Henry coefficients reported in the literature within the appropriate temperature ranges (Bhanage et al., 1997; Deshpande et al., 1998), as given in **Table 2**. It was, therefore, assumed that the concentrations of gaseous components in the liquid medium were in equilibrium with applied gaseous partial pressures and that reaction solution (~90 mole % toluene) could be approximated to resemble that of pure toluene. Where duplicate measurements were available, i.e. at 60°C, the arithmetic mean of reported Henry coefficient measurements was used.

Table 2: Henry coefficients for hydrogen and carbon monoxide in toluene.

Temperature (°C)	H_{CO} (bar.L.mol^{-1})	H_{H2} (bar.L.mol^{-1})
60[a]	187.5	616.9
60[b]	185.0	617.0
70[a]	202.6	767.4
80[b]	230.0	907.0
90[b,*]	260.0	1191.0

[a]Bhanage et al., 1997, [b]Deshpande et al., 1998, *Extrapolated between reported values at 80°C and 100°C.

3. Results and discussion

3.1 Influence of temperature

The influence of temperature on the reaction kinetics was evaluated by varying the reaction temperature in the range 60 to 90°C while keeping all other reaction conditions constant at standard conditions. Product distribution-time results at the different temperatures are shown in **Figure 1**.

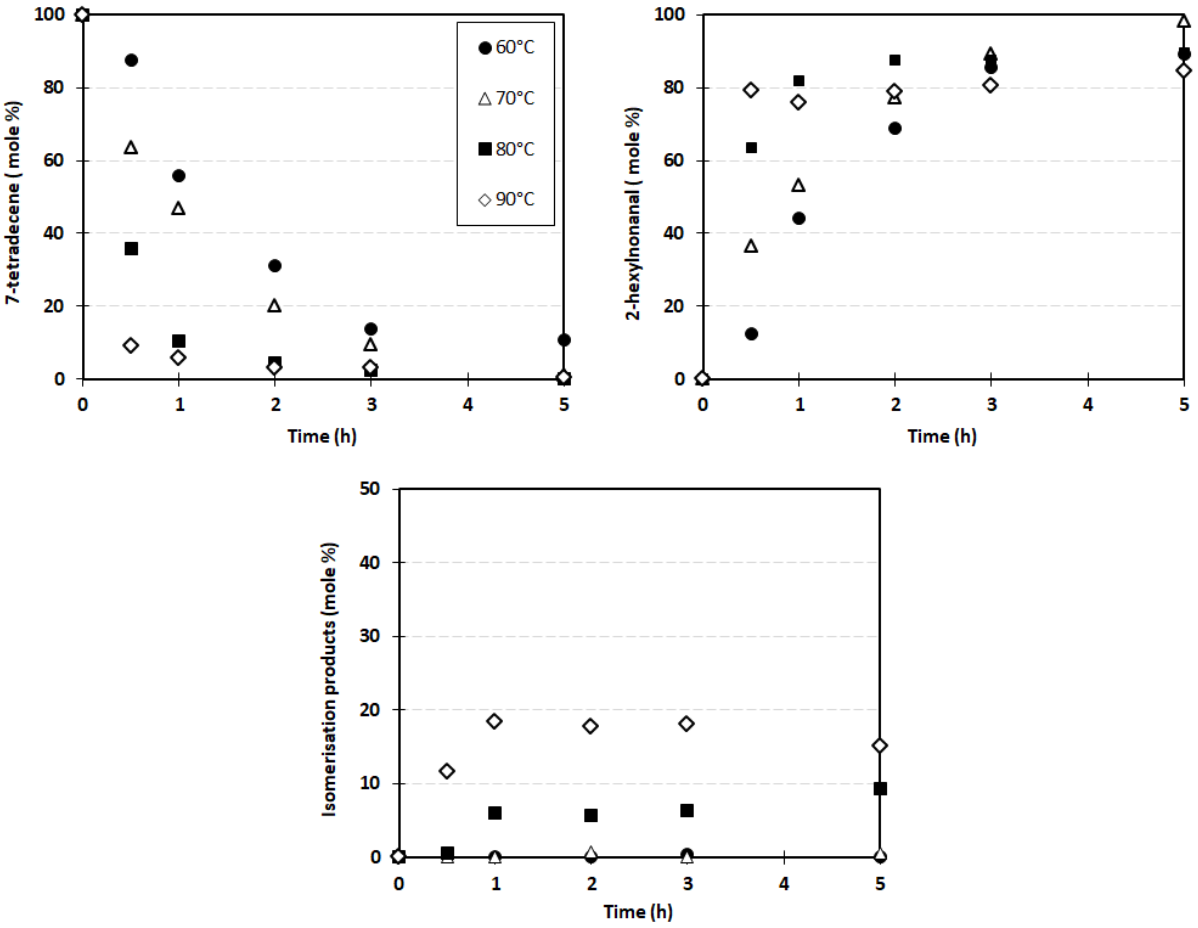

Figure 1: Influence of reaction temperature on the hydroformylation of 7-tetradecene using bulky phosphite catalyst at 1mM catalyst concentration and 30 bar (H_2:CO,, 1:1).

The consumption of 7-tetradecene resulted in the formation of both the primary hydroformylation product 2-hexylnonanal and iso-products. Iso-products represent the combination of possible isomeric alkene (6-, 5-tetradecenes, etc.) and isomeric aldehyde (2-pentyldecanal, 2-butylundecanal, etc.) products formed during the hydroformylation of 7-tetradecene, as reported previously (Breckwoldt and Van der Gryp, 2018). The formation of

primary hydroformylation product 2-hexylnonanal increased with temperature up to 70°C before decreasing due to increasing formation of iso-products with higher temperature. Even at the maximum temperature of 90°C, isoalkenes reached no more than 5 mole%; therefore iso-products are comprised almost completely of corresponding isomeric aldehydes. This result justified the grouping of isoalkenes and isoaldehydes into the single iso-product pseudo-component. Thus, it appears that the product distribution results at the different reaction temperatures follow an apparent parallel reaction scheme due to the competing hydroformylation and isomerisation-product pathways. It was therefore proposed in this study that the kinetics of the hydroformylation of post-metathesis product 7-tetradecene using Rh-tris(2,4-ditertbutylphenyl)-phosphite catalyst system can be described by the reaction scheme shown in **Figure 2** and the system of interdependent ordinary differential mole balance equations (**Equations 1-3**).

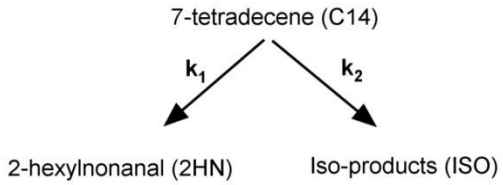

Figure 2: Parallel reaction scheme for the hydroformylation of 7-tetradecene.

$$\frac{d(C_{C14})}{dt} = -k_{1(obs)}C_{C14} - k_{2(obs)}C_{C14} \qquad (1)$$

$$\frac{d(C_{2HN})}{dt} = k_{1(obs)}C_{C14} \qquad (2)$$

$$\frac{d(C_{ISO})}{dt} = k_{2(obs)}C_{C14} \qquad (3)$$

Where,

$k_{1(obs)}$ is the observed rate of consumption of 7-tetradecene to 2-hexylnonanal (h^{-1})

$k_{2(obs)}$ is the observed rate of consumption of 7-tetradecene to isomerisation products (h^{-1})

C_{C14} is the concentration of 7-tetradecene in the reactor ($mol.L^{-1}$)

C_{2HN} is the concentration of 2-hexylnonanal in the reactor ($mol.L^{-1}$)

C_{ISO} is the concentration of isomerisation products in the reactor ($mol.L^{-1}$)

Based on the proposed reaction scheme shown in **Figure 2**, the observed reaction rates (k_{obs}) for the different reaction temperatures were calculated by regression (see **Section 2.4**) and the results are summarized in **Table 3** (Entries 1-4). For brevity, the fitted results compared to the experimental distribution-time data at 70°C are shown in **Figure 3**, although the product-distribution results over the entire temperature range were found to be similarly well described. It is clear from these results that the proposed reaction scheme well describes the hydroformylation of post-metathesis product with Rh-tris(2,4-di-tertbutylphenyl)phosphite catalyst over the investigated temperature range.

Table 3: Observed rate constants for the hydroformylation of 7-tetradecene at different operating conditions.

Entry	T (°C)	P_{CO} (bar)	P_{H2} (bar)	Rh (mM)	Observed rate constant (h^{-1})	
					k_1	k_2
1	60	15	15	1.0	0.55 ± 0.03	0.001 ± 0.01
2	70	15	15	1.0	0.88 ± 0.02	0.02 ± 0.01
3	80	15	15	1.0	2.00 ± 0.12	0.20 ± 0.03
4	90	15	15	1.0	4.11 ± 0.45	0.88 ± 0.12
5	70	15	15	0.7	0.44 ± 0.02	0.03 ± 0.01
6	70	15	15	0.5	0.13± 0.002	0.01 ± 0.002
7	70	15	20	1.0	0.93 ± 0.18	0.05 ± 0.04
8	70	15	25	1.0	0.97 ± 0.06	0.05 ±0.02
9	70	25	15	1.0	0.64 ± 0.02	0.02 ± 0.001

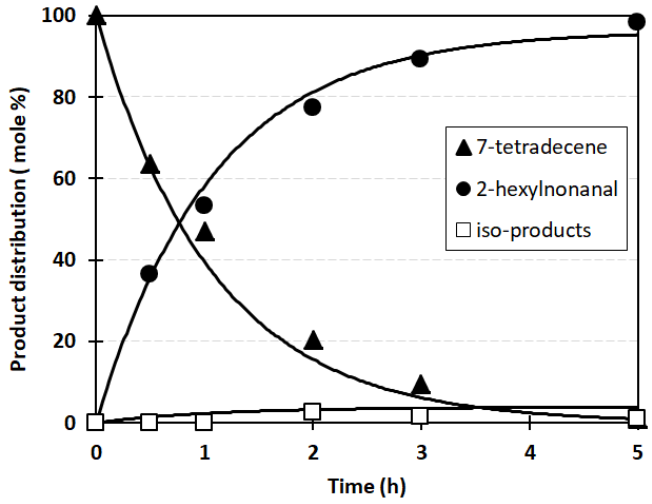

Figure 3: Comparison of experimental data with proposed reaction scheme. Result shown at 70°C and 30 bar (H_2:CO, 1:1) at 1 mM catalyst concentration.

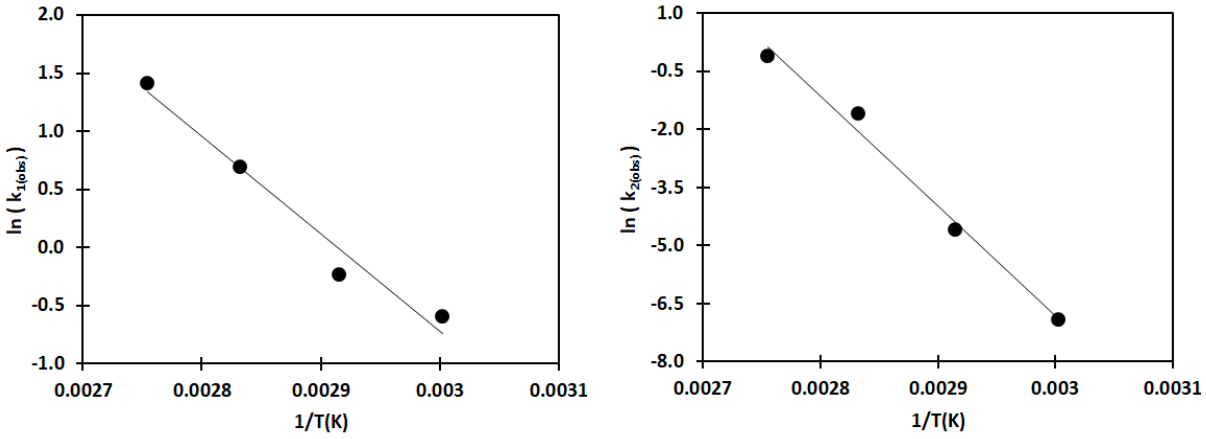

Figure 4: Arrhenius plots for the observed reaction rate constants for the hydroformylation of 7-tetradecene.

From the observed reaction rate constants at the different temperatures, the activation energies were determined from the slope of the Arrhenius plots, as shown in **Figure 4**, with magnitudes of 68 kJ.mol^{-1} and 229 kJ.mol^{-1}, for the hydroformylation and iso-products, respectively. The magnitude of the hydroformylation activation energy in this study is comparable to that previously reported for the hydroformylation of 7-tetradecene using biphasic Rh-TPPTS catalyst (70 kJ.mol^{-1}) (Haumann et al., 2002). Comparably lower activation energies (49-57 kJ.mol^{-1}) were observed during the hydroformylation of other long-chain linear terminal alkenes (1-decene and 1-dodecene) using homogeneous hydroformylation catalysts (Bhanage et al., 1997; Divekar et al., 1993). These results suggest a higher energy barrier for the hydroformylation of the linear internal alkene as compared to the terminal alkenes, as is to be expected due to lower reactivity of the internal double bond. The activation energy for the isomerisation reaction in this study is high, probably due to thermodynamic reasons, since the equilibrium lies against the isomerisation of the internal alkene double toward the more terminal alkene. It is furthermore clear from the magnitudes of activation energies that the hydroformylation of 7-tetradecene should be operated at a low temperature, preferably below 70°C. If the temperature is raised, the isomerisation products will become energetically favoured ($E_2 > E_1$) and iso-product formation will increase. This correlates well with the experimental results in **Figure 1**, which showed that for temperatures below 70°C, iso-products are suppressed, while at higher temperatures, iso-products become significant. At 80°C, for example, 2-hexylnonanal formation decreased to 89% from 98% at 70°C due to an increase in iso-products formed at the higher temperature.

3.2 Influence of catalyst concentration

The influence of catalyst concentration on the reaction kinetics was investigated by varying the catalyst concentration between 0.5 to 1 mM while keeping all other reaction conditions constant as per the standard reaction conditions at 70°C, 30 bar ($CO:H_2$, 1:1), ligand-to-metal molar ratio of 20 and initial 7-tetradecene concentration of 1 M. Results are shown in **Figure 5**.

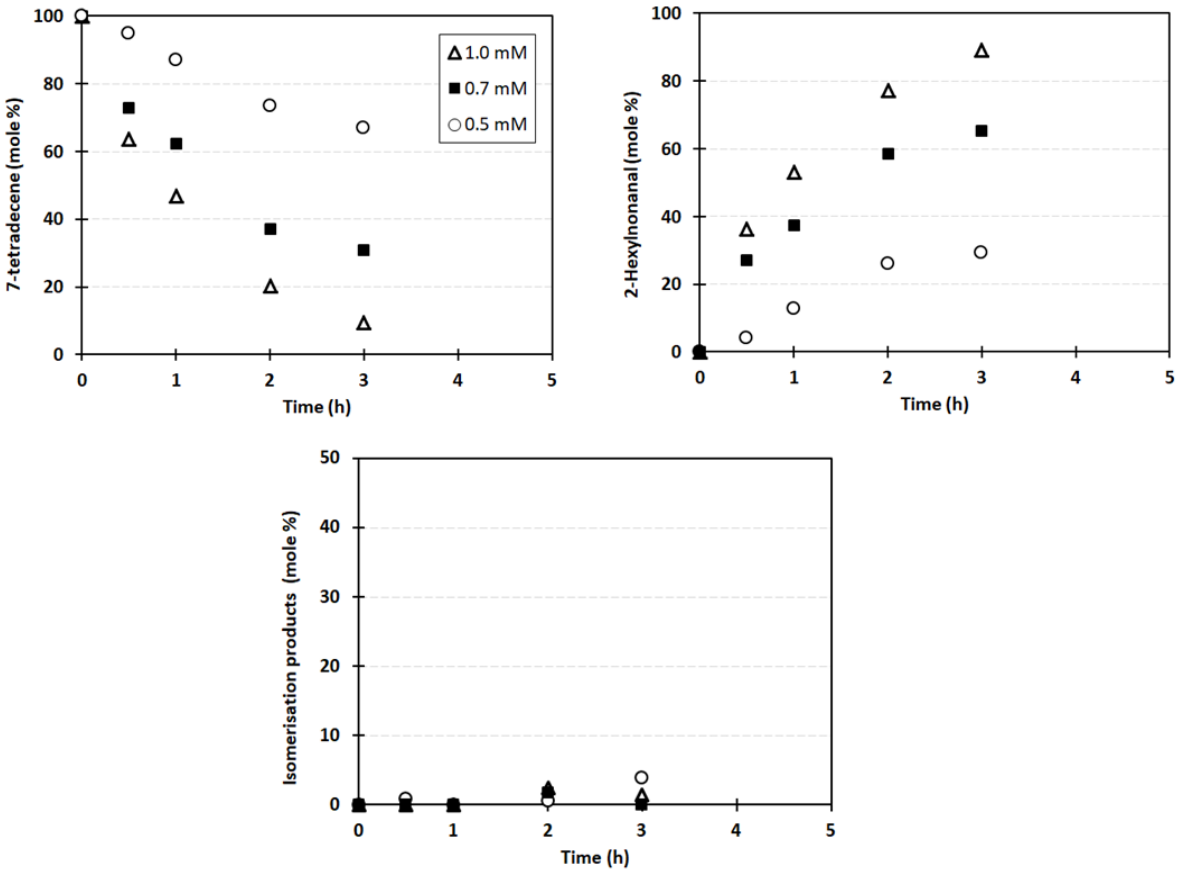

Figure 5: Influence of catalyst concentration on the hydroformylation of 7-tetradecene using bulky phosphite catalyst at 70°C, 30 bar (H_2:CO , 1:1) and ligand-to-metal molar ratio of 20.

The formation of the hydroformylation product 2-hexylnonanal increased with increasing concentration of the catalyst. This is to be expected from the hydroformylation mechanism as increasing the catalyst concentration will increase the amount of active catalyst species, thus leading to higher reaction rates. The hydroformylation products increased three-fold over 3 h (30 to 89%) by doubling the catalyst concentration. Iso-products were insignificant due to the chosen low operating temperature (70°C). It was furthermore observed that hydroformylation rate was negligible below a certain critical concentration, where after the rate increased linearly

with increasing catalyst concentration (**Table 3**, Entries 2, 5 and 6). The value of the critical concentration, below which the reaction would not proceed, was estimated from linear extrapolation of the observed reaction rates with varied catalyst concentrations and found to be 0.4 mM. Deshpande et al. (1988, 1989) similarly observed a critical catalyst concentration for the rhodium-catalysed hydroformylation of 1-hexene and vinyl acetate, beyond which the rate of reaction increased with first-order dependence in catalyst concentration. They proposed that this could be a result of substrate-inhibition kinetics due to the formation of inactive rhodium species at a high alkene concentration relative to the catalyst; however, the reason for this still remains unclear.

3.3 Influence of hydrogen and carbon monoxide partial pressures

In order to determine the influence of hydrogen and carbon monoxide partial pressures on the reaction kinetics, the equimolar syngas feed ($CO:H_2$, 1:1) was replaced with two separate hydrogen and carbon monoxide feed cylinders in order to provide the desired H_2:CO molar ratio.

3.3.1 Hydrogen partial pressure

The influence of hydrogen partial pressure on the hydroformylation reaction was evaluated at constant carbon monoxide partial pressure (15 bar), while all other parameters were kept constant as per standard conditions. Results are summarized in **Figure 6** and **Table 3** (Entries 2, 7 and 8).

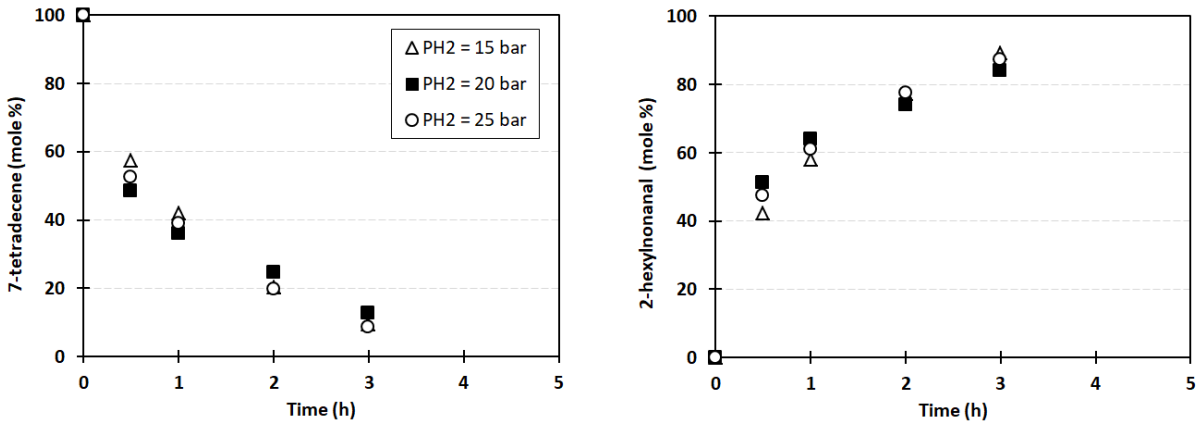

Figure 6: Influence of hydrogen partial pressure on the hydroformylation of 7-tetradecene using bulky phosphite catalyst at 1mM catalyst concentration and P_{CO} = 15 bar.

It appears from the results that the reaction remains unaffected by increasing the hydrogen partial pressure within the investigated range (15 to 25 bar). Hydrogen pressure independence was also observed previously by Guven et al. (2014) using bulky phosphite modified catalyst. This may be explained by considering that the rhodium complex $HRh(CO)_3L$ (L = bulky phosphite) remains the resting state of the catalyst as was observed previously via *in situ* studies (Jongsma et al., 1991) and that the rate-determining step occurs early on during the hydroformylation mechanism (Van Rooy et al., 1995). Probably, the large steric hindrance of the bulky alkyl groups of the alkene surrounding the internal double bond affects this overall reaction rate.

3.3.2 Carbon monoxide partial pressure

Increasing the carbon monoxide pressure from 15 to 25 bar at constant hydrogen partial pressure (15 bar) appears to have a negative influence on the hydroformylation of 7-tetradecene with bulky phosphite catalyst (**Figure 7**).

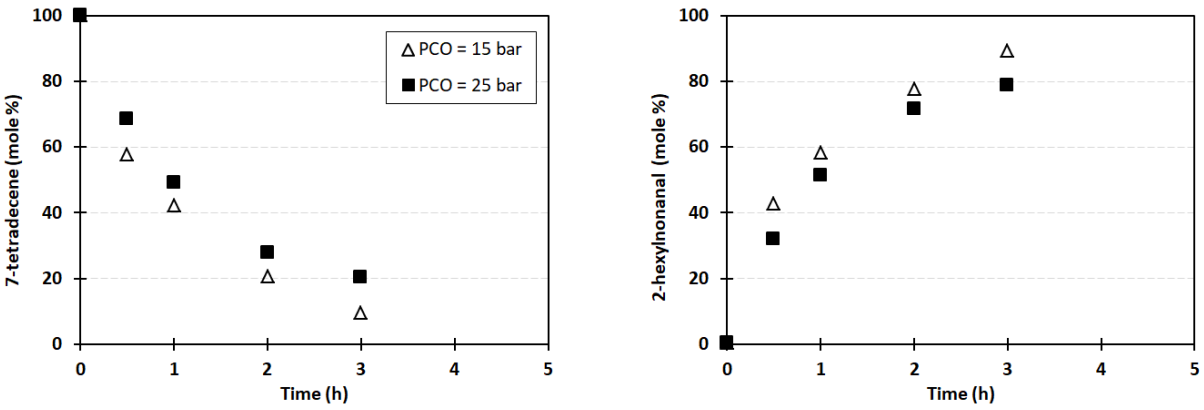

Figure 7: Influence of carbon monoxide partial pressure on the hydroformylation of 7-tetradecene using bulky phosphite catalyst at 1mM catalyst concentration and P_{H2} = 15 bar.

After 3 h, the 2-hexylnonanal product formation decreased by increasing the carbon monoxide partial pressure (90% at 15 bar to 80% at 25 bar). This behaviour is to be expected for the hydroformylation reaction using bulky phosphite-modified catalyst due to the preferred resting state of the catalyst being the $HRh(CO)_3L$ complex, as evidenced by IR (Kamer et al., 2004). Consequently, an equilibrium dissociation of a single CO molecule is required to yield the catalytically active co-ordinatively unsaturated $HRh(CO)_2L$ complex to allow co-ordination of the alkene to the metal. Increasing the partial pressure of carbon monoxide therefore shifts the

equilibrium towards the resting state species which reduces the number of catalytically active species present during the reaction, thereby decreasing the observed reaction rate. Variation of the carbon monoxide pressure had no notable influence on iso-product formation since iso-products remained insignificant due to the chosen low temperature. Observed reaction rate constants were calculated at the different carbon monoxide pressures and are given in **Table 3** (Entries 2 and 9). From the observed rate constants, it is confirmed that the rate of hydroformylation is inhibited with increasing carbon monoxide pressure (k_{obs} decreases from 0.88 ± 0.02 at 15 bar to 0.64 ± 0.02 at 25 bar).

3.4 Modelling of the reaction rate

The mechanistic cycle proposed by the group of Van Leeuwen (Van Rooy et al., 1995; Van Rooy et al., 1996) for the hydroformylation reaction using bulky phosphite ligand (**Figure 8**) was considered in order to describe the kinetics of the hydroformylation of 7-tetradecene observed at the different operating conditions (**Table 3**). The general hydroformylation mechanism begins with dissociation of single carbonyl ligand from the resting tricarbonyl complex **1** to yield the 16-electron, catalytically active metal-hydride complex **2**, which allows reversible alkene coordination to yield the π-complex **3**. Hydride migration of **3** with the alkene gives the unsaturated rhodium-alkyl complex **4**. Subsequent carbon monoxide coordination is required to yield the saturated rhodium-alkyl complex **5**, and generates the 16-elecltron rhodium-acyl species **6** via migratory insertion of carbon monoxide. Complex **6** may undergo hydrogenolysis to produce the product aldehyde and regeneration of catalytically active 16-electron complex **2**. Alternatively, **6** may coordinate with another carbon monoxide molecule to form the 18-electron acyl complex **7** in equilibrium with **6** (Kubis et al., 2012). Even though the reaction mechanism involves a number of reaction steps and theoretical studies predict that transition states involving both alkene coordination and migratory insertion of the alkene into the rhodium-hydrides species do exist (Zuidema et al., 2008), the simplified reaction steps given by **Equations 4-6** were sufficient in order to derive the rate equation, where $HRhL(CO)_2(alkene^*)$ represents an approximation of the rate-determining transition-state.

$$HRhL(CO)_3 \underset{k_{-1}}{\overset{k_1}{\rightleftharpoons}} HRhL(CO)_2 + CO \qquad (\mathbf{4})$$

$$HRhL(CO)_2 + \text{alkene} \xrightarrow{k} HRhL(CO)_2(alkene^*) \qquad (\mathbf{5})$$

$$HRhL(CO)_2(alkene^*) + CO + H_2 \xrightarrow{fast} HRhL(CO)_2 + \text{aldehyde} \qquad (\mathbf{6})$$

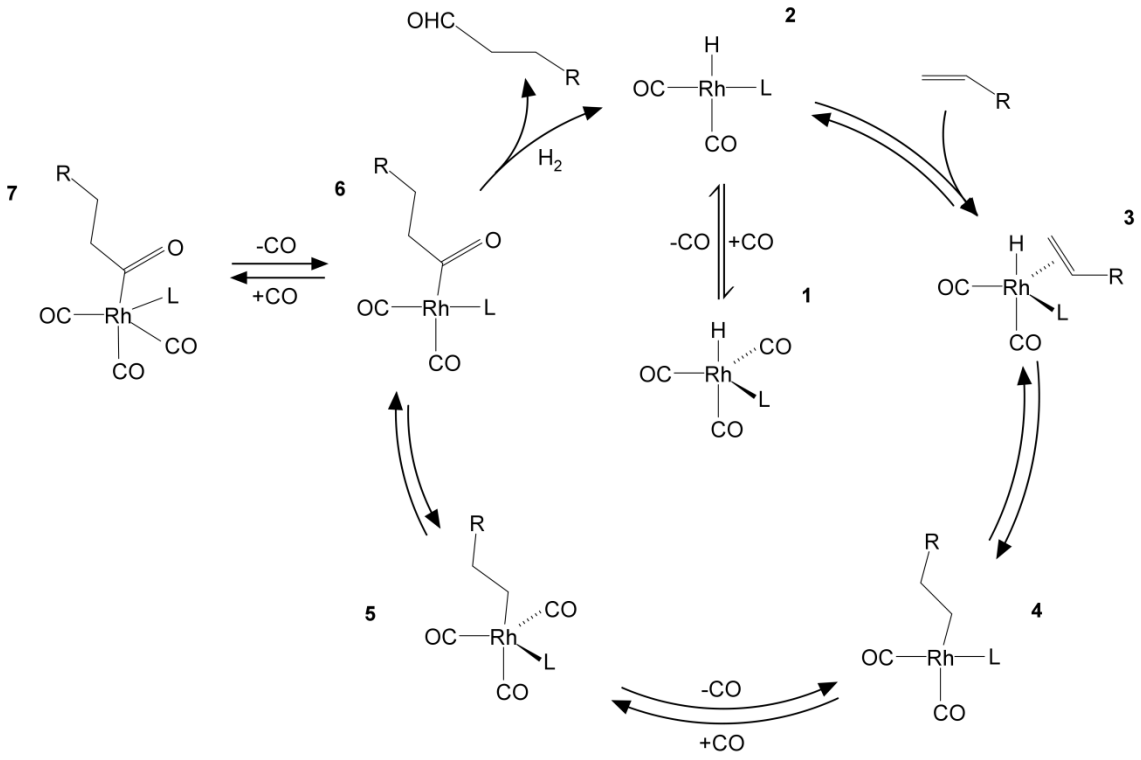

Figure 8: Reaction mechanism for the rhodium-catalysed hydroformylation reaction using bulky phosphite ligand (Van Rooy et al., 1995; Van Rooy et al., 1996).

It follows that the carbon monoxide dissociation (**Equation 4**) therefore exists as a pre-equilibrium step, while **Equation 6** is fast. Consequently, the concentrations of pre-equilibrium species are relatable by **Equation 7**, and the total concentration of the rhodium catalyst at any point in the cycle is given by **Equation 8**.

$$[HRhL(CO)_2][CO] = K_1[HRhL(CO)_3] \qquad (\mathbf{7})$$

$$[Rh] = [HRhL(CO)_2] + [HRhL(CO)_3] \qquad (\mathbf{8})$$

It thus also follows from **Equation 5**, that the rate of hydroformylation can be expressed as:

$$r_{Hydro} = k[alkene][HRhL(CO)_2] \qquad (\mathbf{9})$$

Combining **Equations 7-9** it can be shown that the rate of hydroformylation becomes:

$$r_{Hydro} = \frac{k[Rh][alkene]}{1 + K[CO]} \qquad (\mathbf{10})$$

As can be seen from **Equation 10**, the derived mechanism-based rate model does not explicitly account for the critical catalyst concentration observed in this study (see Section 3.2). The reason for this is probably the simplicity of the reaction steps in **Equations 7-9** accounting for the overall reaction rate. A critical catalyst concentration correction term (Rh_c) was therefore introduced into the rate model in order to explicitly account for the observed critical catalyst concentration (below which no reaction occurs) and to preserve the linear dependence observed in the experiments above the estimated Rh_c (0.4 mM).

$$r_{Hydro} = \frac{k[Rh - Rh_c][alkene]}{1 + K[CO]} \qquad (\mathbf{11})^{**}$$

The observed reaction rates for the hydroformylation of 7-tetradecene are therefore consistent with the modified mechanism-based model (**Equation 11**), i.e. the reaction rate was found to be first-order in alkene and catalyst concentrations (above the critical catalyst concentration), negative-order in carbon monoxide concentration and zero-order in hydrogen.

The rate of formation of iso-products was modelled as a semi-empirical first-order reaction (**Equation 12**) since the hydroformylation of isoalkenes to corresponding isoaldehydes occurred extremely rapidly; therefore, the rate of iso-product formation is attributed to the rate of isomerisation, and an additional rate constant for the hydroformylation of isoalkenes to isoaldehydes was not necessary. This was justified in earlier discussions due to the low isoalkene formations with respect to isoaldehydes observed across the entire alkene conversion range due to rapid conversion thereof to isoaldehydes. Other researchers similarly found that the rate of isomerisation under hydroformylation conditions could be modelled as a first-order type of reaction (Koeken et al., 2011).

$$r_{Iso} = k[Rh - Rh_c][alkene] \qquad (\mathbf{12})$$

Based on this knowledge, fitting of the pre-exponential factors (k_0) of the Arrhenius Equation (**Equation 13**) and equilibrium constant (K) was determined through regression by minimizing the sum of square errors (SSE) of the objective function (**Equation 14**). The complete hydroformylation kinetics parameter set is summarized in **Table 4**. It should be noted that the frequency factor for the isomerisation reaction rate (k_2) is unusually high as other researchers report typical frequency factors in the order 10^6-10^{22} using different catalyst systems (Disser et al., 2005; Peschel et al., 2012; Kiedorf et al., 2014; Jörke et al., 2015). The higher frequency

**Model only valid above reported critical rhodium concentration (Rh_c)

factor calculated for this system might be attributed to the high sensitivity of temperature on the isomerisation reaction. This is also reflected by the high isomerisation activation energy due to isomerisation having negligible influence at temperatures below 70°C (k_{obs} < 0.02 h^{-1}), while isomerisation products become exponentially more significant with increasing the temperature (k_{obs} > 0.2 h^{-1}), possibly a result of other active species forming at these higher temperatures.

$$k = k_0 \exp\left(\frac{-E_A}{RT}\right) \qquad (\mathbf{13})$$

$$SSE = \sum_{i}^{n}\left(k_{obs,i\,(predicted)} - k_{obs,i\,(measured)}\right)^2 \qquad (\mathbf{14})$$

Table 4: Summary of kinetics parameters for the hydroformylation of 7-tetradecene.

Parameter	**k_1**	**k_2**
k_0 ($L.mol^{-1}.h^{-1}$)	1.25×10^{14}	1.53×10^{36}
E_A ($kJ.mol^{-1}$)	68.5	229.4
K ($L.mol^{-1}$)	26.5	-
SSE	0.021	0.013

Nevertheless, it is clear that the proposed rate model is able to well-describe the observed rate constants over the range of reaction conditions investigated, as indicated by the strong Pearson correlation coefficient (0.998) between experimentally observed and model-predicted reaction rates (**Figure 9**).

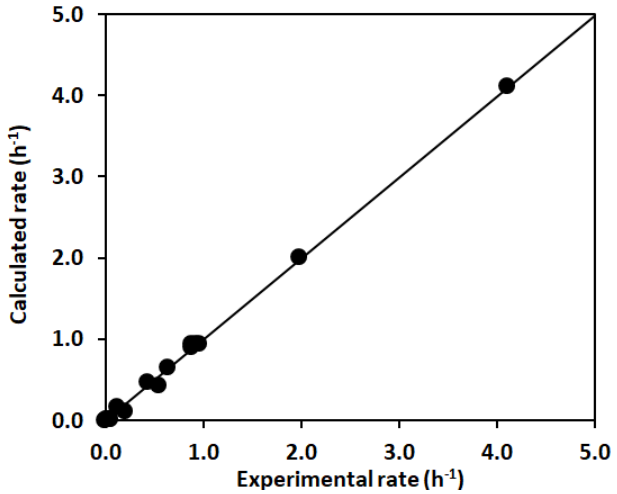

Figure 9: Parity plot showing the comparison of experimentally observed and model-predicted reaction rate constants.

4. Conclusions

Reaction engineering kinetics for the bulky phosphite-modified rhodium catalyst Rh-tris(2,4-ditertbutylphenyl)phosphite system were evaluated for the hydroformylation of the post-metathesis product 7-tetradecene. The reaction system was found to be well-described by a system of three ordinary differential mole balance equations and phenomenological mechanism-based hydroformylation rate law equation derived for bulky phosphite ligand coordinated to rhodium. The reaction rate was first order in alkene and catalyst concentration (above a critical catalyst concentration) and the reaction was independent of hydrogen partial pressure, which indicates that the rate-determining step occurs early in the mechanistic cycle. The reaction rate is inhibited with increasing carbon monoxide pressure. The activation energy for the hydroformylation reaction was determined to be 68 $kJ.mol^{-1}$ and an excellent correlation of mechanistic-based rate model and experimental rate data validates the theoretical approach used to describe the kinetics of this substrate-catalyst system. The kinetic modelling approach applied also takes benefit from the fact that kinetic data were generated over a wide alkene conversion range. Together with our previous work (Breckwoldt and Van der Gryp, 2018), the potential practical application of Rh-tris(2,4-ditertbutylphenyl)phosphite catalyst system for the industrial-scale hydroformylation of higher internal alkenes of the post-metathesis type, may be realized.

Conflicts of interest

There are no conflicts to declare.

Acknowledgements

The support of the DST-NRF Centre of Excellence in Catalysis (CoE) towards this research is hereby acknowledged. Opinions expressed and conclusions arrived at, are those of the author and are not necessarily to be attributed to the CoE. The authors also wish to thank the Department of Process Engineering, University of Stellenbosch for additional financial support.

References

Bhanage, B., Divekar, S., Deshpande, R. and Chaudhari, R. 1997. Kinetics of hydroformylation of l-dodecene using homogeneous HRh(CO)(PPh3)3 catalyst. Journal of Molecular Catalysis A: Chemical. 115, 247-257.

Breckwoldt, N. and Van der Gryp, P. 2018. Hydroformylation of post-metathesis product using commercial rhodium-based catalysts. Reaction Kinetics, Mechanisms and Catalysis. 125, 689-705.

Breit, B., Winde, R., Mackewitz, T., Paciello, R. and Harms, K. 2001. Phosphabenzenes as monodentate π-acceptor ligands for rhodium-catalyzed hydroformylation. Chemistry-A European Journal. 7, 3106-3121.

Cornils, B. and Hermann, W. (Eds.) 2002. Applied homogeneous catalysis with organometallic compounds. Wiley-VCH.

Deshpande, R. and Chaudhari, R. 1988. Kinetics of hydroformylation of 1-hexene using homogeneous HRh(CO)(PPh3)3 complex catalyst. Industrial and Engineering Chemistry Research. 27, 1996-2002.

Deshpande, R. and Chaudhari, R. 1989. Hydroformylation of vinyl acetate using homogeneous HRh (CO)(PPh3)3 catalyst: a kinetic study. Journal of Molecular Catalysis. 57, 177-191.

Deshpande, R., Bhanage, B., Divekar, S., Kanagasabapathy, S. and Chaudhari, R. 1998. Kinetics of hydroformylation of ethylene in a homogeneous medium: comparison in organic and aqueous systems. Industrial and Engineering Chemistry Research. 37, 2391-2396

Deshpande, R., Kelkar, A., Sharma, A., Julcour-Lebigue, C. and Delmas, H. 2011. Kinetics of hydroformylation of 1-octene in ionic liquid-organic biphasic media using rhodium sulfoxantphos catalyst. Chemical Engineering Science. 66, 1631-1639.

Disser, C., Muennich, C. and Luft, G. 2005. Hydroformylation of long-chain alkenes with new supported aqueous phase catalysts. Applied Catalysis A: General. 296, 201-208.

Divekar, S., Deshpande, R. and Chaudhari, R. 1993. Kinetics of hydroformylation of 1-decene using homogeneous HRh(CO)(PPh3)3 catalyst: a molecular level approach. Catalysis Letters. 21, 191-200.

Dry, M. 2002. The Fischer-Tropsch process: 1950–2000. Catalysis Today. 71, 227-241.

Du Toit, J., Jordaan, M., Huijsmans, C., Jordaan, J., van Sittert, C. and Vosloo, H. 2014. Improved metathesis lifetime: chelating pyridinyl-alcoholato ligands in the second generation Grubbs precatalyst. Molecules. 19, 5522-5537.

Du Toit, J., van der Gryp, P., Loock, M., Tole, T., Marx, S., Jordaan, J. and Vosloo, H. 2016. Industrial viability of homogeneous olefin metathesis: Beneficiation of linear alpha olefins with the diphenyl-substituted pyridinyl alcoholato ruthenium carbene precatalyst. Catalysis Today. 275, 191-200.

Fogler, H. 2014. Elements of chemical reaction engineering. Pearson Education.

Fox, J. 2015. Applied regression analysis and generalized linear models. Sage Publications.

Franke, R., Selent, D. and Börner, A. 2012. Applied hydroformylation. Chemical Reviews, 112, 5675-5732.

Güven, S., Hamers, B., Franke, R., Priske, M., Becker, M. and Vogt, D. 2014. Kinetics of cyclooctene hydroformylation for continuous homogeneous catalysis. Catalysis Science and Technology. 4, 524-530.

Haumann, M., Yildiz, H., Koch, H. and Schomäcker, R. 2002. Hydroformylation of 7-tetradecene using Rh-TPPTS in a microemulsion. Applied Catalysis A: General. 236, 173-178.

Jongsma, T., Challa, G. and Van Leeuwen, P. 1991. A mechanistic study of rhodium tri (ot-butylphenyl) phosphite complexes as hydroformylation catalysts. Journal of Organometallic Chemistry. 42, 121-128.

Jordaan, M. and Vosloo, H. 2007. Ruthenium catalyst with a chelating pyridinyl-alcoholato ligand for application in linear alkene metathesis. Advanced Synthesis and Catalysis. 349, 184-192.

Jörke, A., Triemer, S., Seidel-Morgenstern, A. and Hamel, C. 2015. Kinetic Investigation exploiting local parameter subset selection: isomerization of 1-decene using a Rh-biphephos catalyst. Chemie Ingenieur Technik. 87, 713-725.

Kamer, P., van Rooy, A., Schoemaker, G.C. and van Leeuwen, P. 2004. In situ mechanistic studies in rhodium catalyzed hydroformylation of alkenes. Coordination Chemistry Reviews. 248, 2409-2424.

Kiedorf, G., Hoang, D., Müller, A., Jörke, A., Markert, J., Arellano-Garcia, H., Seidel-Morgenstern, A. and Hamel, C. 2014. Kinetics of 1-dodecene hydroformylation in a thermomorphic solvent system using a rhodium-biphephos catalyst. Chemical Engineering Science. 115, 31-48.

Koeken, A., van den Broeke, L., Benes, N. and Keurentjes, J. 2011. Triphenylphosphine modified rhodium catalyst for hydroformylation in supercritical carbon dioxide. Journal of Molecular Catalysis A: Chemical. 346, 94-101.

Kubis, C., Sawall, M., Block, A., Neymeyr, K., Ludwig, R., Börner, A. and Selent, D. 2014. An operando FTIR spectroscopic and kinetic study of carbon monoxide pressure influence on rhodium-catalyzed olefin hydroformylation. Chemistry–A European Journal. 20, 11921-11931.

Kubis, C., Selent, D., Sawall, M., Ludwig, R., Neymeyr, K., Baumann, W., Franke, R. and Börner, A. 2012. Exploring between the extremes: conversion-dependent kinetics of phosphite-modified hydroformylation catalysis. Chemistry-A European Journal. 18, 8780-8794.

Mol, J. 2004. Industrial applications of olefin metathesis. Journal of Molecular Catalysis A: Chemical. 213, 39-45.

Peschel, A., Hentschel, B., Freund, H. and Sundmacher, K. 2012. Design of optimal multiphase reactors exemplified on the hydroformylation of long chain alkenes. Chemical engineering journal. 188, 126-141.

Pruett, R. and Smith, J. 1969. Low-pressure system for producing normal aldehydes by hydroformylation of alpha-olefins. The Journal of Organic Chemistry. 34, 327-330.

Van der Gryp, P., Marx, S. and Vosloo, H. 2012. Experimental, DFT and kinetic study of 1-octene metathesis with Hoveyda–Grubbs second generation precatalyst. Journal of Molecular Catalysis A: Chemical. 355, 85-95.

Van Leeuwen, P. and Claver, C. (Eds.). 2002. Rhodium catalyzed hydroformylation (Vol. 22). Springer Science and Business Media.

Van Leeuwen, P. and Roobeek, C. 1983. Hydroformylation of less reactive olefins with modified rhodium catalysts. Journal of Organometallic Chemistry. 258, 343-350.

Van Rooy, A., de Bruijn, J., Roobeek, K., Kamer, P. and Van Leeuwen, P. 1996. Rhodium-catalysed hydroformylation of branched 1-alkenes; bulky phosphite vs. triphenylphosphine as modifying ligand. Journal of Organometallic Chemistry. 507, 69-73.

Van Rooy, A., Orij, E., Kamer, P. and van Leeuwen, P. 1995. Hydroformylation with a rhodium/bulky phosphite modified catalyst. A comparison of the catalyst behavior for Oct-1-ene, Cyclohexene, and Styrene. Organometallics. 14, 34-43.

Zoller, U. 2009. Handbook of detergents part F: Production. CRC Press.

Zuidema, E., Escorihuela, L., Eichelsheim, T., Carbó, J., Bo, C., Kamer, P. and Van Leeuwen, P. 2008. The Rate-Determining Step in the Rhodium–Xantphos-Catalysed Hydroformylation of 1-Octene. Chemistry-A European Journal. 14, 1843-1853.

CHAPTER 6

MANUSCRIPT 3

Hydroformylation of the post-metathesis product 7-tetradecene using rhodium(I) Schiff base derived precatalysts

Nicholas C.C. Breckwoldt[1] Neill J. Goosen[1], Percy Van der Gryp[2] and Gregory S. Smith[3]

[1]Department of Process Engineering, University of Stellenbosch, Private Bag X1, Matieland 7602, South Africa.

[2]School of Chemical and Minerals Engineering, Research Focus Area for Chemical Resource Beneficiation, North-West University, Hoffmann Street, Potchefstroom 2522, South Africa

[3]Department of Chemistry, University of Cape Town, Rondebosch, 7701, South Africa.

This chapter has been published in the form of a journal article:

Breckwoldt, N., Goosen, N., Van der Gryp, P. and Smith, G. 2019. Hydroformylation of the post-metathesis product 7-tetradecene using Schiff based derived rhodium(I) precatalysts. Journal of Applied Catalysis A: General. 573, 49-55.

Abstract

The rhodium-catalysed hydroformylation of the post-metathesis product 7-tetradecene using aryl- (**1**) and ferrocenyl- (**2**) Schiff base derived precatalyst complexes was investigated. It was found that the reaction temperature (75 to 115°C), pressure (30 to 60 bar, CO/H_2 = 0.5 - 2) and 7-tetradecene-to-precatalyst molar ratio (1000:1 to 6000:1) had a significant influence on the hydroformylation performance. Turnover numbers up to 4310 were observed and the selectivity data show a temperature and pressure-dependent conversion of 7-tetradecene to the primary branched aldehyde product 2-hexylnonanal and isomeric branched aldehydes. A cooperative effect between rhodium and ferrocene was observed as hydroformylation performance results obtained with the heterobimetallic precatalysts (**2**) differ from that achieved using the monometallic catalyst system (**1**) under mild reaction conditions. Both precatalysts performed optimally at a temperature of around 95°C. Lifetime studies with the precatalysts were conducted and the precatalysts were found to remain active over at least three consecutive reaction cycles.

1. Introduction

Hydroformylation is an important industrial reaction for the metal-catalysed conversion of alkenes with syngas (hydrogen and carbon monoxide) to produce aldehydes (Van Leeuwen and Claver, 2002; Frey, 2014). Several million tons of aldehydes are produced each year by means of the hydroformylation reaction, which in turn, serve as precursors to a wide variety of higher value products within pharmaceutical, detergent and plasticizer industries (Cornils and Hermann, 2002). The reaction is catalytically driven and current research focuses primarily on the use of well-defined rhodium or cobalt-based complexes as hydroformylation catalysts (Franke et al., 2012). In general, rhodium-based complexes are preferred owing to their higher reactivity and selectivities under more mild reaction conditions.

Rhodium complexes bearing hemilabile ligands have been widely studied in the field of catalysis due to their unique structural features and coordination properties (Adams and Weller, 2017). One particular interesting class of these types of ligands are the Schiff bases which are readily prepared via the condensation reaction of a primary amine and an aldehyde to produce imines (C=N) (Wilkinson et al., 2016). These ligands are important in chemistry for the preparation of Schiff base derived metal complexes and have been applied in a variety of transition-metal catalysed reactions as reviewed by Abu-Dief and Mohamed (2015), including polymerisation, oxidation, hydrosilylation, epoxidation and Diels-Alder reactions, amongst others. Furthermore, Schiff base derived metal complexes often demonstrate excellent thermal stability under high temperature conditions and are stable in the presence of air and moisture; such properties contributing significantly toward their successful application as catalytic metal complexes (Gupta and Sutar, 2008).

The incorporation of a second different metal yielding a heterobimetallic catalyst system has also been suggested recently as a promising catalyst design strategy and is motivated by the premise that two different metals in close proximity might lead to cooperative effects (Van der Vlugt, 2012; Buchwalter et al., 2015). In particular, the incorporation of relatively inexpensive and abundantly available first-row transition-metal metallocenes such as ferrocene is a candidate of interest and has been often reported as an ancillary with rhodium to yield hydroformylation precatalysts (Lally et al., 2000; Hierso et al., 2004; Trzeciak et al., 2005; Peng et al., 2008; Kuhnert et al., 2008; Bebbington et al., 2010; Madalska et al., 2014; Stockmann et al., 2014).

Using the above-described catalyst design concepts, our group has recently prepared and evaluated the performance of several novel rhodium(I) hydroformylation precatalyst complexes bearing Schiff base derived N^O chelates (**Figure 1**) (Hager et al., 2012; Maqeda et al., 2015;

Matsinha et al., 2015; Siangwata et al., 2015; Siangwata et al., 2016). These precatalysts have shown excellent activity and chemoselectivity in the hydroformylation of 1-octene to corresponding aldehydes, which in turn, serve as valuable intermediates for the preparation of plasticizer alcohols such as diiso-nonyl phthalate (Taddei and Mann, 2013).

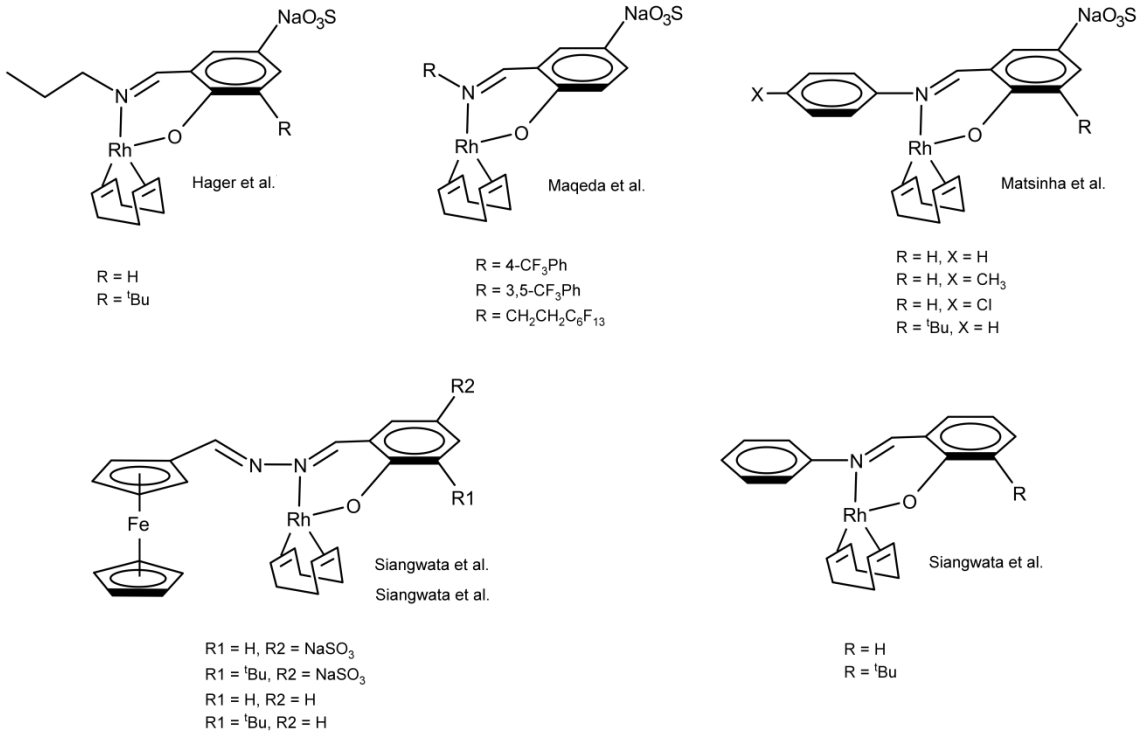

Figure 1: Schiff base derived rhodium(I) hydroformylation precatalysts available in the literature.

Although the hydroformylation of α-alkenes was quite extensively studied, interest in the hydroformylation of internal alkenes has also increased significantly in the industrial context, as several important feedstocks, such as Raffinate II streams (i.e. internal butene mixtures) derived from the steam cracking process (Van Leeuwen and Claver, 2002) and alkene streams produced via Fischer-Tropsch synthesis (De Klerk, 2011) contain internal alkenes. Therefore, catalyst systems which display high activity in the hydroformylation of internal alkenes and selectivity towards either linear or branched aldehydes have been the subject of high demand in this area (Clark, 2015). We were therefore prompted to expand our application and evaluation of monometallic and heterobimetallic Schiff base derived complexes as internal alkene hydroformylation catalysts. In line with our standing interest in the beneficiation of low value α-alkene feedstocks, such as the metathesis of 1-octene to synthetically valuable higher alkenes

(Jordaan et al., 2006; Jordaan et al., 2007; Van der Gryp et al., 2012; Du Toit et al., 2016), and subsequent functionalization thereof to high value products with a host of opportunities in the detergent/surfactant range (Breckwoldt and Van der Gryp, 2018), we decided to investigate the hydroformylation of the post-metathesis product 7-tetradecene using rhodium(I) aryl- (**1**) and ferrocenyl- (**2**) Schiff base derived precatalysts (**Figure 2**) (Siangwata et al., 2016).

It is therefore the aim of this study to evaluate and understand the reaction engineering of these hydroformylation precatalysts as applied to the hydroformylation of 7-tetradecene as a model internal alkene substrate system.

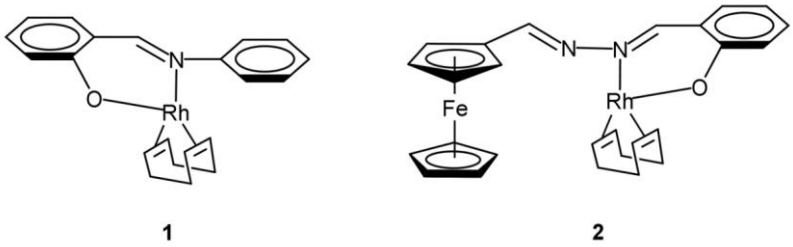

Figure 2: Schiff base derived aryl- (**1**) and ferrocenyl- (**2**) rhodium(I) precatalysts evaluated in this study.

2. Experimental

2.1 Preparation of precatalysts

The rhodium(I) aryl- (**1**) and ferrocenyl- (**2**) Schiff base derived precatalysts (**Figure 2**) were prepared according to previously reported methods (Siangwata et al., 2016).

2.2 Chemicals used

7-Tetradecene (>98%) was synthesized as reported by Van der Gryp et al. (2012) via 1-octene metathesis using Hoveyda-Grubbs second generation precatalyst (98%, Sigma-Aldrich). Toluene was used as reaction solvent (> 99%, ACE Chemicals). Syngas was used as received from Afrox Ltd.

2.3 Hydroformylation procedure

Hydroformylation experiments conducted with precatalysts **1** and **2** were performed in a 100 mL stainless steel reactor with Teflon insert, thermocouple-regulated temperature control and pressure gauge. In a typical reaction, toluene (6 mL), catalyst precursor (0.0097 mmol, 1.79 or 2.39 mg) and 7-tetradecene (9.69 mmol, 1.90 g) were added to the reaction vessel before being sealed and placed into an oil bath. The oil bath was then heated with stirring until reactor

contents had reached the desired temperature set-point. The reaction vessel was pressurized with syngas (CO/H_2) and the reaction allowed to proceed over the indicated reaction time. The resulting product distributions were determined via GC-MS according to analytical methods reported previously (Breckwoldt and Van der Gryp, 2018).

2.4 Lifetime studies

To evaluate the lifetime of the precatalysts, reactions were performed at 95°C, pressure of 40 bar ($CO:H_2$, 1:1) and initial 7-tetradecene-to-precatalyst molar ratio of 1000:1 (based on the first reaction). After each 8 hour reaction, the post-reaction mixture was sampled (10 uL) and fresh 7-tetradecene (1.90 g, 9.69 mmol) was added. This procedure was repeated over three reaction cycles. Between each cycle, the reactor was depressurized of syngas for sampling and fresh substrate addition, then flushed with syngas and re-pressurised to the desired operating pressure. Conversion (X) during the lifetime experiments was defined as follows:

$$X = \frac{N_{C14,consumed}}{N_{C14,added}} \times 100\%$$

Where,

$N_{C14,consumed}$ is the number of moles of 7-tetradecene consumed during the reaction

$N_{C14,add}$ is the number of moles of fresh 7-tetradecene added before the reaction

3. Results and discussion

3.1 Preliminary screening

As was reported previously (Siangwata et al., 2016), optimised reaction conditions to obtain high yields of aldehydes during the hydroformylation reaction using Schiff base derived precatalysts **1** and **2** were established at 95°C and 40 bar. Therefore, preliminary evaluations with **1** and **2** for the hydroformylation of 7-tetradecene were performed under these reaction conditions. In **Figure 3**, the reaction scheme for the hydroformylation of post-metathesis product 7-tetradecene is illustrated. The resulting product distributions were analysed according to the conversion of 7-tetradecene, corresponding aldehyde and isoalkene product formations and the turnover number (TON). The TON was calculated on the basis of the total aldehydes formed per mole of rhodium catalyst following the definition of TON proposed by Bligaard et al. (2016). Aldehydes were further characterised according to their content, as expressed by the 2HN:Iso ratio, i.e. the molar ratio of primary branched aldehyde product 2-hexylnonanal (2HN) and isoaldehydes (Iso) formed.

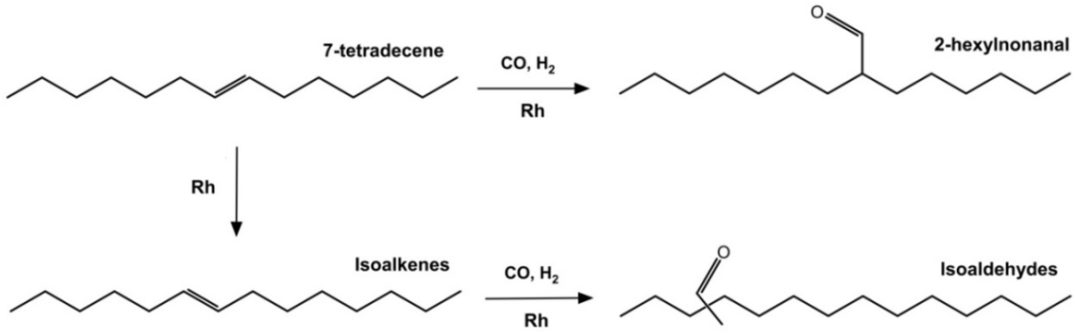

Figure 3: Hydroformylation of 7-tetradecene reaction network.

Both precatalysts were active in the hydroformylation of 7-tetradecene at 95°C as indicated by near complete conversions and a high chemoselectivity (above 87%) to aldehydes (**Table 1,** Entries 2 and 6). **Figure 4** gives a typical product-distribution-time profile showing the evolution of hydroformylation products formed during the hydroformylation reaction. Interestingly, little to no hydroformylation products were observed over the first two hours of the reaction which suggests that the precatalysts undergo an initial induction period. The existence of the induction period may be explained either as a result of the slow formation of the catalytically active rhodium-hydride complex, or alternatively, a vacant catalytically active site should be opened for migration of the sterically crowded internal double bond to the metal. Thereafter, consumption of 7-tetradecene resulted in the formation of 2-hexylnonanal, isomeric alkenes and isomeric aldehyde products. All the isomeric aldehydes were grouped together into a single pseudo-component termed "isoaldehydes". Isomerisation of 7-tetradecene was also observed in parallel to the hydroformylation reaction and lead to the formation of isomeric tetradecenes which were grouped together as "isoalkenes". The rate of isomerisation of 7-tetradecene to isoalkenes was significant during the first two hours of the reaction after catalyst induction, after which isoalkenes reach a maximum of around 20%. Thereafter, the hydroformylation of isoalkenes to corresponding isoaldehydes predominates and contributes towards isoaldehydes being the major hydroformylation product at the end of the reaction.

Table 1: Influence of temperature on hydroformylation reaction.[a]

Entry	Precatalyst	Temperature (°C)	Conv. (%)	Isoalkenes (%)	Aldehydes (%)[b]	(2HN:Iso)	TON
1	**1**	75	0	-	-	-	-
2	**1**	85	13	3	10	77:23	220
3	**1**	95	94	6	88	39:61	1930
4	**1**	105	94	7	87	41:59	1920
5	**1**	115	79	6	73	27:73	1610
6	**2**	75	0	-	-	-	-
7	**2**	85	88	11	77	51:49	1680
8	**2**	95	97	5	92	39:61	2030
9	**2**	105	97	3	94	32:68	2070
10	**2**	115	92	4	88	27:73	1930

[a]Reactions carried out at 40 bar ($CO:H_2$, 1:1) in toluene (6 mL) with 6.69 mmol of 7-tetradecene and 7-tetradecene-to-precatalyst molar ratio of 2200:1 over 8 hours. [b]Total aldehydes formed which includes the primary aldehyde product 2-hexylnonanal and isoaldehydes (expressed as mole percentage).

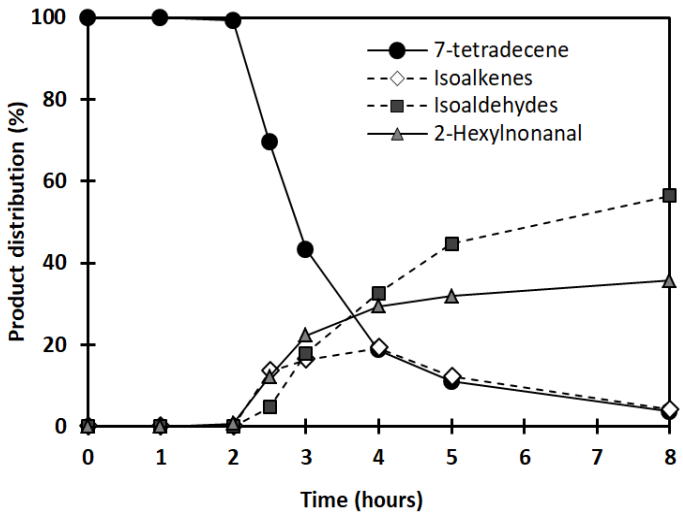

Figure 4: Production-distribution-time profiles for a typical hydroformylation reaction shown at 95°C and 40 bar ($CO:H_2$, 1:1) and 7-tetradecene-to-precatalyst molar ratio of 2200:1.

Regioselectivities (2HN/Iso) of 0.65 and 0.64 are observed after 8 hours for precatalysts **1** and **2**, respectively. The linear aldehyde product pentadecanal, formed via consecutive isomerisation reactions to the terminal alkene before hydroformylation, was detected in only minimal quantities of less than 5% of total aldehydes formed. Therefore, hydroformylation with

1 and **2** showed a preference for the branched aldehydes. In terms of hydroformylation activity, TONs of 1914 and 2016 were calculated for precatalysts **1** and **2**, respectively, which are comparable to that reported for 1-octene hydroformylation under similar reaction conditions (Siangwata et al., 2016). High TONs account for the high reactivity of the internal double bond using precatalyst **1** and **2**. These N^O chelate systems, however, show lower regioselectivity toward the primary aldehyde product 2-hexylnonanal when compared to previously reported monophosphine and monophosphite catalyst systems evaluated for 7-tetradecene hydroformylation (Breckwoldt and Van der Gryp, 2018). This is probably because the N^O chelate systems are only activated at comparably higher temperatures. Lazzaroni and co-workers (Lazzaroni et al., 1989) found that isomerisation is due to a β-hydride elimination of secondary alkyl species and is more favourable at high temperatures.

3.2 Influence of reaction temperature

The influence of temperature on the catalytic performance of precatalysts **1** and **2** was investigated by varying the temperature between 75 and 115°C while keeping a constant pressure (40 bar and $CO:H_2$, 1:1). Results are shown in **Table 1** (Entries 1-10) and **Figure 5**. At the lowest temperature of 75°C, no hydroformylation products were observed for both precatalysts after 8 hours. This can possibly be explained due to the strong co-ordination of the N^O chelate ligands to the rhodium centre that inhibits activation of internal double bond with the metal and leads to a much longer induction period. Higher temperatures are therefore required in order to activate the internal double bond with the precatalyst and to generate product turnovers. Interestingly, operating at a higher temperature of 85°C gave TONs of 208 and 1653 for precatalysts **1** and **2**, respectively, and indicates that heterobimetalilc catalyst system (**2**) performs better than the monometallic system (**1**), at least under these conditions. This is most likely due to the presence of the ferrocenyl group where ferrocene acts as an electron reservoir (Feringa and Van den Beuken, 1998; Park and Hong, 2012), thus stabilizing the electron density around the catalytically active rhodium centre via the conjugated imine π-electron system. This effect could lower the activation energy barrier of the reaction, thus leading to higher reaction rates. Other authors similarly observed improved catalytic activities when employing ferrocenyl-based ligands under mild conditions compared to their monometallic analogues (Stockmann et al., 2014).

As the temperature increases from 85 to 105°C, the TON increased and near quantitative conversion of 7-tetradecene (ca. 94%) was achieved. However, the TON starts to decrease as the temperature is increased further to 115°C and might be attributed to one of two factors; either degradation of the catalyst due to the high temperature environment or decreasing solubility of syngas in the reaction medium at the high temperature which could lower the accessibility of

syngas, thereby also lowering the hydroformylation rate. The regioselectivity (2HN:Iso) also decreases with temperature due to a decrease in primary aldehyde 2-hexylnonanal formation while isoaldehyde formation increases. These observations appear to suggest an optimum temperature for the hydroformylation of 7-tetradecene using precatalysts **1** and **2**. In terms of both TON and selectivity (chemo- and regio-), the optimum temperature is at around 95°C.

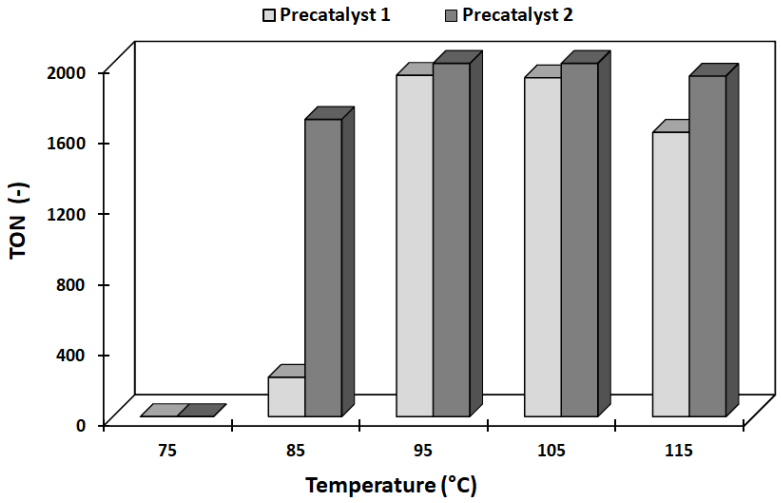

Figure 5: Influence of reaction temperature on the TON. Reactions performed at 40 bar ($CO:H_2$, 1:1) in toluene with 7-tetradecene-to-precatalyst molar ratio of 2200:1 over 8 hours.

3.3 Influence of catalyst loading

Hydroformylation precatalysts such as **1** and **2** are expensive to prepare and apply in an industrial context due the expensive rhodium content. It is therefore important from an economic point of view to investigate the influence of catalyst loading on the performance of the hydroformylation reaction. The influence of the precatalyst loading was investigated by varying the 7-tetradecene-to-precatalyst molar ratio in the range 1000:1 to 6000:1 under standard conditions (95°C and 40 bar). The results are summarized in **Table 2** and **Figure 6**.

It is clear from the results that as the 7-tetradecene-to-precatalyst molar ratio increases with precatalyst **1**, i.e. as the amount of precatalyst used decreases, aldehyde product formation decreases (~87% at 1000:1 to 70% at 6000:1). Similarly using precatalyst **2,** aldehyde formation decreases with increasing 7-tetradecene-to-precatalyst molar ratio (~96% at 1000:1 to 66% at 6000:1). Variation of the precatalyst loading had little effect on the regioselectivity of the reaction as can be seen from **Figure 6** with relatively constant 2HN/Iso ratios over the precatalyst loading range. The precatalyst loading did, however, have a significant influence on

the TON. The TON increased linearly with increasing 7-tetradecene-to-precatalyst molar and indicates that more substrate is consumed per catalytically active rhodium species at a lower precatalyst concentration. TONs up to 4220 were observed, which are to our knowledge, the highest reported using similar rhodium(I) hydroformylation precatalysts bearing N^O chelates (Hager et al., 2012; Maqeda et al., 2015; Matsinha et al., 2015; Siangwata et al., 2015; Siangwata et al., 2016).

Table 2: Influence of catalyst loading on the hydroformylation reaction.[a]

Precatalyst	7-tetradecene-to-pecatalyst	Conv. (%)	Isoalkene (%)	Aldehydes (%)[b]	(2H:Iso)	TON
1	1000	93	5	88	41:59	880
1	2200	94	6	88	39:61	1930
1	4000	92	9	83	40:60	3320
1	6000	87	15	72	42:58	4310
2	1000	98	2	96	38:62	960
2	2200	97	5	92	39:61	2030
2	4000	94	6	88	38:62	3500
2	6000	82	14	68	41:59	4070

[a]Reactions carried out at 95°C and 40 bar ($CO:H_2$, 1:1) in toluene (6 mL) with 6.69 mmol of 7-tetradecene over 8 hours.
[b]Total aldehydes formed which includes the primary aldehyde product 2-hexylnonanal and isoaldehydes (expressed as mole percentage).

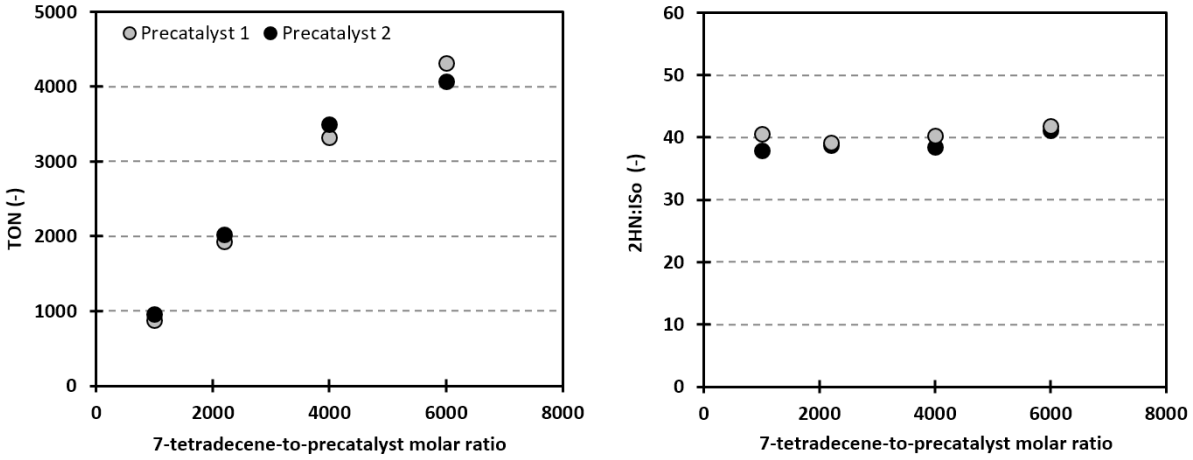

Figure 6: Influence of precatalyst load on hydroformylation performance. Reactions performed at 95°C and 40 bar ($CO:H_2$, 1:1) in toluene over 8 hours.

3.4 Influence of pressure

Additional hydroformylation experiments were performed in order to determine the influence of pressure on the hydroformylation reaction using precatalysts **1** and **2**, as shown in **Table 3**. Increasing the pressure from 30 to 50 bar while keeping the temperature (95°C) and CO:H_2 ratio (1:1) constant gave improved conversion and chemoselectivity to aldehydes when using both precatalysts, which in turn, resulted in higher TONs (**Table 1**, Entries 1-6). This is to be expected as increasing the pressure will improve the solubility and accessibility of gaseous reagents (H_2 and CO), thus leading to increased hydroformylation reaction rates. In addition to increased activity, the regioselectivity was also improved in favour of the primary aldehyde product 2-hexylnonanal by increasing the syngas pressure (2HN/Iso of 0.57 at 30 bar to 0.78 at 50 bar with **1** and 0.48 at 30 bar to 0.78 at 50 bar with **2**). This can be attributed to a decreased level of alkene isomerisation occurring at the higher pressures. It is worthy of mention that no hydrogenation products were observed within the investigated pressure range. It is therefore clear from an operational point of view that the reaction preferably be operated at a higher pressure. Since near quantitative conversion of 7-tetradecene was observed at the higher pressures after 8 hours, the reaction time was reduced in a further study and the influence of hydrogen and carbon monoxide pressures on the hydroformylation reaction were separately investigated (**Table 1**, Entries 7-9). By doubling only the hydrogen partial pressure, all of the 7-tetradecene was converted completely to aldehydes with maximum TON (2200) after just 5 h and the regioselectivity was also improved compared to the equimolar (1:1) syngas feed (**Table 1**, Entry 8 vs. 7). Therefore, hydrogen partial pressure positively influences the reaction rate and could indicate that oxidative dihydrogen addition to the rhodium acyl species is rate-determining. Doubling the carbon monoxide pressure also led to an improvement in the TON (**Table 1**, Entry 9 vs. 7). As expected, increasing the carbon monoxide pressure leads to improved regioselectivity due to suppressing the β-hydride elimination reaction of the rhodium-alkyl species; presumably the carbon monoxide insertion preferably takes place at higher carbon monoxide pressure.

Table 3: Influence of reaction pressure on the hydroformylation reaction.[a]

Entry	Precatalyst	P_{H2} (bar)	P_{CO} (bar)	Conv. (%)	Iso-C14 (%)	Aldehydes (%)[b]	(2HN:Iso)	TON
1	**1**	15	15	67	18	49	36:64	1070
2	**1**	20	20	94	6	88	39:61	1930
3	**1**	25	25	99	2	97	44:56	2140
4	**2**	15	15	89	14	75	33:67	1640
5	**2**	20	20	97	5	92	39:61	2030
6	**2**	25	25	99	0	99	43:57	2180
7	**2**[c]	20	20	89	12	77	42:58	1690
8	**2**[c]	40	20	100	0	100	47:53	2200
9	**2**[c]	20	40	97	0	97	49:51	2130

[a]Reactions carried out at 95°C in toluene (6 mL) with 6.69 mmol of 7-tetradecene and 7-tetradecene-to-precatalyst molar ratio of 2200:1 over 8 hours. [b]Total aldehydes formed which includes the primary aldehyde product 2-hexylnonanal and isoaldehydes (expressed as mole percentage). [c]Results after 5 hour reaction.

3.5 Catalyst lifetime

In considering the commercial use of homogeneous precatalysts such as **1** and **2**, the catalyst lifetime is an important factor to consider. In order to evaluate the lifetime of the precatalysts, a sequence of three consecutive reactions were performed in order to mimic a pseudo-continuous operation. Thus, at the end of each reaction, fresh 7-tetradecene (1.90 g, 9.69 mmol) was added to the post-reaction mixture which was then reused in the next catalytic run. Even though higher TONs were observed by operating at a high 7-tetradecene-to-precatalyst load (see Section 3.3) a lower 7-tetradecene-to-precatalyst load of 1000:1 (i.e. the maximum catalyst loading) was used in the lifetime study in order to ensure a reasonable catalyst concentration throughout each consecutive reaction. Results are shown in **Figure 7**. It is clear from these results that both precatalysts **1** and **2** were still active after second and third consecutive additions of 7-tetradecene. There is, however, a decrease in conversion observed across the consecutive reactions, mostly probably due to dilution of the catalyst concentration following addition of fresh alkene. Lowering the catalyst concentration lowers the accessibility of the substrate to the metal centre and leads to lower reaction rates. Beyond the 2nd run, an increase in conversion is observed and might be ascribed to a change in active catalytic species present during the reaction. Despite presumed change in catalytic species, an increase in the total cumulative TONs up to 1660 and 2110 was observed over the complete reaction cycle compared to TONs of 880 and 960 after a single reaction, for precatalysts **1** and **2**, respectively and confirms that the catalytically active species remains active for hydroformylation. Reactions performed in the presence of heterobimetallic precatalyst show potentially improved

hydroformylation performance compared to the monometallic precatalyst system as indicated by higher cumulative TON over the consecutive reaction cycles.

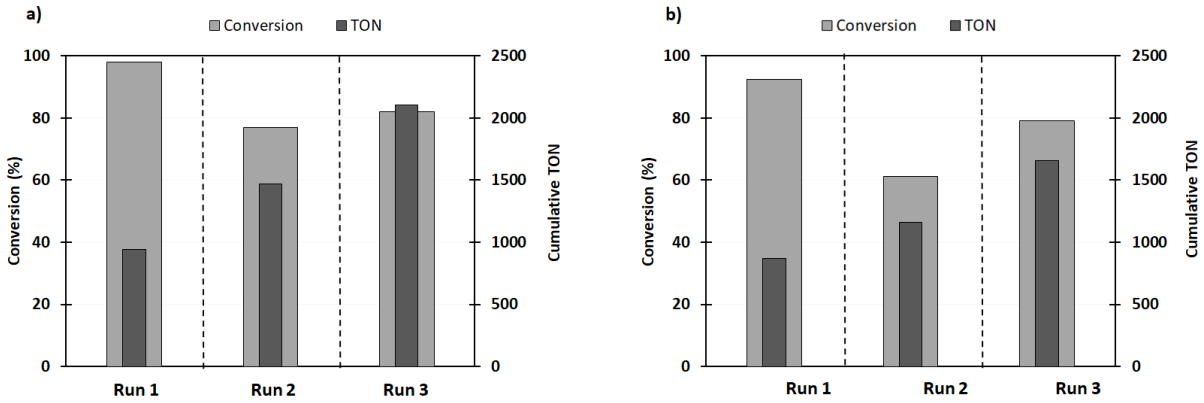

Figure 7: Catalyst life studies with a) precatalyst **2** and b) precatalyst **1**. Reactions performed at 95°C and 40 bar ($CO:H_2$, 1:1) and initial 7-tetradecene-to-precatalsyt molar ratio of 1000:1 over 8 hours.

4. Conclusions

In this study, the rhodium-catalysed hydroformylation of the post-metathesis product 7-tetradecene using aryl-(**1**) and ferrocenyl-(**2**) Schiff base derived precatalysts was evaluated by varying reaction operating conditions such as temperature (75-115°C), precatalyst loading (7-tetradecene-to-precatalyst molar ratio between 1000:1 and 6000:1) and total pressure (30-60 bar, CO/H_2 = 0.5-2). Turnover numbers up to 4220 were observed and product selectivities show that the precatalysts show temperature and pressure-dependent conversion of 7-tetradecene to both the primary branched aldehyde product 2-hexylnonanal and isomeric branched isoaldehydes. Even though precatalysts **1** and **2** show lower selectivities to the primary aldehyde product 2-hexylnonanal compared to commercial phosphorus-modified rhodium catalysts (Breckwoldt and Van der Gryp, 2018), it is no drawback, as the alkyl-branched isoaldehyde products may be of equal synthetic value. Further functionalization of these aldehydes to alcohols could be used for the production of detergent products with economic values roughly six times that of the olefinic feedstock (Dry, 2002). Furthermore, there is evidence to suggest a cooperative effect between two different metal centres as results obtained with the heterobimetallic precatalyst (**2**) differ from that achieved using the monometallic catalyst system (**1**) under mild reaction conditions. In terms of the lifetime of the

precatalysts, it was found that precatalysts **1** and **2** remain active after at least three reaction cycles under pseudo-continuous conditions, thus increasing the total TON achievable by each precatalyst. In the next phase of our study, we aim to evaluate the reaction engineering kinetics and rate law modelling using Schiff base derived precatalysts for the prototype post-metathesis product hydroformylation reaction system.

Acknowledgements

The support of the DST-NRF Centre of Excellence (CoE) in Catalysis towards this research is hereby acknowledged. Opinions expressed and conclusions arrived at, are those of the author and are not necessarily to be attributed to the CoE. The authors also wish to thank the University of Stellenbosch and University of Cape Town for additional financial support towards this research and Shepherd Siangwata for skilled guidance and assistance in preparing the precatalysts used for the study.

References

Abu-Dief, A. and Mohamed, I. 2015. A review on versatile applications of transition metal complexes incorporating Schiff bases. Beni-Suef University Journal of Basic and Applied Sciences. 4, 119-133.

Adams. G. and Weller A. 2017. POP-type ligands: Variable coordination and hemilabile behaviour. Coordination Chemistry Reviews. 355, 150-172.

Bebbington, M., Bontemps, S., Bouhadir, G., Hanton, M., Tooze, R., van Rensburg, H. and Bourissou, D. 2010. A 1,1′-ferrocenyl phosphine-borane: synthesis, structure and evaluation in Rh-catalyzed hydroformylation. New Journal of Chemistry. 34, 1556-1559.

Bligaard, T., Bullock, R., Campbell, C., Chen, J., Gates, B., Gorte, R., Jones, C., Jones, W., Kitchin, J. and Scott, S. 2016. Toward benchmarking in catalysis science: best practices, challenges, and opportunities. ACS Catalysis. 6, 2590-2602.

Breckwoldt, N. and Van der Gryp, P. 2018. Hydroformylation of post-metathesis product using commercial rhodium-based catalysts. Reaction Kinetics, Mechanisms and Catalysis. 125, 689-705.

Buchwalter, P., Rosé, J. and Braunstein, P. 2015. Multimetallic catalysis based on heterometallic complexes and clusters. Chemical Reviews. 115, 28-126.

Clarke, M. 2015. Branched selective hydroformylation: a useful tool for organic synthesis. Current Organic Chemistry. 9, 701-718.

Cornils, B. and Herrmann, W. (Eds.). 2002. Applied homogeneous catalysis with organometallic compounds (Vol. 4). Wiley-VCH.

De Klerk, A. 2011. Fischer-Tropsch refining. Wiley-VCH.

Dry, M. 2002. The Fischer-Tropsch process: 1950–2000. Catalysis Today. 71, 227-241.

Du Toit, J., Van der Gryp, P., Loock, M., Tole, T., Marx, S., Jordaan, J. and Vosloo, H. 2016. Industrial viability of homogeneous olefin metathesis: Beneficiation of linear alpha olefins with the diphenyl-substituted pyridinyl alcoholato ruthenium carbene precatalyst. Catalysis Today. 275, 191-200.

Franke, R. Selent, D. and Börner, A. 2012. Applied hydroformylation. Chemical Reviews. 112, 5675-5732.

Frey, G. 2014. 75 Years of oxo synthesis - The success story of a discovery at the OXEA Site Ruhrchemie. Journal of Organometallic Chemistry. 754, 5-7.

Gupta, K. and Sutar, A. 2008. Catalytic activities of Schiff base transition metal complexes. Coordination Chemistry Reviews. 252, 1420-1450.

Hager, E., Makhubela, B. and Smith, G. 2012. Aqueous-phase hydroformylation of 1-octene using hydrophilic sulfonate salicylaldimine dendimers. Dalton Transactions. 41, 13927-13935.

Hierso, J., Lacassin, F., Broussier, R., Amardeil, R. and Meunier, P. 2004. Synthesis and characterisation of a new class of phosphine-phosphonite ferrocenediyl dinuclear rhodium complexes. Journal of Organometallic Chemistry. 689, 766-769.

Jordaan, M., Van Helden, P., Van Sittert, C. and Vosloo, H. 2006. Experimental and DFT investigation of the 1-octene metathesis reaction mechanism with the Grubbs 1 precatalyst. Journal of Molecular Catalysis A: Chemical. 254, 145-154.

Jordaan, M. and Vosloo, H. 2007. Ruthenium catalyst with a chelatingp-alcoholato ligand for application in linear alkene metathesis. Advanced Synthesis and Catalysis. 349, 184-192.

Kühnert, J., Ecorchard, P. and Lang, H. 2008. Heterometallic transition-metal complexes based on 1-carboxy-1′-(diphenylphosphanyl) ferrocene,(tmeda/pmdta) zinc (II), and gold (I) Units. European Journal of Inorganic Chemistry. 32, 5125-5137.

Lally, M., Broussier, R. and Gautheron, B. 2000. Ferrocene-based phosphonite–phosphine ligands, Pd and Rh complexes. Tetrahedron Letters. 41, 1183-1185.

Lazzaroni, R., Raffaelli, A., Settambolo, R., Bertozzi S. and Vitulli, G. 1989. Reversbility of metal-alkyl intermediate formation in the rhodium-catalyzed deuterioformylation of 1-hexene. Organometallics. 8, 2323-2327.

Madalska, M., Lönnecke, P. and Hey-Hawkins, E. 2014. Aryl-based ferrocenyl phosphine ligands in the rhodium (I)-catalyzed hydroformylation of olefins. Journal of Molecular Catalysis A: Chemical. 383, 137-142.

Maqeda, L. Makhubela, B. and Smith, G. 2015. Synthesis, characterization and evaluation of fluorocarbon-containing rhodium(I) complexes for biphasic hydroformylation reactions. Polyhedron. 91, 128-135.

Matsinha, L., Mapolie, S. and Smith, G. 2015. Recoverable and recyclable water-soluble sulphonated salicylaldimine Rh(I) complexes for 1-octene hydroformylation in auqueous biphasic media. Dalton Transactions. 44, 1240-1248.

Park, J. and Hong, S. 2012. Cooperative bimetallic catalysis in asymmetric transformations. Chemical Society Reviews. 41, 6931-6943.

Peng, X., Wang, Z., Xia, C. and Ding, K. 2008. Ferrocene-based bidentate phosphonite ligands for rhodium (I)-catalyzed enantioselective hydroformylation. Tetrahedron Letters. 49, 4862-4864.

Siangwata, S., Baartzes, N., Makhubela, B. and Smith, G. 2015. Synthesis, characterisation and reactivity of water-soluble ferrocenylimine-Rh(I) complexes as aqueous-biphasic hydroformylation catalyst precursors. Journal of Organometallic Chemistry. 769, 26-32.

Siangwata, S., Chulu, S., Oliver, C. and Smith, G. 2016. Rhodium-catalysed hydroformylation of 1-octene using aryl and ferrocenyl Schiff base-derived ligands. Applied Organometallic Chemistry. 1-9.

Stockmann, S., Lönnecke, P., Bauer, S. and Hey-Hawkins, E. 2014. Heterobimetallic complexes with ferrocenyl-substituted phosphaheterocycles. Journal of Organometallic Chemistry. 751, 670-677.

Taddei, M. and Mann, A. (Eds.). 2013. Hydroformylation for organic synthesis. Springer.

Trzeciak, A., Štěpnička, P., Mieczyńska, E. and Ziółkowski, J. 2005. Rhodium (I) complexes with 1′-(diphenylphosphino) ferrocenecarboxylic acid as active and recyclable catalysts for 1-hexene hydroformylation. Journal of Organometallic Chemistry. 690, 3260-3267.

Van den Beuken, E. and Feringa, B. 1998. Bimetallic catalysis by late transition metal complexes. Tetrahedron. 54, 12985-13011.

Van der Gryp, P., Marx, S. and Vosloo, H. 2012. Experimental, DFT and kinetic study of 1-octene metathesis with Hoveyda-Grubbs second generation precatalyst. Journal of Molecular Catalysis A: Chemical. 355, 85-95.

Van der Vlugt, J. 2012. Cooperative catalysis with first-row late transition metals. European Journal of Inorganic Chemistry. 3, 363-375.

Van Leeuwen, P. and Claver, C. (Eds.). 2002. Rhodium catalyzed hydroformylation (Vol. 22). Springer Science and Business Media.

Wilkinson, S., Sheedy, T. and New, E. 2016. Synthesis and characterization of metal complexes with Schiff base ligands. Journal of Chemical Education. 93, 351-354.

CHAPTER 7

MANUSCRIPT 4

Kinetic evaluation of the hydroformylation of the post-metathesis product 7-tetradecene using a heterobimetallic rhodium-ferrocenyl Schiff base derived precatalyst

Nicholas C.C. Breckwoldt[1] , Gregory. S. Smith[2], Percy van der Gryp[3] and Neill J. Goosen[1]

[1]Department of Process Engineering, University of Stellenbosch, Private Bag X1, Matieland 7602, South Africa.

[2]Department of Chemistry, University of Cape Town, Rondebosch, South Africa.

[3]School of Chemical and Minerals Engineering, Research Focus Area for Chemical Resource, Beneficiation, North-West University, Hoffmann Street, Potchefstroom 2522, South Africa.

This chapter has been submitted for publication in the form of a journal article:

Breckwoldt, N., Smith, G., Van der Gryp, P. and Goosen, N. Kinetic evaluation of the hydroformylation of the post-metathesis product 7-tetradecene using a heterobimetallic rhodium-ferrocenyl Schiff base derived precatalyst. Submitted to Reaction Kinetics, Mechanisms and Catalysis (24 April 2019).

Abstract

Reaction engineering kinetics for the hydroformylation of the post-metathesis product 7-tetradecene using a heterobimetallic rhodium-ferrocenyl Schiff base derived precatalyst was investigated with variation of reaction temperature (85–105°C), precatalyst loading (0.25-0.52 mM), carbon monoxide partial pressures (20–40 bar) and hydrogen partial pressures (20–40 bar). The experimental product-time distributions for the parallel hydroformylation and isomerisation reaction system are well described by four interdependent pseudo first-order differential mole balance equations. The effects of temperature in the Arrhenius equation, precatalyst concentration, carbon monoxide and hydrogen partial pressures have been incorporated into a phenomenological mechanism-based rate equation. The rate of hydroformylation is first order in alkene, carbon monoxide and hydrogen, with fractional dependence in precatalyst concentration. Activation energy for the hydroformylation reaction was calculated to be 62 kJ.mol^{-1}, which is comparable to that determined for the commercialized phosphorus-modified catalyst systems.

1. Introduction

The hydroformylation of alkenes is one of the most important industrial transition-metal-catalysed processes in the chemical industry (Cornils and Hermann, 2002; Van Leeuwen and Claver, 2002). The reaction involves the addition of hydrogen (H_2) and carbon monoxide (CO) across the alkene double bond to yield aldehydes as major products. A number of transition metals, such as rhodium (Rh), cobalt (Co), ruthenium (Ru) and palladium (Pd) can catalyse the hydroformylation reaction (Franke et al., 2012). However, most commercial hydroformylation processes currently employ rhodium-based catalysts due to superior activity and selectivity afforded by rhodium as compared to other transition metals.

Employing bimetallic complexes that contain two metal centres can also be beneficial during catalytic reactions (Park and Hong, 2012; Van der Vlugt, 2012; Timerbulatova et al., 2013). This stems from potential cooperative effects between two proximal metals that may lead to overall improved catalytic activity performance as compared to conventional monometallic catalyst systems. Heterobimetallic complexes containing two different metal centres can potentially offer a more diverse application as catalysts, whereby each metal is responsible for performing a different function (Feringa and Van den Bekuen, 1998; Brakto and Gómez, 2013). For example, one of the metals can act as the catalytically active site, while the second metal may be responsible for increasing or decreasing the electron density around the active metal during the catalytic cycle (Brakto and Gómez, 2013).

Due to ferrocene's synthetic versatility, which readily allows for the potential fine-tuning of catalytic properties, several heterobimetallic rhodium-ferrocene complexes have been reported and evaluated as hydroformylation precatalysts (Lally et al., 2000; Hierso et al., 2004; Trzeciak et al., 2005; Peng et al., 2008; Kühnert et al., 2008; Bebbington et al., 2010; Madalska et al., 2014; Stockmann et al., 2014). These catalyst complexes predominantly make use of phosphorus donor sites in order to affect the desired electronic and steric modification by the ferrocenyl substituent. In some instances, improved catalytic activity in favour of the heterobimetallic catalyst could be observed over the monometallic catalyst as an indication of cooperative effects.

Complexation of the metals to bidentate hemilabile (chelating) Schiff base derived ligands represents another very interesting catalyst design motif owing to the excellent thermal stability and high activity observed using these types of metal complexes for a wide range of catalytic reactions (Gupta and Sutar, 2008). More recently in this regard, our group has developed and reported on the application of novel heterobimetallic rhodium-ferrocenyl complexes bearing Schiff base derived N'O chelates as hydroformylation precatalysts

(Siangwata et al., 2015; Siangwata et al., 2016; Breckwoldt et al., 2019). The precatalysts displayed high activity and gave high conversion (up to 540 h^{-1} and 99%, respectively) in the hydroformylation of both terminal and internal alkenes and have moderate to high regioselectivity towards corresponding branched aldehydes. Evidence of cooperative effect by including the ferrocene group was observed, as indicated by improved catalytic performance of the heterobimetallic catalyst system as compared to the monometallic system under selected operating conditions (Breckwoldt et al., 2019).

Herein, we would like to expand our evaluation of heterobimetallic rhodium(I)-ferrocenyl Schiff base derived complexes by exploring the reaction kinetics of such precatalyst systems in hydroformylation. While there are several kinetic modelling investigations reported for different hydroformylation systems using homogeneous monometallic rhodium-based catalysts (Deshpande et al., 1988; Bhanage et al., 1997; Deshpande et al., 1998; Nair et al., 1999; Kiss et al., 1999; Rosales et al., 2007; Bernas et al., 2008; Rosales et al., 2008; Güven et al., 2014; Li et al., 2017; Breckwoldt et al., 2019), there are none reported which focus on the hydroformylation using heterobimetallic precatalyst systems, to the best of our knowledge.

In line with our ongoing interest in the beneficiation of higher internal alkene post-metathesis product streams to detergent-range series of products, it was decided to investigate the hydroformylation of the post-metathesis product 7-tetradecene as a model substrate system for this study. The objectives of the investigation were thus three-fold: (i) to evaluate the parametric influences of process conditions affecting the kinetics of the hydroformylation of 7-tetradecene using the Schiff base derived heterobimetallic rhodium-ferrocenyl precatalyst, (ii) to apply a suitable phenomenological rate equation model that can be used in the reaction-engineering context and (iii) to estimate all necessary kinetic rate parameters.

2. Materials and methods

2.1 Chemicals and precatalyst used

7-Tetradecene (>98%) was prepared via 1-octene metathesis using Hoveyda-Grubbs second-generation precatalyst (98%, Sigma-Aldrich) as per methods and conditions reported previously (Van der Gryp et al., 2012). Toluene (>99%, ACE Chemicals) was used as solvent during all hydroformylation experiments. A prepared syngas mix ($CO:H_2$, 1:1) as well as separate hydrogen and carbon monoxide gas cylinders were supplied and used as received from Afrox Ltd. for the kinetic experiments. The ferrocenyl-rhodium(I) Schiff base derived precatalyst complex (**Figure 1**) was prepared according to published procedures (Siangwata et al., 2016).

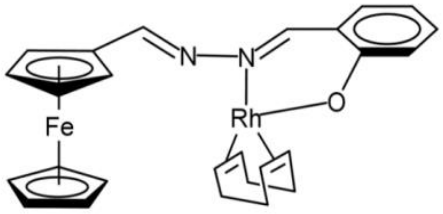

Figure 1: Heterobimetallic Schiff base derived ferrocenyl-rhodium(I) precatalyst used in this study.

2.2 Reaction conditions for the kinetic study

To study the kinetics of the hydroformylation reaction, hydroformylation experiments were performed under the range of reaction conditions given in **Table 1**. Standard reaction conditions were considered as the following: reaction temperature of 95°C, initial 7-tetradecene molar concentration of 1 mol.L^{-1}, precatalyst molar concentration of 0.52×10^{-3} mol.L^{-1}, partial pressure of carbon monoxide (P_{CO}) equal to 20 bar and partial pressure of hydrogen (P_{H2}) equal to 20 bar, in line with conditions typically reported for these types of N'O chelate systems (Siangwata et al., 2015; Siangwata et al., 2016; Breckwoldt et al., 2019). While investigating the influence of the different reaction conditions (either temperature, precatalyst concentration, carbon monoxide or hydrogen partial pressure) on the kinetics, all other parameters were kept constant as per standard reaction conditions.

Table 1: Range of reaction conditions investigated in this study.

Parameter (Units)	Parameter Range
Precatalyst concentration (mol.L^{-1})	0.25–0.52 (10^{-3})
Carbon monoxide partial pressure (bar)	20–40
Hydrogen partial pressure (bar)	20–40
Temperature (°C)	85–105
Reaction volume (L)	6.0 (10^{-3})

2.3 Hydroformylation procedure

Hydroformylation kinetics experiments were performed using a stainless steel pressure reactor containing a Teflon insert. The reactor was fitted with thermocouple and pressure-indicating regulator to control the reaction temperature and syngas pressure, respectively. For each standard reaction, toluene (6 mL), rhodium precatalyst (0.0097 mmol, 2.39 mg) and 7-tetadecene (9.69 mmol, 1.90 g) were charged to the reactor, which was then sealed and placed in an oil bath for heating. After heating the reactor to the desired reaction temperature, the reactor was pressurized with syngas. All standard reactions were performed using a syngas feed with H_2:CO ratio of 1:1 prepared by Afrox. Where the influence of varied H_2:CO ratio was investigated, custom syngas feed mixtures were prepared using separate hydrogen and carbon monoxide gas cylinders according to the same methodology reported previously (Breckwoldt et al., 2019). Preliminary kinetic testing of the precatalyst showed initial induction periods, presumably due to the time required to form the catalytically active rhodium-hydride species (Breckwoldt et al., 2019). Therefore, all of the kinetic data reported in this study were collected at the end of the induction period which marked the start of the reaction (time zero). The induction period was determined via GC-MS experiments; before the end of the induction period, no products were detected, whereas just after the induction period, consumption of the substrate and formation of products could be observed as an indicator of the formation of active catalyst. The total syngas pressure was kept constant during all of the hydroformylation experiments. After pressurizing the reactor for the desired reaction time, the hydroformylation reaction was stopped by depressurizing the reactor of syngas. Samples of the post-reaction mixture were taken and analysed via GC-MS: Agilent 7890A GC, Zebron ZB-1701 capillary column (60 m × 250 µm × 0.25 µm) and Agilent 5975C single quadrupole mass detector; column pressure 23.787 psi (He); split ratio 25:1; oven temperature 45°C for 1 min, 45–250°C at 10 °C.min-1 for 20 min; detector temperature of 280°C. Separate hydroformylation experiments were conducted at the different reaction time intervals (following catalyst induction) in order to generate the observed product-distribution-time profiles. From these profiles, the kinetic rate data could be determined. The average experimental uncertainty with respect to the different product formations (7-tetradecene, isoalkenes, 2-hexylnoanal and isoaldehydes) was estimated to be ± 1 mole %.

2.4 Methodology framework for describing the kinetics

The general algorithm proposed by Fogler (2014) for analysing the kinetic batch reactor data was applied in this study (**Figure 2**). **Figure 3** illustrates the reaction network for the hydroformylation of 7-tetradecene. The reaction network consists of three main reactions, namely: hydroformylation of 7-tetradecene to the direct hydroformylation product

2-hexylnonanal, 7-tetradecene isomerisation to isomeric tetradecenes and hydroformylation thereof to corresponding isomeric aldehydes. Isomeric tetradecenes and aldehydes were grouped together as the pseudo-components 'isoalkenes' and 'isoaldehydes', respectively. A similar reaction network was previously adopted and applied successfully to describe the kinetics of the 7-tetradecene hydroformylation system (Breckwoldt et al., 2019).

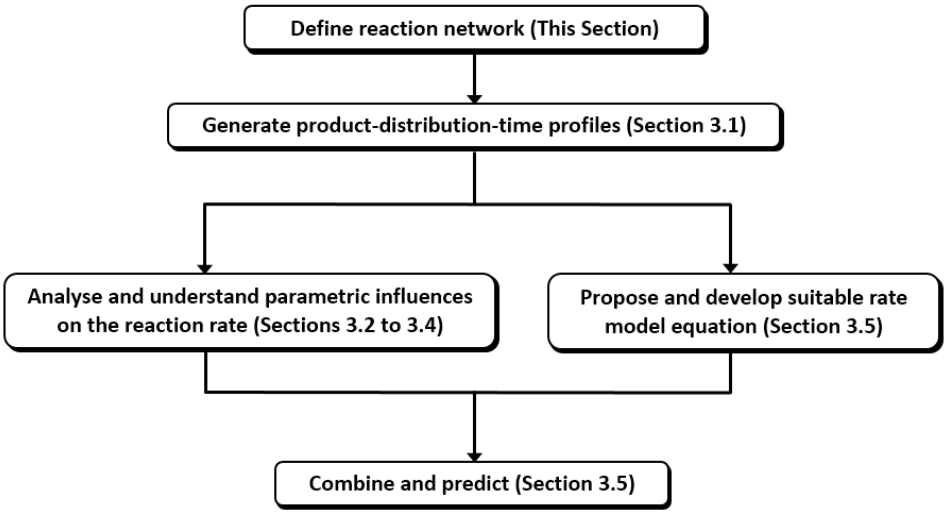

Figure 2: Methodology framework applied in study for describing kinetics of the hydroformylation reaction.

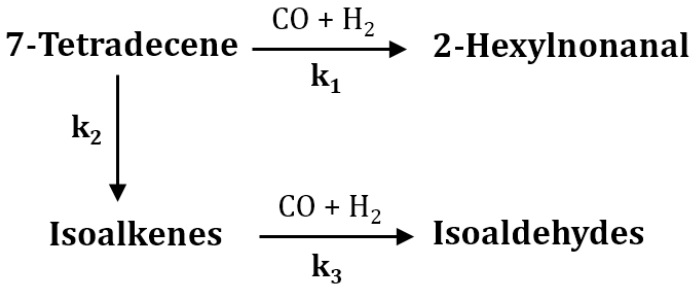

Figure 3: Reaction network for 7-tetradecene hydroformylation.

Based on the depicted reaction network, the corresponding system of four elementary differential mole-balance equations (**Equations 1-4**) was proposed and solved simultaneously in order to obtain the observed kinetic rate data (rate constants $k_{1,obs}$, $k_{2,obs}$ and $k_{3,obs}$). The solutions were obtained numerically using the fourth-order Runge-Kutta approximation in Matlab ® in combination with least squares regression procedure (Breckwoldt et al., 2019).

$$\frac{d(C_{C14})}{dt} = -k_{1(obs)}C_{C14} - k_{2(obs)}C_{C14} \qquad (\mathbf{1})$$

$$\frac{d(C_{2HN})}{dt} = k_{1(obs)}C_{C14} \qquad (\mathbf{2})$$

$$\frac{d(C_{ISOALK})}{dt} = k_{2(obs)}C_{C14} - k_{3(obs)}C_{C14} \qquad (\mathbf{3})$$

$$\frac{d(C_{ISOALD})}{dt} = k_{3(obs)}C_{C14} \qquad (\mathbf{4})$$

where $k_{1(obs)}$ is the observed rate of consumption of 7-tetradecene to 2-hexylnonanal (h^{-1}), $k_{2(obs)}$ is the observed rate of consumption of 7-tetradecene to isoalkene products (h^{-1}), $k_{3(obs)}$ is the observed rate of consumption of isoalkenes to isoaldehyde products (h^{-1}), C_{C14} is the concentration of 7-tetradecene in the reactor ($mol.L^{-1}$), C_{2HN} is the concentration of 2-hexylnonanal in the reactor ($mol.L^{-1}$), C_{ISOALK} is the concentration of isoalkene products in the reactor ($mol.L^{-1}$) and C_{ISOALD} is the concentration of isoaldehyde products in the reactor ($mol.L^{-1}$).

3. Results and discussion

3.1 Typical product-distribution-time profiles

Figure 4 shows a typical product-distribution-time profile during the hydroformylation of 7-tetradecene using the Schiff base derived ferrocenyl-rhodium(I) precatalyst. The consumption of 7-tetradecene resulted in the formation of the expected products (2-hexylnonanal, isoalkenes and isoaldehydes) during the hydroformylation reaction. Isomerisation of 7-tetradecene to isoalkenes was significant at the beginning of the reaction, reaching a peak product formation at around 1 h (at 95°C); thereafter hydroformylation of the isoalkenes to isoaldehydes predominates. Due to the high rate of isomerisation, isoaldehydes are typically the major product at the end of the reaction. Based on the proposed kinetic reaction network equations (**Equations 1-4**) the calculated values of each of the observed rate constants ($k_{1,obs}$, $k_{2,obs}$ and $k_{3,obs}$) are summarized in **Table 2** for the different temperatures, precatalyst concentrations, hydrogen partial pressures and carbon monoxide partial pressures. It is clear from these

results, as shown in **Figure 4** for standard reaction conditions, that the proposed kinetic reaction network model describes the hydroformylation of 7-tetradecene satisfactorily within the investigated reaction condition ranges.

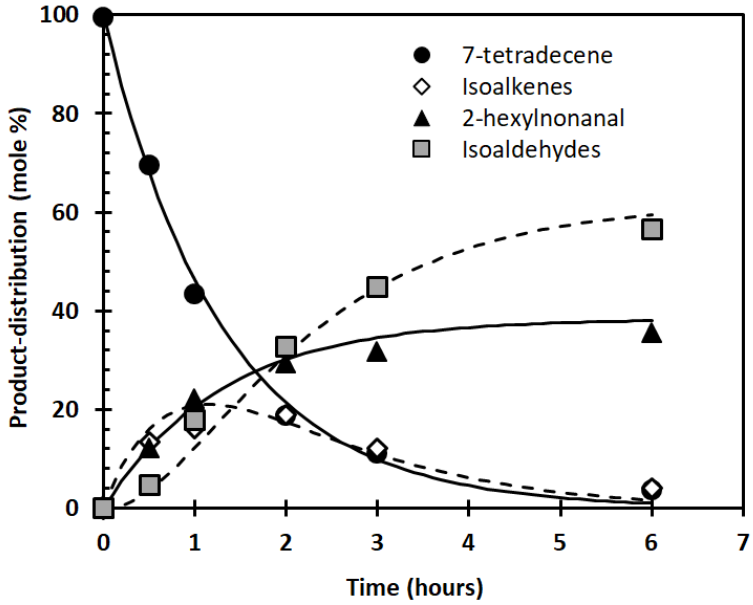

Figure 4: Typical product-distribution-time profile for the hydroformylation reaction using Schiff base derived ferrocenyl-rhodium(I) precatalyst. Reaction performed at 95°C, 40 bar ($CO:H_2$, 1:1), precatalyst concentration 0.52 × 10^{-3} mol.L^{-1}, initial 7-tetradecene concentration 1 mol.L^{-1} in toluene (6 mL). Solid lines represent solved mole balance equation model.

Table 2: Observed rate constants for the hydroformylation of 7-tetradecene at varied operating conditions.

Entry	T	P_{CO}	P_{H2}	Rh	Observed rate constant (h^{-1})		
	(°C)	(bar)	(bar)	(mM)	k_1	k_2	k_3
1	85	20	20	0.52	0.20	0.23	0.80
2	95	20	20	0.52	0.29	0.46	0.94
3	95	20	40	0.52	0.65	0.74	2.60
4	95	40	20	0.52	0.54	0.53	2.45
5	95	20	20	0.25	0.19	0.35	0.90
6	105	20	20	0.52	0.60	1.25	1.44

3.2 Influence of temperature

The influence of temperature on the reaction rate was evaluated at the three different temperatures (85, 95 and 105°C) while keeping all other reaction conditions constant at standard conditions. As we reported previously (Breckwoldt et al., 2019), these types of Schiff base derived precatalyst systems are essentially inactive at temperatures below 85°C, while performance decreases at temperatures above 105°C; hence our selection of the temperature range 85-105°C for evaluation in this study. As is to be expected, the reaction rate was found to increase with temperature according to the Arrhenius equation (**Equation 5**) within the evaluated temperature range:

$$k_i = k_{i,0} \exp\left(\frac{-E_{A,i}}{RT}\right) \qquad (\mathbf{5})$$

From the slope of the linearized Arrhenius plot (**Figure 5**), the hydroformylation activation energy (E_1) could be estimated and was found to be 62 kJ.mol^{-1}. This value of the activation energy is in good agreement to that reported previously for the hydroformylation of 7-tetradecene using the homogeneous bulky phosphite-modified rhodium catalyst (68 kJ.mol^{-1}) (Breckwoldt et al., 2019). Similarly, the activation energies for the isomerisation of 7-tetradecene to isoalkenes (E_2) and hydroformylation to isoaldehydes (E_3) could be determined with values of 95 kJ.mol^{-1} and 33 kJ.mol^{-1}, respectively. Although the product-distribution profiles (**Figure 4**) will be governed by the relative reaction rates (k_1, k_2 and k_3), the relative values of the calculated activation energies (E_1, E_2 and E_3) are also consistent with the experimental product-distribution-time profiles. As the temperature is increasing, an increase in the relative rate of isomerisation to hydroformylation will become more favourable from an energy viewpoint ($E_2 > E_1$), leading to significant isoalkene product formation. Eventually, all isoalkenes products formed will be converted to corresponding isoaldehydes from an energy viewpoint ($E_3 < E_2$).

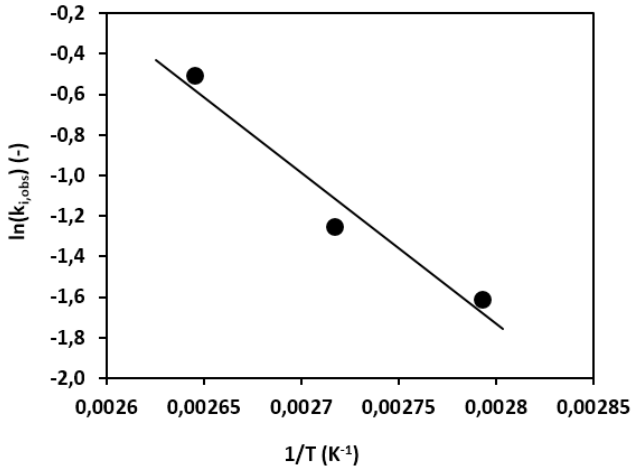

Figure 5: Arrhenius plot showing the influence of temperature on the observed hydroformylation rate.

3.3 Influence of catalyst concentration

The rate of hydroformylation was investigated at different precatalyst concentrations, as shown in **Figure 6.** In general, the reaction rate was found to be positively influenced by increasing the precatalyst concentration, which is consistent with previous studies in the literature using conventional monometallic homogeneous rhodium-based catalysts (Deshpande et al., 1988; Bhanage et al., 1997; Deshpande et al., 1998; Nair et al., 1999; Kiss et al., 1999; Rosales et al., 2007; Bernas et al., 2008; Rosales et al., 2008; Güven et al., 2014; Li et al., 2017; Breckwoldt et al., 2019). However, a more complex dependency of the hydroformylation rate on the precatalyst concentration was observed when employing the heterobimetallic precatalyst in this study. At a low precatalyst concentration, the rate of hydroformylation appears to increase more quickly than with increasing the precatalyst at a higher concentration. This behaviour is indicative of a fractional order dependence on precatalyst concentration since not all of the precatalyst becomes active with equal turnover frequencies as the precatalyst concentration is increasing. One possible explanation for this behaviour is due to the resting state of the catalyst, whereby the amount of rhodium entering the catalytic cycle at any given time does not increase linearly with increasing the amount of rhodium. Another possibility is displacement of some of the ligand to yield a unmodified catalyst at a lower precatalyst concentration due to higher relative carbon monoxide concentration. As the precatalyst concentration is increased, equilibrium should favour the ligand-modified catalyst, which explains the deceleration of the reaction rate with increasing the precatalyst concentration.

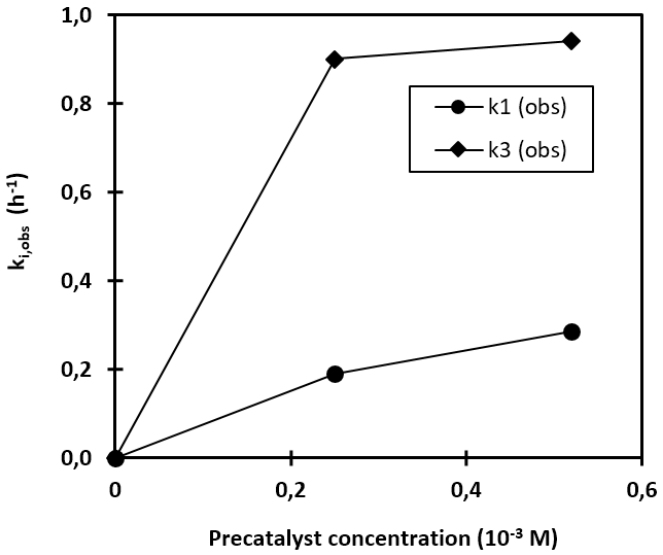

Figure 6: Influence of precatalyst concentration on the rate of hydroformylation. Reactions performed at 95°C, 40 bar ($CO:H_2$, 1:1), initial 7-tetradecene concentration of 1 $mol.L^{-1}$ in toluene (6 mL).

3.4 Influence of hydrogen and carbon monoxide partial pressures

3.4.1 Hydrogen partial pressure

The rate of hydroformylation increased linearly with increasing the hydrogen partial pressure (**Figure 7**).

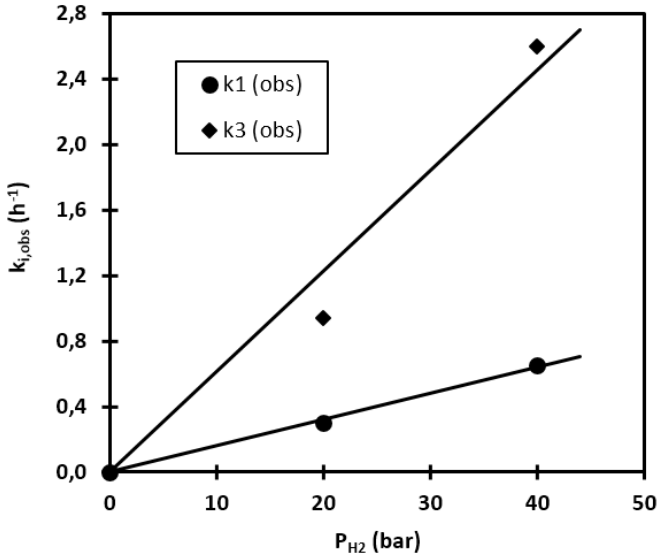

Figure 7: Influence of hydrogen partial pressure on the rate of hydroformylation. Reactions performed at 95°C, precatalyst concentration 0.52 × 10^{-3} $mol.L^{-1}$, P_{CO} of 20 bar, initial 7-tetradecene concentration 1 $mol.L^{-1}$ in toluene (6 mL).

Linear dependence in hydrogen pressure was also observed previously under homogeneous catalytic conditions using rhodium-based catalysts and was reported to be consistent with oxidative addition of hydrogen to the rhodium-acyl species as the rate-determining step during the overall catalytic cycle (Deshpande et al., 1988; Bhanage et al., 1997; Deshpande et al., 1998; Nair et al., 1999).

3.4.2 Carbon monoxide partial pressure

Unlike other conventional homogeneous hydroformylation systems conducted in organic solvent such as toluene (Deshpande et al., 1988; Bhanage et al., 1997; Deshpande et al., 1998), the rate of hydroformylation vs. carbon monoxide partial pressure did not display typical substrate-inhibited kinetics within comparable carbon monoxide partial pressure ranges (**Figure 8**).

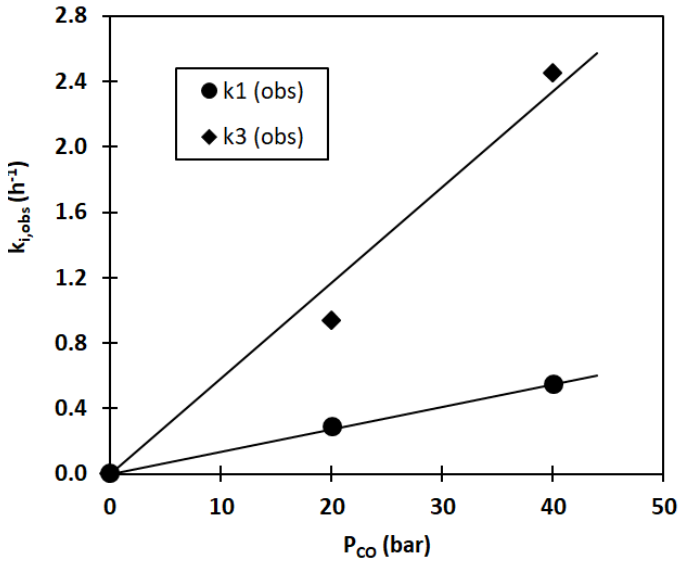

Figure 8: Influence of carbon monoxide partial pressure on the rate of hydroformylation. Reactions performed at 95°C, precatalyst concentration 0.52 × 10^{-3} mol.L^{-1}, P_{H2} of 20 bar, initial 7-tetradecene concentration 1 mol.L^{-1} in toluene (6 mL).

As per the mechanism of rhodium-catalysed hydroformylation proposed by Evans et al. (1968), substrate inhibition kinetics with increasing carbon monoxide partial pressure result from the undesired formation of inactive 'dead-end' dicarbonyl and tricarbonyl acyl species due to increased carbon monoxide solubility at higher pressures. These inactive carbonyl acyl species are unable to complete the hydroformylation cycle, hence inhibiting the overall reaction rate. At lower carbon monoxide partial pressures, a positive influence of carbon monoxide is observed since the concentration is too low to form the inactive rhodium carbonyl species in significant amount (Deshpande et al., 1998). The observed positive linear dependence of the

reaction rate with respect to carbon monoxide partial pressure observed in this study is therefore consistent with a catalytic regime that does not involve significant accumulation of these inactive rhodium carbonyl species within the ranges investigated. This might be explained due to the relatively lower solubility of carbon monoxide in toluene at the higher operating temperatures in this study, which are required when employing these N'O chelate type precatalyst systems. Presumably, much higher carbon monoxide pressures would be required to sufficiently increase the solubility of carbon monoxide at a higher reaction temperature and to observe the rate-diminishing effects of inactive rhodium species formed at these pressures. Since the total investigated syngas pressure is well within typical industrial operating range (40-60 bar), higher carbon monoxide pressures were not investigated.

3.5 Kinetic modelling of the reaction network

Since a phenomenological rate model based on the mechanism of hydroformylation using a heterobimetallic Schiff base derived rhodium(I) precatalyst has not been developed before, the generalized mechanism-based rate equation (**Equation 6**) derived in the work of Shaharun et al. (2010) was adopted and applied in this study, taking into account the consistency with the parametric effects observed in the hydroformylation experiments. Species concentrations are denoted by square brackets and K_1 is an equilibrium constant.

$$R_{Hydro} = \frac{k[\text{Precatalyst}][\text{alkene}]P_{CO}P_{H_2}}{1 + K_1 P_{CO}} \qquad (\mathbf{6})$$

The developed rate equation is based on the following simplified reaction steps (**Equations 7-9**) adapted for Schiff base derived chelate ligands (denoted as N⁀O), where **Equation 7** is treated as a catalyst pre-equilibrium step and oxidative dihydrogen addition of the rhodium-acyl species (**Equation 9**) is assumed to be the rate-determining step in the overall catalytic cycle. Application of such a model appears appropriate, since a linear dependence of reaction rate to increasing hydrogen partial pressures observed in the experiments is consistent with dihydrogen addition as the rate-determining step during hydroformylation. The mathematical derivation of the rate equation is described in detail (Shaharun et al., 2010).

$$HRh(CO)(N⁀O) + CO \underset{k_{-1}}{\overset{k_1}{\rightleftharpoons}} HRh(CO)_2(N⁀O) \qquad (\mathbf{7})$$

$$HRh(CO)_2(N⁀O) + \text{alkene} \underset{k_{-2}}{\overset{k_2}{\rightleftharpoons}} HRh(CO)(N⁀O)(\text{acyl}) \qquad (\mathbf{8})$$

$$Rh(CO)(N⁀O)(\text{acyl}) + H_2 \xrightarrow{k} HRh(CO)(N⁀O) + \text{aldehyde} \qquad (\mathbf{9})$$

Even though **Equation 6** could satisfactorily describe the rate data, it was found that the rate data could be more accurately fitted if the rate equation was modified slightly to include a fractional order dependence term with respect to the precatalyst concentration (**Equation 10**). The reason for this is due to the non-linear, positive fractional-order dependence observed in the hydroformylation experiments, which is not explicitly accounted for in **Equation 6**, and probably also the relatively simplicity of **Equations 7-9** in describing the overall reaction rate.

$$R_{Hydro} = \frac{k[Precatalyst]^{x}[alkene]P_{CO}P_{H_2}}{1 + K_1P_{CO}} \qquad (\mathbf{10})$$

A separate isomerisation rate equation was incorporated to account for the isomerisation rate data (k_2). Isomerisation was modelled as first-order in the alkene and independent of hydrogen and carbon monoxide concentrations in accordance with the literature (Koeken et al., 2011; Kiedorf et al., 2014), with modification to account for fractional precatalyst dependence (**Equation 11**).

$$R_{Iso} = [Precatalyst]^{x}[alkene] \qquad (\mathbf{11})$$

Estimation of the kinetic rate model parameters (k_0, K_α and x) for **Equations 10** and **11** with known activation energies from the Arrhenius plots was performed using a non-linear least square regression algorithm in order to minimize the objective function (**Equation 12**). A summary of the complete rate model parameters are summarized in **Table 3**.

$$SSE = \sum_{i}^{n}\left(k_{obs,i\,(pred)} - k_{obs,i\,(measured)}\right)^2 \qquad (\mathbf{12})$$

Table 3: Summary of hydroformylation rate model parameters.

Parameter	k_1	k_2	k_3
k_0 (units)[a]	2.0 x 10^8	2.0 x 10^{15}	3.0 x 10^3
K_1 (bar^{-1})	0.01	-	0.00
x (-)	0.75	0.63	0.40
E_A ($kJ.mol^{-1}$)	62	95	33
SSE	0.01	0.04	0.14
Pearson correlation (-)	0.98	0.93	0.94

[a]Units of k_1 and k_3: $mol^{-x}.L^{x}.bar^{2}.h^{-1}$; units for k_2: $mol^{-x}.L^{x}.h^{-1}$.

From the regression results, it is clear that the observed reaction rates could be well described by the proposed kinetic model over the investigated operating ranges, as indicated by a strong linear Pearson correlation coefficient (>0.94) between experimentally observed and model-predicted rate data (**Figure 9**). This observation that the rate data for the heterobimetallic catalyst system could be described well by the rate-law model derived for conventional monometallic catalyst systems indicates that similar mechanism-based modelling principles can also be extended to describe the kinetics of these heterobimetallic catalyst systems. This result was expected since rhodium remains the primary catalytically active site in the heterobimetallic catalyst complex, in line with our previous evidence showing that the ferrocenyl ligand alone is inactive in hydroformylation (Siangwata et al., 2016). This is also consistent with our more recent evidence (Breckwoldt et al., 2019) of improved catalytic activity in the case of the heterobimetallic complex as most likely being electronic in nature, the influence of which is inherently incorporated into the observed reaction rate.

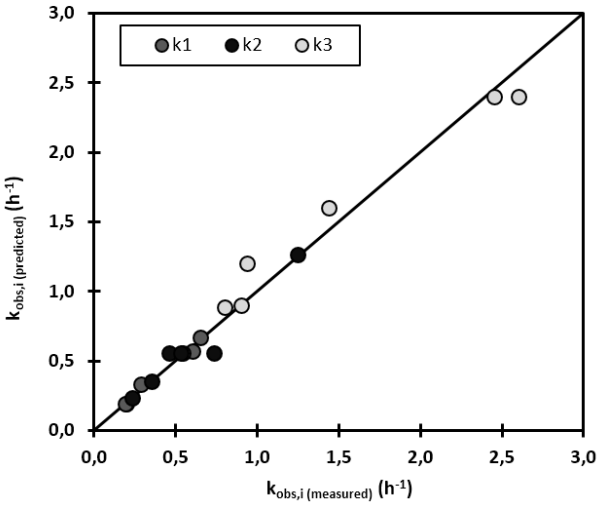

Figure 9: Comparison of experimentally observed and model-predicted hydroformylation rate data.

4. Conclusions

Reaction kinetics for the hydroformylation of the post-metathesis product 7-tetradecene using heterobimetallic Schiff base derived ferrocenyl-rhodium precatalyst were investigated. A system of elementary differential mole balance equations was proposed and solved to describe the reaction network comprised of parallel hydroformylation and isomerisation pathways. The proposed reaction network model allowed the observed hydroformylation reaction rates to be estimated, which were found to be first order with respect to the alkene, hydrogen partial pressure and carbon monoxide pressure and a positive fractional order with respect to the precatalyst concentration. The parametric influences of the different reaction conditions affecting the overall reaction rate using the heterobimetallic complex are therefore consistent with those typically observed using conventional monometallic catalyst systems. A generalized mechanism-based rate law equation consistent with the parametric effects was applied to describe the observed kinetic rate data and all necessary kinetic rate parameters were estimated with overall satisfactory agreement to experimental product-distribution-time profiles over a wide alkene conversion range. The activation energy of the hydroformylation reaction was calculated to be 62 $kJ.mol^{-1}$, which is comparable with conventional phosphorus-modified rhodium catalyst systems. The kinetic model serves as a starting point for the development of suitable reactor models for alkene hydroformylation using heterobimetallic catalysts. Through optimal selection of the metallocene group with variable electron-withdrawing and electron-donating substituents, it is imaginable that such heterobimetallic catalyst systems can be employed to improve the effectiveness of rhodium in an industrial context.

Acknowledgements

The support of the DST-NRF Centre of Excellence (CoE) in Catalysis towards this research is hereby acknowledged. Opinions expressed and conclusions arrived at, are those of the author and are not necessarily to be attributed to the CoE. The authors also wish to thank the University of Stellenbosch and University of Cape Town for additional financial support towards this research and Shepherd Siangwata for skilled guidance and assistance in preparing the precatalyst used for the study.

References

Bebbington, M., Bontemps, S., Bouhadir, G., Hanton, M., Tooze, R., van Rensburg, H. and Bourissou, D. 2010. A 1,1′-ferrocenyl phosphine-borane: synthesis, structure and evaluation in Rh-catalyzed hydroformylation. New Journal of Chemistry. 34, 1556-1559.

Bernas, A., Maki-Arvela, P., Lehtonen, J. Salmi, T. and Murzin, D. 2008. Kinetic modeling of propene hydroformylation with Rh/TPP and RH/CHDPP Catalysts. Industrial and Engineering Chemistry Research. 47, 4317-4324.

Bhanage, B., Divekar, S., Deshpande, R. and Chaudhari, R. 1997. Kinetics of hydroformylation of l-dodecene using homogeneous HRh(CO)(PPh3)3 catalyst. Journal of Molecular Catalysis A: Chemical. 115, 247-257.

Bratko, I. and Gómez, M. 2013. Polymetallic complexes linked to a single-frame ligand: cooperative effects in catalysis. Dalton Transactions. 42, 10664-10681.

Breckwoldt, N. Goosen, H. Vosloo and P. Van der Gryp. 2019. Kinetic evaluation of the hydroformylation of post-metathesis product 7-tetradecene using bulky phosphite-modified rhodium catalyst. Reaction Chemistry and Engineering. 4,695-704.

Breckwoldt, N. Goosen, P. Van der Gryp, and G. Smith. 2019. Hydroformylation of the post-metathesis product 7-tetradecene using rhodium(I) Schiff base derived precatalysts. Journal of Applied Catalysis A: General. 573, 49-55.

Cornils, B., and Hermmann, W. 2002. Applied homogeneous catalysis with organometallic compounds: a comprehensive handbook in three volumes. Wiley-VCH.

Deshpande, R. and Chaudhari, R. 1988. Kinetics of hydroformylation of 1-hexene using homogeneous HRh(CO)(PPh3)3 complex catalyst. Industrial and Engineering Chemistry Research. 27, 1996-2002.

Deshpande, R., Bhanage, B.M.; Divekar, S., Kanagasabapathy, S., Chaudhari, R. 1998. Kinetics of hydroformylation of ethylene in a homogeneous medium: comparison in organic and aqueous systems. Industrial and Engineering Chemistry Research. 37, 2391–2396.

Evans, D., Osborn, J. and Wilkinson, G. 1968. Hydroformylation of alkenes by use of rhodium complex catalysts. Journal of the Chemical Society A: Inorganic, Physical, Theoretical. 11, 3133-3142.

Fogler, H. 2014. Elements of chemical reaction engineering. Pearson Education.

Franke, R., Selent, D. and Börner, A. 2012. Applied hydroformylation. Chemical Reviews. 112, 5675-5732.

Gupta, K. and Sutar, A. 2008. Catalytic activities of Schiff base transition metal complexes. Coordination Chemistry Reviews. 252, 1420-1450.

Güven, S., Hamers, B., Franke, R., Priske, M., Becker, M. and Vogt, D., 2014. Kinetics of cyclooctene hydroformylation for continuous homogeneous catalysis. Catalysis Science and Technology. 4, 524-530.

Hierso, J., Lacassin, F., Broussier, R., Amardeil, R. and Meunier, P. 2004. Synthesis and characterisation of a new class of phosphine-phosphonite ferrocenediyl dinuclear rhodium complexes. Journal of Organometallic Chemistry. 689, 766-769.

Kiedorf, G., Hoang, D., Müller, A., Jörke, A., Markert, J., Arellano-Garcia, H., Seidel-Morgenstern, A. and Hamel, C. 2014. Kinetics of 1-dodecene hydroformylation in a thermomorphic solvent system using a rhodium-biphephos catalyst. Chemical Engineering Science. 115, 31-48.

Kiss, G., Mozeleski, E., Nadler, K. VanDriessche, E. and DeRoover, C. 1999. Hydroformylation of ethene with triphenylphosphine modified rhodium catalyst: kinetic and mechanistic studies. Journal of Molecular Catalysis A: Chemical. 138, 155-176.

Koeken, A., van den Broeke, L., Benes, N. and Keurentjes, J. 2011. Triphenylphosphine modified rhodium catalyst for hydroformylation in supercritical carbon dioxide. Journal of Molecular Catalysis A: Chemical. 346, 94-101.

Kühnert, J., Ecorchard, P. and Lang, H. 2008. Heterometallic transition-metal complexes based on 1-carboxy-1′-(diphenylphosphanyl) ferrocene,(tmeda/pmdta) Zinc (II), and gold (I) units. European Journal of Inorganic Chemistry. 32, 5125-5137.

Lally, M., Broussier, R. and Gautheron, B. 2000. Ferrocene-based phosphonite–phosphine ligands, Pd and Rh complexes. Tetrahedron Letters. 41, 1183-1185.

Li, X., Zhang, K. Qin, L. and Ma, H. 2017. Kinetic studies of hydroformylation of 1-butene using homogeneous Rh/PPh3 complex catalyst. Molecular Catalysis. 443, 270-279.

Madalska, M., Lönnecke, P. and Hey-Hawkins, E. 2014. Aryl-based ferrocenyl phosphine ligands in the rhodium (I)-catalyzed hydroformylation of olefins. Journal of Molecular Catalysis A: Chemical. 383, 137-142.

Nair, V., Mathew, S., Chaudhari, R. 1999. Kinetics of hydroformylation of styrene using homogeneous rhodium complex catalyst. Journal of Molecular Catalysis A: Chemical. 143, 99-110.

Park, J. and Hong, S. 2012. Cooperative bimetallic catalysis in asymmetric transformations. Chemical Society Reviews. 41, 6931-6943.

Peng, X., Wang, Z., Xia, C. and Ding, K. 2008. Ferrocene-based bidentate phosphonite ligands for rhodium (I)-catalyzed enantioselective hydroformylation. Tetrahedron Letters. 49, 4862-4864.

Rosales, M., Chacon, G., Gonzalez, A., Pacheco, I., Baricelli, P. and Melean, L. 2008. Kinetics and mechanisms of homogeneous catalytic reactions Part 9. Hydroformylation of 1-hexene catalyzed by a rhodium system containing a tridentated phosphine. Journal of Molecular Catalysis A: Chemical. 287, 110-114

Rosales, M., Gonzalez, A., Guerrero, Y., Pacheco, I. and Sanchez-Delgado, R. 2007. Kinetics and mechanisms of homogeneous catalytic reactions Part 6. Hydroformylation of 1-hexene by use of Rh(acac)(CO)2/dppe [dppe = 1,2-bis(diphenylphosphino)ethane] as the precatalyst. Journal of Molecular Catalysis A: Chemical. 270, 241-249.

Shaharun, B. Dutta, H. Mukhtar and S. Maitr. 2010. Hydroformylation of 1-octene using rhodium-phosphite catalyst in a thermomorphic solvent system. Chemical Engineering Science. 65, 273-281.

Siangwata, S., Baartzes, N., Makhubela, B. and Smith, G. 2015. Synthesis, characterisation and reactivity of water-soluble ferrocenylimine-Rh(I) complexes as aqueous-biphasic hydroformylation catalyst precursors. Journal of Organometallic Chemistry. 769, 26-32.

Siangwata, S., Chulu, S., Oliver, C. and Smith, G. 2016. Rhodium-catalysed hydroformylation of 1-octene using aryl and ferrocenyl Schiff base-derived ligands. Applied Organometallic Chemistry. 1-9.

Stockmann, S., Lönnecke, P., Bauer, S. and Hey-Hawkins, E. 2014. Heterobimetallic complexes with ferrocenyl-substituted phosphaheterocycles. Journal of Organometallic Chemistry. 751, 670-677.

Timerbulatova, M., Gatus, M., Vuong, K., Bhadbhade, M., Algarra, A., Macgregor, S. and Messerle, B. 2013. Bimetallic complexes for enhancing catalyst efficiency: probing the relationship between activity and intermetallic distance. Organometallics. 32, 5071-5081.

Trzeciak, A., Štěpnička, P., Mieczyńska, E. and Ziółkowski, J. 2005. Rhodium (I) complexes with 1′-(diphenylphosphino) ferrocenecarboxylic acid as active and recyclable catalysts for 1-hexene hydroformylation. Journal of Organometallic Chemistry. 690, 3260-3267.

Van den Beuken, E. and Feringa, B. 1998. Bimetallic catalysis by late transition metal complexes. Tetrahedron. 54, 12985-13011.

Van der Gryp, P., Marx, S. and Vosloo, H. 2012. Experimental, DFT and kinetic study of 1-octene metathesis with Hoveyda-Grubbs second generation precatalyst. Journal of Molecular Catalysis A: Chemical. 355, 85-95.

Van der Vlugt, J. 2012. Cooperative catalysis with first-row late transition metals. European Journal of Inorganic Chemistry. 3, 363-375.

Van Leeuwen, P. and Claver, C. (Eds.) 2002. Rhodium catalyzed hydroformylation (Vol. 22). Springer Science and Business Media.

CHAPTER 8

CONCLUSIONS AND RECOMMENDATIONS

In this chapter, the main findings and conclusions of this study are presented (Section 8.1), followed by recommendations for future work in Section 8.2.

8.1 Conclusions

8.1.1 Overall aim

This study aimed to broadly evaluate and understand the performance of rhodium-based catalysts for the model hydroformylation reaction of the post-metathesis product 7-tetradecene. The study produced several novel contributions (defined Section 1.5) relating specifically to the application of commercial (Chapters 5 and 6) and non-commercial (Chapters 7 and 8) rhodium-based catalyst systems. These contributions form part of the broader scope of the RSA Olefin programme for the upgrading of low-value olefin feedstocks to higher value detergent-range products in South Africa. A wide distribution of products was identified for the model hydroformylation reaction of 7-tetradecene, as shown in **Figure 8.1**. The findings of the study are summarized below with respect to the application of the different commercial (Section 8.1.2) and non-commercial (Section 8.1.3) catalyst systems.

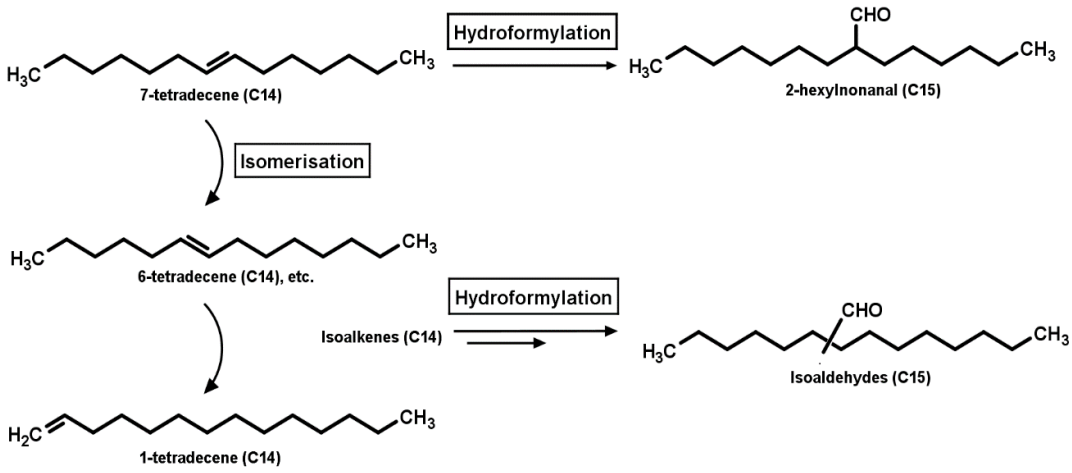

Figure 8.1: Possible products and reaction network for the post-metathesis product 7-tetradecene hydroformylation reaction evaluated in this study.

8.1.2 Hydroformylation with commercial rhodium catalysts

In terms of rhodium-based catalysts which are commercially available, the hydroformylation performance of Rh-tris(2,4-ditertbutylephenyl)phosphite (**1**), Rh-triphenylphosphine (**2**) and Rh-triphenylphosphite (**3**) catalyst systems were evaluated (Chapter 4). The performance of the catalysts was determined according to selectivity and activity (turnover numbers) parameters. In terms of turnover numbers, under optimized conditions (70°C, 30 bar), it was found that **1** was roughly three times more active as compared to **2** and **3** catalyst systems. This was ascribed to strong π-acceptor properties of the bulky phosphite ligand that promote more facile

dissociation of carbonyl ligand during catalytic cycle, which lead to higher reaction rates. In terms of selectivity, under optimized conditions, **1** was exclusively hydroformylation-selective toward the targeted aldehyde product 2-hexylnonanal (> 99% selectivity, TON of 980), while **2** and **3** were both hydroformylation- and isomerisation-selective, resulting in lower selectivity performance. It could thus be concluded that **1** is the most effective commercial catalyst systems for the hydroformylation of the post-metathesis product under the investigated condition ranges.

In order to facilitate reactor sizing and design of such reaction systems, it was further proposed and demonstrated in this study that the kinetics of the hydroformylation of 7-tetradecene using **1** could be well described by the set of three pseudo first-order ordinary differential mole balance equations, as given by **Equations 8.1-8.3** (Chapter 5).

$$\frac{dC_{C14}}{dt} = -k_{1(obs)}C_{C14} - k_{2(obs)}C_{C14} \qquad (8.1)$$

$$\frac{dC_{2HN}}{dt} = k_{1(obs)}C_{C14} \qquad (8.2)$$

$$\frac{dC_{ISO}}{dt} = k_{2(obs)}C_{14} \qquad (8.3)$$

A mechanism-derived rate equation for the bulky-phosphite ligand coordinated to rhodium was applied and incorporated to describe the observed hydroformylation reaction rate data ($k_{i,obs}$). Excellent correlation of the mechanism-based rate equation with the experimentally determined product-time distributions was found over a wide substrate conversion range; this being one of only few studies reporting such a systematic evaluation of the kinetics of the hydroformylation using bulky phosphite-modified rhodium catalyst, and the first for the hydroformylation of post-metathesis product. Activation energy for hydroformylation reaction was determined to be 68 kJ.mol^{-1}.

8.1.3 Hydroformylation with Schiff base derived rhodium precatalysts

In terms of non-commercialized catalyst systems, the hydroformylation performance of monometallic **4** and heterobimetallic **5** Schiff base derived precatalyst complexes bearing bidentate N'O chelate ligands was evaluated (Chapter 6). The precatalysts exhibit induction phenomena, rendering both precatalysts inactive at temperatures below 85°C. The precatalysts performed optimally at 95°C (40 bar) with approximately 40:60 regio-selective split in favour of the isoaldehydes. These precatalyst systems are therefore much less selective than the commercial catalyst system reported in this study. However, significantly higher turnover numbers, up to 4310, could be achieved at a lower catalyst loadings compared to the

commercial catalyst systems; albeit at higher reaction temperatures. These are the highest reported turnover numbers for these N'O chelate type precatalyst systems in hydroformylation, to the best of the author's knowledge. Evidence of a cooperative effect of including an additional metallocenes metal (ferrocene) was also reported, which can potentially motivate the application of heterobimetallic catalysts to enhance the efficacy of rhodium in an industrial context. Moreover, precatalysts **4** and **5** remain active after at least three consecutive reaction cycles under pseudo-continuous conditions, thus increasing the total product turnovers achievable by each of the precatalysts.

The kinetics of the model reaction using the heterobimetallic ferrocenyl-rhodium(I) Schiff base derived precatalyst **5** have also been investigated (Chapter 7). Whereas a set of three differential mole balance equations was found to be suitable for describing the kinetics of **1**, it was found that the kinetics with **5** could be better described by a set of four pseudo first-order ordinary differential mole-balance equations, as given by **Equations 8.4-8.7**.

$$\frac{d(C_{C14})}{dt} = -k_{1(obs)}C_{C14} - k_{2(obs)}C_{C14} \qquad (8.4)$$

$$\frac{d(C_{2HN})}{dt} = k_{1(obs)}C_{C14} \qquad (8.5)$$

$$\frac{d(C_{ISOALK})}{dt} = k_{2(obs)}C_{C14} - k_{3(obs)}C_{C14} \qquad (8.6)$$

$$\frac{d(C_{ISOALD})}{dt} = k_{3(obs)}C_{C14} \qquad (8.7)$$

A mechanism-based rate equation consistent with the parametric influences (CO, H_2, catalyst and substrate concentrations) typically observed for conventional monometallic catalyst systems was applied in this study to describe the kinetics of the heterobimetallic catalyst. Excellent agreement between the mechanism-based rate equation and rate data was observed and may be used as a starting point for the development of suitable reactor models for alkene hydroformylation using heterobimetallic catalysts. To the best of the author's knowledge, there are no reports of the kinetics using Schiff base derived heterobimetallic rhodium-ferrocenyl precatalysts in hydroformylation. The activation energy for the hydroformylation reaction was determined to be 62 kJ.mol^{-1}, which is comparable to that observed using the commercial bulky phosphite catalyst system (68 kJ.mol^{-1}).

8.2 Recommendations for future work

Based on the findings of this study, the following avenues of investigation are recommended for consideration in future work:

i) Heterobimetallic catalysis

In this study, evidence of cooperative effect of including an additional metal was reported using the heterobimetallic Schiff base derived rhodium-ferrocene precatalyst. In the future, it is proposed that similar heterobimetallic complexes could be designed by incorporating different metallocene groups (ruthenium, osmium, etc.), which could potentially offer improved catalytic performance. Moreover, the variation of electron-withdrawing and electron-donating substituent groups forming part of the catalyst design could aid in optimizing the performance of such catalyst systems in order to be more competitive (in terms of activity and selectivity) with the current state-of-the-art commercial catalyst systems.

ii) One-pot metathesis-hydroformylation

As mentioned at the beginning of this dissertation, multi-step catalytic reaction sequences involving the hydroformylation reaction are attracting much interest as a new and interesting avenue for organic synthesis. In contrast to the isolated treatment of α-alkene metathesis in previous studies and the hydroformylation of the post-metathesis product in this study (both required for foundational work), combining these two fields to yield a one-pot 'metathesis-hydroformylation' technology may be a very interesting and synthetically attractive avenue of investigation in the future. Several one-pot syntheses involving the metathesis reaction have already been reported in the literature (Cossy et al., 2002; Lee et al., 2003; Ajamian et al., 2004), among others, although none have been reported which combine metathesis with hydroformylation, to the best of the author's knowledge.

iii) Economic potential

While directly comparing the catalytic performance of different catalyst systems to identify the "best" catalyst can be very challenging (since most catalyst systems perform optimally at very different reaction conditions), a more robust approach for comparing the performance of the different catalyst systems, from a commercial perspective, may be to perform a detailed economic assessment of the different catalyst systems. A detailed outline for assessing the economic potential of chemical processes is described in Douglas (1988). Such a study should ideally be performed by combining both metathesis and hydroformylation aspects, which could

aid in the identification of possible economic resistances to the commercialisation of such a beneficiation process.

References

Ajamian, A. and Gleason, J. 2004. Two birds with one metallic stone: single-pot catalysis of fundamentally different transformations. Angewandte Chemie International Edition. 43, 3754-3760.

Douglas, J. 1988. Conceptual design of chemical processes. McGraw-Hill.

Cossy, J., Bargiggia, F. and BouzBouz, S. 2002. Tandem reaction by using compatible catalysts: cross-metathesis reaction and hydrogenation. Tetrahedron letters. 43, 6715-6717.

Lee, H., Kim, H., Tae, H., Kim, B. and Lee, J. 2003. One-pot three-component tandem metathesis/Diels–alder reaction. Organic letters. 5, 3439-3442.

APPENDIX A

PERMISSIONS TO REPRODUCE PUBLISHED WORK

A.1 Permission to reproduce Chapter 4

SPRINGER NATURE LICENSE
TERMS AND CONDITIONS

Feb 18, 2019

This Agreement between Mr. Nicholas Breckwoldt ("You") and Springer Nature ("Springer Nature") consists of your license details and the terms and conditions provided by Springer Nature and Copyright Clearance Center.

License Number	4531770633478
License date	Feb 18, 2019
Licensed Content Publisher	Springer Nature
Licensed Content Publication	Reaction Kinetics, Mechanisms and Catalysis
Licensed Content Title	Hydroformylation of post-metathesis product using commercial rhodium-based catalysts
Licensed Content Author	Nicholas C. C. Breckwoldt, Percy van der Gryp
Licensed Content Date	Jan 1, 2018
Licensed Content Volume	125
Licensed Content Issue	2
Type of Use	Thesis/Dissertation
Requestor type	academic/university or research institute
Format	print and electronic
Portion	full article/chapter
Will you be translating?	no
Circulation/distribution	<501
Author of this Springer Nature content	yes
Title	Student
Institution name	Stellenbosch University
Expected presentation date	Feb 2019
Requestor Location	Mr. Nicholas Breckwoldt Department of Process Engineering Stellenbosch University Stellenbosch, Western Cape 7600

A.2 Permission to reproduce Chapter 5

No permission required. Please see online 'Licenses, Copyright & Permissions" policy of the Royal Society of Chemistry (RSC) at http://www.rsc.org/journals-books-databases/journal-authors-reviewers/licences-copyright-permissions/#reuse-permission-requests.

Accessed February 2019.

A.3 Permission to reproduce Chapter 6

A.4 Permission to reproduce Chapter 7

SPRINGER NATURE LICENSE
TERMS AND CONDITIONS

Sep 10, 2019

This Agreement between Mr. Nicholas Breckwoldt ("You") and Springer Nature ("Springer Nature") consists of your license details and the terms and conditions provided by Springer Nature and Copyright Clearance Center.

License Number	4665520709655
License date	Sep 10, 2019
Licensed Content Publisher	Springer Nature
Licensed Content Publication	Reaction Kinetics, Mechanisms and Catalysis
Licensed Content Title	Kinetic evaluation of the hydroformylation of the post-metathesis product 7-tetradecene using a heterobimetallic rhodium-ferrocenyl Schiff base derived precatalyst
Licensed Content Author	Nicholas C. C. Breckwoldt, Gregory S. Smith, Percy Van der Gryp et al
Licensed Content Date	Jan 1, 2019
Licensed Content Volume	128
Licensed Content Issue	1
Type of Use	Thesis/Dissertation
Requestor type	academic/university or research institute
Format	print and electronic
Portion	full article/chapter
Will you be translating?	no
Circulation/distribution	1 - 29
Author of this Springer Nature content	yes
Title	Student
Institution name	Stellenbosch University
Expected presentation date	Sep 2019
Requestor Location	Mr. Nicholas Breckwoldt Department of Process Engineering Stellenbosch University

APPENDIX B

ANALYSIS OF UNCERTAINTY

B.1. The measurand (Y)

Let Y be any measured quantity (termed the 'measurand') which is determined by any number of input quantities $(X_1, X_2, \dots X_N)$. Then Y can be expressed as some function (f) in terms of these input quantities (Equation B.1).

$$Y = f(X_1, X_2, \dots X_N) \qquad (B.1)$$

Even though it is not possible to know the exact true value of any input quantity X_i, the best estimate of X_i, represented as x_i, can be obtained. Consequently, only an estimate of Y, represented as $'y'$, can ever be determined (Equation B.2)

$$y = f(x_1, x_2, \dots x_N) \qquad (B.2)$$

B.2 Uncertainty in measurand (y)

The estimated standard uncertainty $u(y)$ of the measurand (y) can be related to the estimated standard uncertainties of the input quantities x_i that are used to determine y. The Law of Propagation of Uncertainty (Equation B.3) defines this relationship, where $u(x_i)$ represents the standard uncertainty of x_i and $u(x_i, x_j)$ represents the covariance between estimates of the inputs x_i and x_j. The covariance $u(x_i, x_j)$ can be determined by Equation B.4, where $r(x_i, x_j)$ is the correlation coefficient between input estimates. If there exists no obvious relationship (i.e. zero correlation) between input x_i and x_j then the covariance $u(x_i, x_j)$ will be zero. Important to note is that $u(x_i, x_i)$ is simply the estimated variance in x_i. Combination of Equation B.3 and B.4 leads to general equation relating the uncertainty for all input estimates to the square of standard uncertainty in y, i.e. $u^2(y)$ (Equation B.5).

$$u_c^2(y) = \sum_{i=1}^{N} \left(\frac{\partial f}{\partial x_i}\right)\left(\frac{\partial f}{\partial x_i}\right) u^2(x_i) + 2\sum_{i=1}^{N-1}\sum_{j=i+1}^{N} \left(\frac{\partial f}{\partial x_i}\right)\left(\frac{\partial f}{\partial x_j}\right) u(x_i, x_j) \qquad (B.3)$$

$$u(x_i, x_j) = r(x_i, x_j) u(x_i) u(x_j) \qquad (B.4)$$

$$u_c^2(y) = \sum_{i=1}^{N} \left(\frac{\partial f}{\partial x_i}\right)\left(\frac{\partial f}{\partial x_i}\right) u^2(x_i) + 2\sum_{i=1}^{N-1}\sum_{j=i+1}^{N} \left(\frac{\partial f}{\partial x_i}\right)\left(\frac{\partial f}{\partial x_j}\right) r(x_i, x_j) u(x_i)(x_j) \qquad (B.5)$$

Careful inspection of Equation B.5 reveals that the standard uncertainty $u^2(y)$ can be determined by element-wise multiplication of the derivative ($\boldsymbol{D}$) and variance-covariance ($\boldsymbol{VC}$) matrices to yield matrix $\boldsymbol{U}$, followed by summation over all elements of $\boldsymbol{U}$.

$$\boldsymbol{D} = \begin{bmatrix} \left(\frac{\partial f}{\partial x_1}\right)\left(\frac{\partial f}{\partial x_1}\right) & \left(\frac{\partial f}{\partial x_1}\right)\left(\frac{\partial f}{\partial x_2}\right) & \cdots & \left(\frac{\partial f}{\partial x_1}\right)\left(\frac{\partial f}{\partial x_N}\right) \\ \left(\frac{\partial f}{\partial x_2}\right)\left(\frac{\partial f}{\partial x_1}\right) & \left(\frac{\partial f}{\partial x_2}\right)\left(\frac{\partial f}{\partial x_2}\right) & \cdots & \left(\frac{\partial f}{\partial x_2}\right)\left(\frac{\partial f}{\partial x_N}\right) \\ \vdots & \vdots & \ddots & \vdots \\ \left(\frac{\partial f}{\partial x_N}\right)\left(\frac{\partial f}{\partial x_1}\right) & \left(\frac{\partial f}{\partial x_N}\right)\left(\frac{\partial f}{\partial x_2}\right) & \cdots & \left(\frac{\partial f}{\partial x_N}\right)\left(\frac{\partial f}{\partial x_N}\right) \end{bmatrix}$$

$$\boldsymbol{VC} = \begin{bmatrix} u(x_1, x_1) & u(x_1, x_2) & \cdots & u(x_1, x_N) \\ u(x_2, x_1) & u(x_2, x_2) & \cdots & u(x_2, x_N) \\ \vdots & \vdots & \ddots & \vdots \\ u(x_N, x_1) & u(x_N, x_2) & \cdots & u(x_N, x_N) \end{bmatrix}$$

$$\boldsymbol{U} = (\boldsymbol{D} \circ \boldsymbol{VC}) = \begin{bmatrix} \left(\frac{\partial f}{\partial x_1}\right)\left(\frac{\partial f}{\partial x_1}\right)u(x_1, x_1) & \left(\frac{\partial f}{\partial x_1}\right)\left(\frac{\partial f}{\partial x_2}\right)u(x_1, x_2) & \cdots & \left(\frac{\partial f}{\partial x_1}\right)\left(\frac{\partial f}{\partial x_N}\right)u(x_1, x_N) \\ \left(\frac{\partial f}{\partial x_2}\right)\left(\frac{\partial f}{\partial x_1}\right)u(x_2, x_1) & \left(\frac{\partial f}{\partial x_2}\right)\left(\frac{\partial f}{\partial x_2}\right)u(x_2, x_2) & \cdots & \left(\frac{\partial f}{\partial x_2}\right)\left(\frac{\partial f}{\partial x_N}\right)u(x_2, x_N) \\ \vdots & \vdots & \ddots & \vdots \\ \left(\frac{\partial f}{\partial x_N}\right)\left(\frac{\partial f}{\partial x_1}\right)u(x_N, x_1) & \left(\frac{\partial f}{\partial x_N}\right)\left(\frac{\partial f}{\partial x_2}\right)u(x_N, x_2) & \cdots & \left(\frac{\partial f}{\partial x_N}\right)\left(\frac{\partial f}{\partial x_N}\right)u(x_N, x_N) \end{bmatrix}$$

B.3 Application of uncertainty in measurement

Equation B.6 represents the mathematical form of the linear calibration curves (refer to Chapter 3, Section 3.2.3) used to relate the volume of the target species (V_i) to the GC area response of the target compound relative to the external standard response (A_i/A_S) in terms of known external standard volume (V_S) and linear correlation coefficients (α, β).

$$V_i = \left[\alpha + \beta\left(\frac{A_i}{A_S}\right)\right]V_S \qquad (B.6)$$

Treating α, β, A/A_S and V_S as input parameters and applying the first partial derivatives of V_i with respect to each of the input parameters (refer to Equation B.5 as to why these derivatives are necessary), yields the following inputs for the derivation matrix ***D***:

$$\left(\frac{\partial V_i}{\partial \alpha}\right) = 1 \qquad \left(\frac{\partial V_i}{\partial (A_i/A_S)}\right) = \beta V_S$$

$$\left(\frac{\partial V_i}{\partial \beta}\right) = \left(\frac{A_i}{A_S}\right) V_S \qquad \left(\frac{\partial V_i}{\partial V_S}\right) = \beta \left(\frac{A_i}{A_S}\right)$$

The variance-covariance matrix (***VC***) can also then be written :

	α	β	A/A_{IS}	V_{IS}
α	$Var\ (\propto)$	$Cov(\beta, \alpha)$	$Cov\left(\frac{A_i}{A_S}, \alpha\right)$	$Cov\ (V_S, \alpha)$
β	$Cov\ (\propto, \beta)$	$Var\ (\beta)$	$Cov\ \left(\frac{A_i}{A_S}, \beta\right)$	$Cov\ (V_S, \beta)$
A_i/A_S	$Cov\ \left(\propto, \frac{A_i}{A_S}\right)$	$Cov\ \left(\beta, \frac{A_i}{A_S}\right)$	$Var\ \left(\frac{A_i}{A_S}\right)$	$Cov\ \left(V_S, \frac{A_i}{A_S}\right)$
V_S	$Cov\ (\propto, V_S)$	$Cov\ (\beta, V_I)$	$Cov\ \left(\frac{A_i}{A_S}, V_S\right)$	$Var\ (V_S)$

Simplification of ***VC***, through identification of relatable parameters having non-zero covariance gave the following matrix (***VC****), where '*' indicates modified variance-covariance matrix. The variance of α and β, and covariance relating α and β were determined from the linear regression procedure to determine the line of best fit to the calibration curve (Equation B.6). The variance of A_i/A_S was estimated through multiple injections of the sample, to record the distribution of A_i/A_S for that sample. Multiple pipette aliquots of external standard (100 uL) were measured gravimetrically (mass correlated to volume with known density data at standard conditions) to determine the variance of V_S. Element-wise multiplication of the derivative (***D***) and the modified variance-covariance (***VC****)* matrices to yield matrix ***U*****,** followed by summation over all elements of ***U*** allowed estimation of the standard uncertainty $u^2(y)$ (refer back to B.2).

	α	β	A_i/A_S	V_S
α	$Var\ (\propto)$	$Cov(\beta, \alpha)$	0	0
β	$Cov\ (\propto, \beta)$	$Var\ (\beta)$	0	0
A_i/A_S	0	0	$Var\left(\frac{A_i}{A_S}\right)$	0
V_S	0	0	0	$Var\ (V_S)$